

# Optimisation of Wind Turbine Foundations

by

Tinotendaishe Daniel Muzofa



*Thesis presented in partial fulfilment of the requirements for  
the degree of Master of Engineering (Structural) in the  
Faculty of Engineering at Stellenbosch University*

Supervisor: Prof. G.P.A.G. Van Zijl

Co-supervisor: Prof. P.W. Day

December 2017

# Declaration

By submitting this thesis electronically, I declare that the entirety of the work contained therein is my own, original work, that I am the sole author thereof (save to the extent explicitly otherwise stated), that reproduction and publication thereof by Stellenbosch University will not infringe any third party rights and that I have not previously in its entirety or in part submitted it for obtaining any qualification.

Date: December 2017

Copyright © 2017 Stellenbosch University  
All rights reserved.

# Abstract

## Optimisation of Wind Turbine Foundations

T.D. Muzofa

*Department of Structural Engineering,  
University of Stellenbosch,  
Private Bag X1, Matieland 7602, South Africa.*

Thesis: MEng (Civil)

December 2017

This study seeks to optimize the foundations of tall wind turbine support structures in South Africa. It is postulated that the concrete quantity can be reduced in gravity based foundations by incorporating the backfill material into the foundation design. The study was based on the development of finite element models consisting of gravity based foundation embedded in a founding material and connected to a wind turbine tower. Three main analyses were computed namely; Static non-linear push over analysis, Cyclic load analysis and Structural eigenvalue analysis. The purpose of the study was to investigate (a) soil-structure interaction in order to assess the infinite vs. finite soil stiffness effect on the natural frequency of the structure, (b) the stress distribution in the foundation in order to replace under-stressed parts with backfill material yet maintaining the same structural stiffness and vibrational behaviour that complies with the soft-stiff structural vibration frequency domain, (c) the feasibility of using high density concrete towards foundation size reduction, as well as water usage reduction. Finally, a structural performance and cost comparison is drawn between a conventional and alternative foundation systems. A conceptual design guideline for the foundation system is also created for both geotechnical and structural design of the foundation.

The study concludes that soil-structure interaction does influence the natural frequency of the wind turbine tower. Stiff soils result in higher natural frequency and less stiff soils result in a lower natural frequency. Secondly the critical sections that require structural concrete in a gravity based foundation are the section directly below the tower base and also the base of the foundation. The rest of the concrete is primarily for rotational stiffness as a counterweight. Lastly, volumetric aggregate replacement is a feasible solution towards increase in the density of concrete and consequently reducing the concrete foundation size. The feasibility being based on the mechanical behaviour of the concrete material. The study recommends that finite element analysis be used in order to develop an optimum wind turbine foundation design.

Key Words: Wind, Turbine, Foundations, Soil-Structure Interaction, Optimisation

# Uittreksel

## Optimering van Windturbine Fondasies

*(“Optimisation of Wind Turbine Foundations”)*

T.D. Muzofa

*Afdeling StruktuurIngen,  
Universiteit van Stellenbosch,  
Privaatsak X1, Matieland 7602, Suid Afrika.*

Tesis: MIng (Siviel)

Desember 2017

Hierdie studie poog om die fundamente van die ondersteunende strukture van hoë windturbines in Suid-Afrika te optimeer. Daar word gepostuleer dat die hoeveelheid beton in swaartekrag gebaseerde fondasies verminder kan word deur die opvulmateriaal in die fondasie-ontwerp in te sluit. Die studie ontwikkel eindige element modelle wat bestaan uit 'n swaartekrag gebaseerde fondasie, ingebed in die ondergrond, en verbind met 'n windturbine toring. Drie hoofontledings is uitgevoer, naamlik; Statiese nie-lineêre omkantelingsanalise, gedrag onder sikliese belasting en strukturele eiewaarde-analise. Die doel van die studie was om (a) grond-struktuur interaksie te ondersoek ten einde die oneindige teenoor. eindige grondstyfheidseffek op die natuurlike frekwensie van die struktuur te assesser, (b) om uit die spanningsverdeling in die fondasie dele met lae spanning met terugvulmateriaal te vervang, maar steeds dieselfde strukturele styfheid en vibrasiegedrag behou wat voldoen aan die sag-stywe strukturele vibrasie frekwensie domein, (c) die haalbaarheid van die gebruik van hoë-digtheid beton ten einde volume-vermindering, sowel as waterverbruik vermindering te bewerkstellig. Laastens word 'n strukturele prestasie en kostevergelyking getref tussen 'n konvensionele en alternatiewe fondamentstelsel. 'n Konseptuele ontwerpstriglyn vir die fondamentstelsel word ook geskep vir beide die geotegniese en strukturele ontwerp van die fondasie.

Die studie lei tot die gevolgtrekking dat grond-struktuur-interaksie die natuurlike frekwensie van die windturbine toring beïnvloed. Stywe grond veroorsaak hoër natuurlike frekwensie en minder stywe gronde lei tot 'n laer natuurlike frekwensie. Tweedens, die kritiese deel wat strukturele beton benodig in 'n swaartekrag gebaseerde fondament, is die gedeelte direk onder die toringbasis en ook die basis van die stigting. Die res van die beton is hoofsaaklik vir rotasiestyfheid as 'n teengewig. Laastens is volumetriese vermindering 'n haalbare oplossing deur gebruik van hoë-digtheid beton wat aggremaat van hoë digtheid bevat. Die haalbaarheid is gebaseer op die meganiese gedrag van die betonmateriaal. Die

studie beveel aan dat eindige element analise gebruik word om 'n optimale ontwerp van windturbines te ontwikkel.

Sleutelwoorde: Wind, Turbine, Grondslae, Grondstruktuurinteraksie, Optimering

# Acknowledgements

I would like to express my sincere gratitude to the following people and organisations:

- **Prof GPAG Van Zijl:** For his guidance, support and motivation through out my entire career and more specifically the MEng Research.
- **Prof Peter Day:** For his guidance and supervision specifically with understanding the soil behaviour and FE modelling of soil.
- **Mr D, Mrs E Muzofa and Family:** For the prayers, mentor-ship and financial support ever since birth.
- **Mandela Rhodes Foundation:** For funding my MEng studies and offering thought leadership through the workshops presented in residence.
- **Loeriesfontein Wind Farm Team:** For granting me access to their project and providing me valuable insight on the pragmatism of wind turbine constructions.
- **Power Construction:** For granting us a case study mix design for wind turbine foundations and also offering to assist with practical insight pertaining to wind turbine foundation construction.
- **Asnath Kessy:** For providing current material costs and rates used in the cost comparison for the study.

# Dedications

*I dedicate this thesis to my Parents and Siblings: Pastors D and E Muzofa, Melody Muzofa, Daisy Magara, Kuda Muzofa and Rutendo Mazhindu.*

# Contents

<b>Declaration</b>	<b>i</b>
<b>Abstract</b>	<b>ii</b>
<b>Uittreksel</b>	<b>iii</b>
<b>Acknowledgements</b>	<b>v</b>
<b>Dedications</b>	<b>vi</b>
<b>Contents</b>	<b>vii</b>
<b>List of Figures</b>	<b>ix</b>
<b>List of Tables</b>	<b>xii</b>
<b>Nomenclature</b>	<b>xiii</b>
<b>1 Introduction</b>	<b>1</b>
1.1 Background . . . . .	1
1.2 Audience . . . . .	1
1.3 Scope . . . . .	2
1.4 Thesis Layout . . . . .	2
<b>2 Literature Review</b>	<b>3</b>
2.1 Foundation Types . . . . .	3
2.2 Design Guidelines . . . . .	6
<b>3 Concrete Mix Optimisation</b>	<b>19</b>
3.1 Introduction . . . . .	19
3.2 Motivation . . . . .	20
3.3 Design . . . . .	21
3.4 Tests . . . . .	22
3.5 Results . . . . .	29
3.6 Conclusion and Recommendations . . . . .	35
<b>4 Foundation Design</b>	<b>36</b>
4.1 Introduction . . . . .	36
4.2 Given Parameters . . . . .	36
4.3 Geotechnical Design . . . . .	37
4.4 Structural Design . . . . .	42



<b>5</b>	<b>Finite Element Modelling</b>	<b>58</b>
5.1	Introduction . . . . .	58
5.2	Material Models . . . . .	58
5.3	Elements . . . . .	63
5.4	Analysis . . . . .	65
<b>6</b>	<b>Results</b>	<b>72</b>
6.1	Static Push Over . . . . .	72
6.2	Cyclic Loading . . . . .	81
6.3	Eigen Frequency Analysis . . . . .	83
<b>7</b>	<b>Cost Comparison</b>	<b>85</b>
7.1	Introduction . . . . .	85
7.2	Typical wind energy project in South Africa . . . . .	85
7.3	Wind energy project cost breakdown . . . . .	85
7.4	Foundation Cost Comparison . . . . .	86
<b>8</b>	<b>Conclusions and Recommendations</b>	<b>88</b>
8.1	Conclusions . . . . .	88
8.2	Recommendations . . . . .	90
8.3	Future Study . . . . .	90
	<b>Appendices</b>	<b>92</b>
<b>A</b>	<b>Concrete Strength and Stiffness Detailed Results</b>	<b>93</b>
A.1	Compressive Strength . . . . .	93
A.2	Tensile Strength . . . . .	94
A.3	E-Modulus . . . . .	95
<b>B</b>	<b>Detailed Bearing Capacity Calculation</b>	<b>96</b>
B.1	Introduction . . . . .	96
<b>C</b>	<b>FEM Material Properties</b>	<b>102</b>
C.1	Concrete . . . . .	102
C.2	Soil . . . . .	103
C.3	Soil-Structure Interaction . . . . .	104
C.4	Steel . . . . .	104
<b>D</b>	<b>Foundation Detailed Drawings</b>	<b>105</b>
	<b>List of References</b>	<b>108</b>

# List of Figures

2.1	(a) Plain slab; (b) Stub and pedestal; (c) Stub tower embedded in tapered slab; (d) Slab held by founding anchors . . . . .	4
2.2	(a) Pile group and cap; (b) Solid mono-pile; (c) Hollow mono-pile . . . . .	4
2.3	Fatigue resistant foundation system . . . . .	5
2.4	Bottom view of iCK foundation . . . . .	6
2.5	Typical construction variants for the load transfer from tower in to foundation. Adapted from Maunu (2006) . . . . .	7
2.6	a) Model assuming linear soil pressure distribution; b) Model based on the subgrade reaction modulus. From Maunu (2006) . . . . .	8
2.7	Soil pressure distribution under a rigid foundation: a) Small applied vertical load V; b) Redistribution after soil plasticizing. Adapted from Maunu (2006) . . . . .	9
2.8	Wind Corridor overlain on hybrid topographical map with wind speed. Adapted from Mawer (2015) . . . . .	11
2.9	Loading of foundation under idealized conditions . . . . .	13
2.10	Circular and octagonal footing with effective foundation area marked out . . . . .	14
2.11	Single loaded pile displacement and reactions . . . . .	15
2.12	Placement of Anchoring Cage (Vestas) . . . . .	16
2.13	Steel Placement Initial (Vestas) . . . . .	17
2.14	Steel Placement Final (Vestas) . . . . .	17
3.1	Exemplifying the various scales of observation for Civil Engineering Structures	19
3.2	Fixed Reinforcement Steel . . . . .	23
3.3	Concrete Pouring Method . . . . .	23
3.4	Concrete Compaction . . . . .	24
3.5	Super Plasticiser sensitivity analysis for Mix 1 . . . . .	25
3.6	Tensile Splitting test (left) and Compressive Strength Test (Right) shown in the Zwick Z250 MTM and Contest 2MN MTM respectively . . . . .	26
3.7	Secant Modulus of Elasticity Test Set Up . . . . .	27
3.8	Drying Shrinkage Measurement Set Up . . . . .	28
3.9	Sieve Analysis for Coarse Aggregate . . . . .	29
3.10	Compression Test Results . . . . .	31
3.11	Sectional View of Mix 1 (left) and Mix 2 (right) . . . . .	32
3.12	Compressive Stiffness Curves . . . . .	33
3.13	Reference Mix Drying Shrinkage Curves . . . . .	33
3.14	Iron Ore Mix Drying Shrinkage Curves . . . . .	34
3.15	Drying Shrinkage Comparative Curves . . . . .	34
4.1	Generic foundation geometry (not to scale) . . . . .	37
4.2	Loading Under Idealised conditions (adapted from DNV/Riso (2002)) . . . . .	39

4.3	SZZ Stresses for Selfweight Load Case . . . . .	43
4.4	SY Y Stresses for Selfweight Load Case . . . . .	43
4.5	SZZ Stresses for Moment Load Case . . . . .	43
4.6	SY Y Stresses for Moment Load Case . . . . .	44
4.7	Radial plane (RP) for STM truss development . . . . .	44
4.8	3D schematisation of the radial plane and truss for STM . . . . .	45
4.9	Legend for Figure 4.10 . . . . .	46
4.10	Couple forces per radial plane (RP) . . . . .	46
4.11	Prokon Output for STM Truss . . . . .	47
4.12	Load Transfer Schematisation . . . . .	48
4.13	Tower Flange Connections 1 (Left) and 2 (Right) . . . . .	48
4.14	Node 1 : Node boundary . . . . .	50
4.15	Typical bending moment diagram for wind turbine foundation.(Way, 2014) . . . . .	51
4.16	Illustration of compression and tension force couple(Way, 2014). . . . .	51
4.17	BTM Free Body Diagram . . . . .	53
4.18	Shear Force Diagram for foundation modelled using the BTM . . . . .	53
4.19	Bending Moment Diagram for foundation modelled using the BTM . . . . .	54
5.1	Model Schematisation <i>Illustration not drawn to actual modelling scale</i> . . . . .	59
5.2	Soil response in compression . . . . .	60
5.3	Concrete Tensile Curve . . . . .	63
5.4	8-node Regular Curved Shell Element Used to Model Tower (CQ40S . . . . .	64
5.5	10-node Regular Tetrahedron Solid Element Used to Model Concrete and Soil (CTE30) . . . . .	64
5.6	Plane Quadrilateral, 8+8 nodes, 3-D Interface Element (CQ481) . . . . .	65
5.7	Excavation mesh: Second Phase . . . . .	66
5.8	Excavation and concrete foundation mesh : Second Phase . . . . .	66
5.9	Foundation backfill mesh : Third Phase . . . . .	67
5.10	Tower on founded concrete foundation mesh : Fourth Phase . . . . .	67
5.11	Model 1 (Left) Model 2 (Right) . . . . .	68
5.12	Cyclic loading procedure depicted in an exaggerated sketch . . . . .	69
5.13	Working frequency for wind turbine foundation (Way, 2014) . . . . .	70
5.14	Single Degree of Freedom Simplification sketch . . . . .	70
6.1	FEM Nodes and Elements queried for Results Calculation . . . . .	73
6.2	Stress Envelope for soil directly below the concrete foundation . . . . .	73
6.3	Initial Gapping at load factor 0.3 . . . . .	74
6.4	25% Gapping at load factor 0.6 . . . . .	74
6.5	50% Gapping at Ultimate Load . . . . .	74
6.6	Foundation Rotations and Tower Top Displacement for Static push over analysis; Model 1 and 2 . . . . .	76
6.7	Normal Stress SZZ . . . . .	77
6.8	Normal Stress SY Y . . . . .	77
6.9	Normal Stress SZZ : Sectional View 1 m below Tower Base . . . . .	78
6.10	Normal Stress SY Y : Sectional View 1 m below Tower Base . . . . .	78
6.11	Normal Stress SZZ :Sectional View 2.9 m below Tower Base . . . . .	78
6.12	Normal Stress SY Y :Sectional View 2.9 m below Tower Base (Worm's Eye View) . . . . .	79
6.13	Linear Elastic Concrete Foundation vs Total Strain Based Crack Model Concrete Foundation . . . . .	80

*LIST OF FIGURES***xi**

6.14 Crackwidth at initial gapping . . . . .	80
6.15 Stress distribution in Reinforcement . . . . .	81
6.16 Cyclic Loading Results . . . . .	82
6.17 Oedometer Test Results . . . . .	82
6.18 First 3 mode shapes for the structural eigenvalue analysis for fine sand soil type category . . . . .	83
B.1 Generic Foundation Geometry . . . . .	97
B.2 Effective Area . . . . .	98

# List of Tables

3.1	Mix Design . . . . .	22
3.2	Relative Density . . . . .	30
3.3	Water Absorption . . . . .	30
3.4	Aggregate Crushing Value . . . . .	30
3.5	Hardened Concrete Density . . . . .	35
4.1	Soil Parameters . . . . .	37
4.2	Characteristic Extreme Load for Normal Load Cases . . . . .	37
4.3	Design 1 Geometry . . . . .	38
4.4	STM Critical Members . . . . .	47
4.5	Area of Steel Comparison . . . . .	55
6.1	First Eigenvalue results: Natural frequency . . . . .	84
6.2	Rotational stiffness values used for SDOF Eigenvalue analysis . . . . .	84
7.1	Cost breakdown of a typical South African wind energy project (Way, 2014) . . . . .	86
7.2	Material cost for Model 1 . . . . .	86
7.3	Material cost for Model 2 . . . . .	87
A.1	Iron Ore 7 Day Compressive Strength . . . . .	93
A.2	Iron Ore 28 Day Compressive Strength . . . . .	93
A.3	Greywacke 13 mm 7 Day Compressive Strength . . . . .	94
A.4	Greywacke 13 mm 28 day Compressive Strength . . . . .	94
A.5	Iron Ore Tensile Strength . . . . .	94
A.6	Greywacke 13 mm Tensile Strength . . . . .	94
A.7	Iron Ore E-Modulus Results . . . . .	95
A.8	Greywacke 13 mm E-Modulus Results . . . . .	95
B.1	Foundation dimensions and equivalent vertical load . . . . .	97
B.2	Effective Area Calculation . . . . .	98
B.3	Bearing Capacity Calculation . . . . .	99
C.1	Linear Elastic Concrete Model material properties . . . . .	102
C.2	Total Strain Based Crack Model material properties . . . . .	103
C.3	Soil Material Properties . . . . .	103
C.4	SSI Material Properties . . . . .	104
C.5	Steel material properties . . . . .	104

# Nomenclature

## Constants

$$g = 9.81 \text{ m/s}^2$$

## Variables

$\alpha$	Rotation angle . . . . .	[ deg ]
$e$	eccentricity loading due to moment . . . . .	[ m ]
$H$	Horizontal Load . . . . .	[ kN ]
$Hz$	Hertz . . . . .	[ s <sup>-1</sup> ]
$R$	Radius . . . . .	[ m ]
$V$	Vertical Load . . . . .	[ kN ]
$\theta$	Rotation angle . . . . .	[ deg ]

## Abbreviations

BTM	Beam Theory Method
E-Modulus	Secant Modulus of Elasticity
FE	Finite Element
FEA	Finite Element Analysis
FEM	Finite Element Model
FoS	Factor of Safety
LVDT	Linear Variable Differential Transformer
MTM	Materials Testing Machine
STM	Strut and Tie Method
SDOF	Single Degree of Freedom
TSBC	Total Strain Based Crack Model

rpm revolutions per minute

REIPPP Renewable Energy Independent Power Producer Procurement Programme

### **Bearing Capacity Factors**

$N_c$	Cohesion Factor
$N_q$	Surcharge Factor
$N_\gamma$	Self-Weight Factor
$s_c$	Cohesion Foundation Shape Factor
$s_q$	Surcharge Foundation Shape Factor
$s_\gamma$	Self-Weight Foundation Shape Factor
$d_c$	Cohesion Founding Shape Factor
$d_q$	Surcharge Founding Shape Factor
$d_\gamma$	Self-Weight Founding Shape Factor
$i_c$	Cohesion Load Inclination Shape Factor
$i_q$	Surcharge Load Inclination Shape Factor
$i_\gamma$	Self-Weight Load Inclination Shape Factor
$q_c$	Cohesion Bearing Capacity
$q_q$	Surcharge Bearing Capacity
$q_\gamma$	Self-Weight Bearing Capacity
$q_u$	Ultimate Bearing Capacity

### **Subscripts**

$c$	Cohesion
$q$	Surcharge
$\gamma$	Self-Weight
$u$	Ultimate

# Chapter 1

## Introduction

### 1.1 Background

The gradual depletion of non-renewable energy resources as well as the environment degradation coupled with greenhouse gas emissions caused by the use of fossil-based fuels has led to a paradigm shift in the global energy industry. A significant amount of research has been focused on sustainable development and implementation of sustainable energy options.

South Africa is the world's thirteenth largest CO<sub>2</sub> emitter and 77 % of country's primary energy is generated from coal. Efforts to reduce greenhouse gas emissions have birthed a renewable energy industry in South Africa. Although in its infancy, the South African wind industry, driven by the Renewable Energy Independent Power Producer Procurement Program (REIPPP), has added more than 1054 MW of wind power to the grid whilst dropping cost of wind power well below the cost of new coal power (GWEC, 2015).

Wind energy technology is being developed at a rapid pace with modern wind turbines requiring higher support structures to access stronger and less turbulent winds. Currently in South Africa, wind farms are installing wind turbines sized between 2 MW and 3.5 MW with hub heights ranging from approximately 80 m to 120 m. Gravity based foundations, also known as shallow or mass gravity pad foundations, are the most commonly used foundation type in South Africa. They are normally circular with a base diameter ranging from 14 m to 21 m. The concrete volume ranges from 240 m<sup>3</sup> to 450 m<sup>3</sup> per foundation. There is a need to optimize the foundations with regard to cost and carbon footprint by reducing the conventionally required amount of concrete.

South Africa does not have a design code to aid local engineers in the design and standardizing of wind turbine foundations. It is envisaged that this study serves as the first steps to compiling a design guideline for wind turbines foundations for South Africa.

### 1.2 Audience

To fully comprehend this thesis some knowledge about structural mechanics, structural- and geotechnical design, the finite element method and material science (mainly concrete and steel) is recommended.



## 1.3 Scope

The study addresses two main optimisation criteria. Firstly, utilisation of backfill as mass replacement for concrete and secondly reducing the water required in the mix design as wind farms are usually located in remote and water scarce areas.

The study involves non-linear computational modelling of the wind turbine towers connected to foundation embedded in a founding material. It also involves experimental tests carried out on a case study concrete mix design used on wind turbine foundations in South Africa. It is important to note that, although all foundation systems is investigated, the primary focus of this research is gravity based foundations as they are the most common type of foundation used in South Africa.

## 1.4 Thesis Layout

The thesis document comprises 8 Chapters. Chapter 2 gives a literature overview of wind turbine foundations, reviewing other research carried out previously on wind turbine foundations. Chapter 3 primarily focuses on the concrete mix design in an attempt to reduce the water requirements per wind turbine foundation. Chapter 4 utilises a worked example to explain the foundation design procedure for both the geotechnical and structural design of a gravity based wind turbine foundation. The foundation design developed in Chapter 4 is implemented in a Finite Element Model (FEM) and the analysis reported in Chapter 5. Chapter 5 also reports on the modelling of an alternative foundation type, which was designed towards reducing the concrete volume in foundation type. Chapter 6 reports on the analyses results. The economic constraints of implementing proposed optimisation recommendations are investigated and reported in Chapter 7. Lastly, the conclusions and recommendations are reported in Chapter 8.

# Chapter 2

## Literature Review

In order to gain understanding of the foundation types available and the design procedure for the current foundation types, literature was reviewed and an industry survey carried out by meeting with companies that have worked, or are currently working with wind turbine projects. A site visit was undertaken to a wind farm under construction in South Africa. This chapter reports on the relevant literature to this study. Section 2.1 gives an overview of wind turbine foundation types whilst Section 2.2 reports on research performed to provide wind turbine design guidelines. Codes and Standards available for wind turbine foundations are also reviewed in Section 2.2.

### 2.1 Foundation Types

Wind turbine superstructures can be founded on various types of foundation. The choice of foundation is usually governed by soil conditions at the particular site. The common foundation types for wind turbines are gravity base foundations (shallow or mass gravity pad foundations), piled foundation and anchored foundation. Figures 2.1 and 2.2 show variants in the common foundation types.

Gravity foundations use large quantities of concrete and steel. However, they are perceived as low-risk foundations. It was noted in meetings held in an industry survey that gravity pad foundations are the most commonly used foundation system in South Africa. However, cases where the founding material was found to have insufficient strength or stiffness to bear the pressure of the gravity foundation system, alternative foundations systems like piled foundations were employed to transfer the load to underlying stronger and stiffer material.

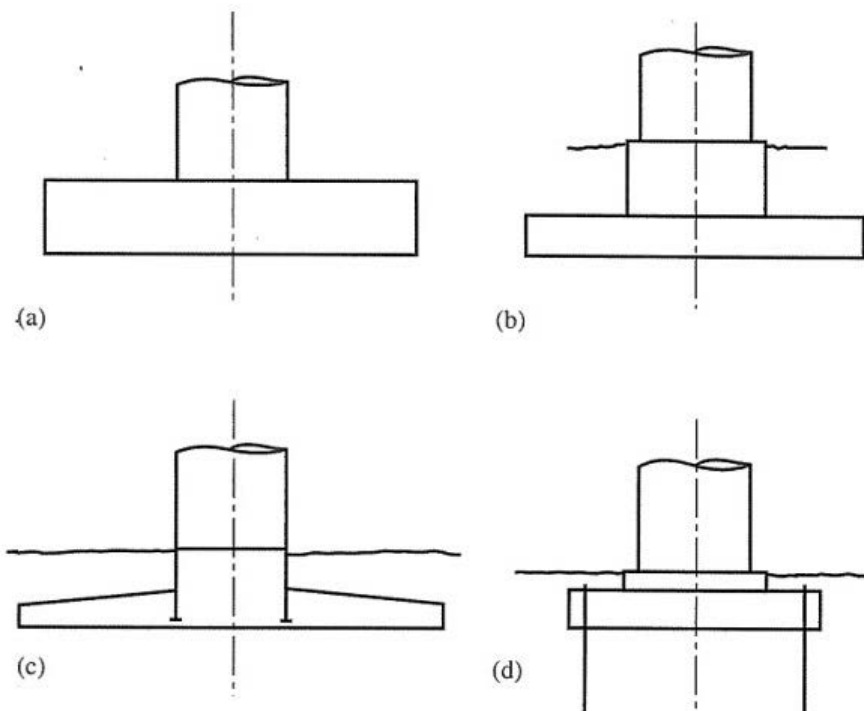


Figure 2.1: (a) Plain slab; (b) Stub and pedestal; (c) Stub tower embedded in tapered slab; (d) Slab held by founding anchors

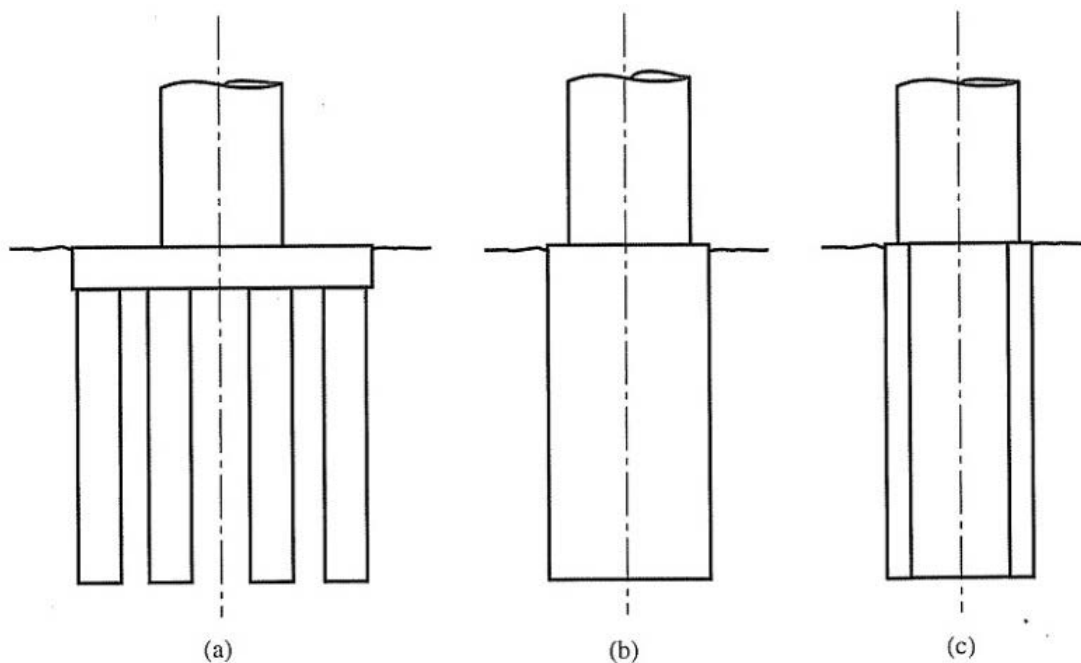


Figure 2.2: (a) Pile group and cap; (b) Solid mono-pile; (c) Hollow mono-pile

There is limited innovation with regard to reducing the concrete and steel required for gravity pad foundations. Although cost reduction would be achieved by reducing the large quantities of steel and concrete, an additional benefit would be the improvement of heat dissipation conditions during construction by a reduced ratio of concrete mass to

surface area, thus reducing the likelihood of thermal cracking due to heat of hydration. Figure 2.3 shows an example of a design developed by Phuly (2010) towards reducing the volumetric amount of concrete and steel required for mass gravity pad foundations. This Phuly (2010) patented design is a fatigue resistant gravity base spread footing. The design has a substantial horizontal, continuous bottom support slab with a stiffened perimeter. It comprises a number of radial reinforcing ribs extending outward from the pedestal and a three-dimensional network of post-tensioned elements. The post-tensioning keeps the structural elements under heavy multi-axial compression with a specific eccentricity that is intended to reduce stress amplitudes and deflections. The design strives to have a desirable combination of sufficient stiffness and significant fatigue resistance (Phuly, 2010).

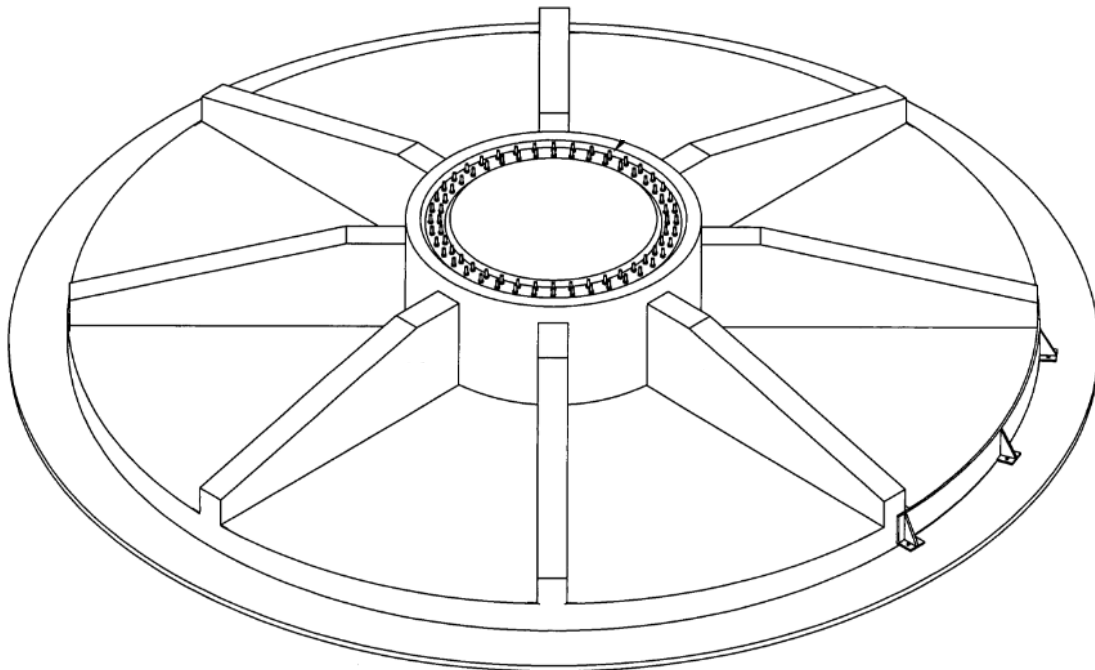


Figure 2.3: Fatigue resistant foundation system  
(Phuly, 2010)

Another innovative design aimed at reducing the construction material is the iCK foundation shown in Figure 2.4.

The iCK foundation consists of

- A top slab whose function is to achieve uniform distribution of pressure on the ground
- A central reinforced ring
- Several radial reinforced beams or stiffening ribs that form a composite section with the top slab
- A pedestal.

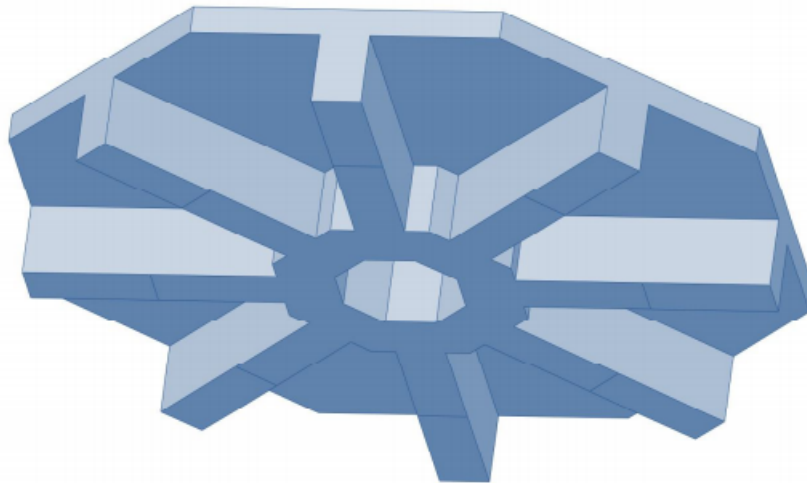


Figure 2.4: Bottom view of iCK foundation  
(Rey and Puertos, 2012)

The iCK foundation differs from the conventional ribbed foundation by having a T-section with compressions distributed across the top of the T head (Rey and Puertos, 2012). The disadvantage of the iCK foundation is that it assumes a load case without a cyclic lateral load on the supported tower. A lateral load induces a moment which alters the distribution of stresses. Compressive stresses alternate from top to bottom i.e. the top surface of the windward side of the foundation experiences tensile stress and compression stresses at the bottom surface, whilst on the leeward side of the foundation the opposite occurs. This is elaborated in Section 4.4.

## 2.2 Design Guidelines

There is currently no universal procedure for wind turbine foundation design. Literature offers guideline options, which are reported on in this section. There are also research master's theses that focused on the design of wind turbine foundations by Maunu (2006), Svensson (2010) and Nicholson (2011). It should be noted however that, although these guidelines are available, the main focus has been on the geotechnical design and its influence on the geometry of the foundation. Limited information is available with regard to the structural design (reinforcement). It was found that wind turbine suppliers provide the foundation designer with a loading document detailing the loading at the top of the foundation stub. The foundation designer is also provided with a document depicting the reinforcement layout. This information regarding the reinforcement layout is deemed as proprietary information and the turbine supplier reserves all patent, copyrights, trades secrets and any other proprietary rights (Vestas, 2011*a*).

### 2.2.1 Pekka Maunu (2006)

Maunu (2006) studied the design of wind turbine foundation slabs. His research reports on different structural design principles. He carried out his study by comparing various techniques to model the wind turbine foundation. Maunu also modelled a full three dimensional foundation and subjected it to a moment and axial design load. According

to Maunu (2006) the global dimensions of the wind turbine foundation slabs are governed by the normative regulations regarding safety against overturning. The considerations to be made when designing a foundation include the following:

- **Ultimate Limit State:** *Foundation verified against structural failure under extreme static loads*
  - Stability of soil related to substantial pore water pressure under the foundation
  - Flexural resistance of foundation
  - Shear resistance of foundation
  - Concentrated force specifically at the connection between the foundation and the tower
- **Serviceability Limit State**
  - Crack width
  - Settlement
  - Limitation of stresses to ensure durability
- **Fatigue Limit State:** *Dynamic analysis including fatigue calculations for both concrete and steel due to the cyclic loading on the foundation; this was however mentioned as not typically required.*
  - Concrete : Cyclic nature of load increase crack propagation.
  - Steel : Reinforcement fatigue

Maunu (2006) also reported on the variants for the tower to foundation connection, namely an I girder bent to form a ring beam and a pre-stressed anchor bolt cage as shown in Figure 2.5

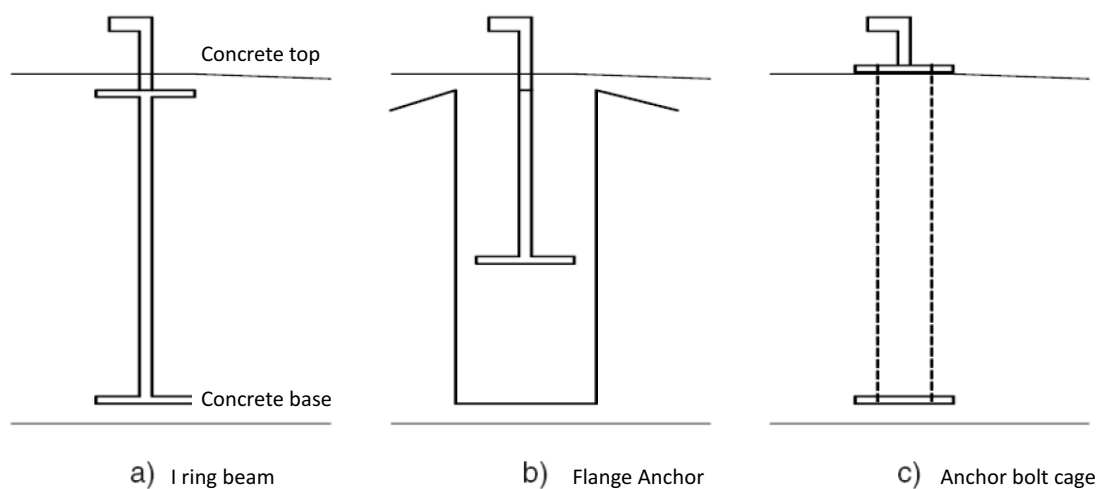


Figure 2.5: Typical construction variants for the load transfer from tower in to foundation. Adapted from Maunu (2006)

Maunu (2006) also considers the two design principles of linear pressure distribution based on beam theory, and the Winkler type spring foundation. The linear pressure distribution is regarded as conservative for large slabs. The Winkler type spring foundation is characterised by modelling the soil as a collection of discrete linear springs with a modulus of subgrade reaction. Although the Winkler type spring method is the most widely used method, the determination of the modulus of subgrade reaction is problematic, as it is not purely determined by the soil properties, but depends on the whole system: loading, dimensions and soil type. Figure 2.6 shows the above mentioned principles.

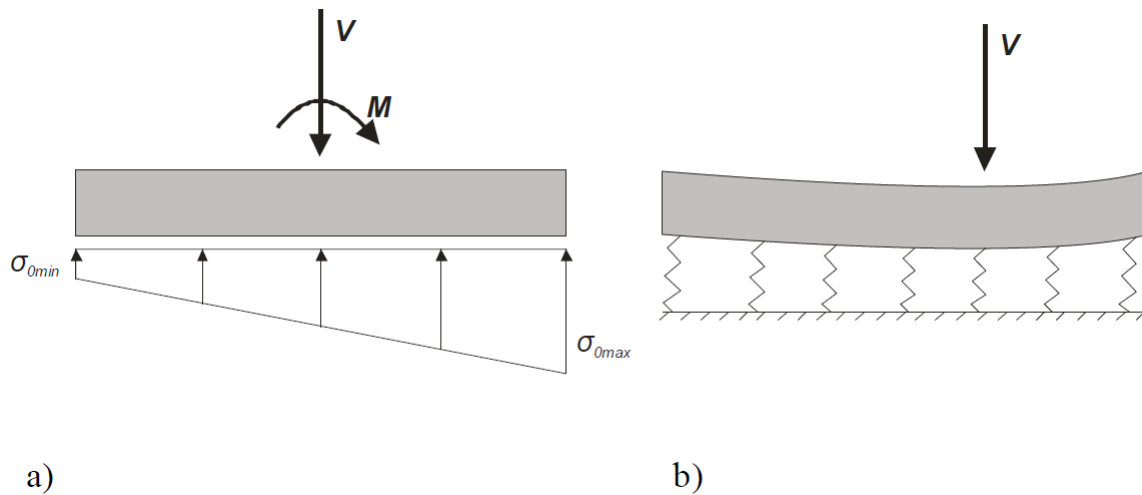


Figure 2.6: a) Model assuming linear soil pressure distribution; b) Model based on the subgrade reaction modulus. From Maunu (2006)

Lastly, Maunu (2006) describes the soil pressure distribution under a rigid foundation for a small applied load, as well as for a load that causes plasticity of soil as shown in Figure 2.7. Maunu (2006) concludes that the most critical part of the structure is the steel ring anchorage in the slab. Reinforcement surrounding the load transfer zone is highly stressed and consequently significant tensile cracking is encountered in this region, nonetheless, minor flexural cracking occurred and no global shear cracking was witnessed by Maunu (2006).

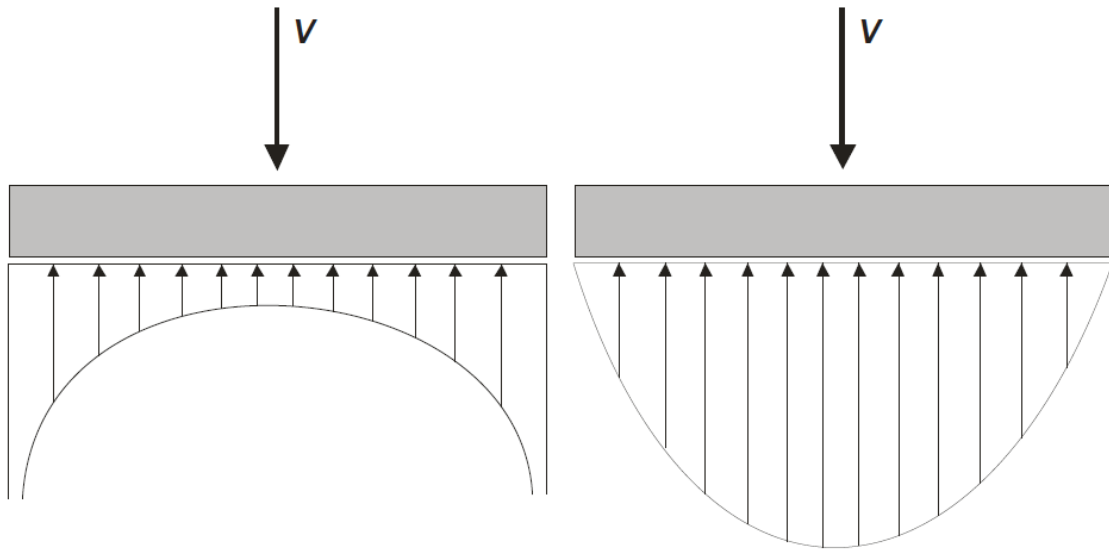


Figure 2.7: Soil pressure distribution under a rigid foundation: a) Small applied vertical load  $V$ ; b) Redistribution after soil plasticizing. Adapted from Maunu (2006)

### 2.2.2 John Corbett Nicholson (2011)

Nicholson (2011) carried out a study on The Design of Wind Turbine Tower and Foundation Systems Optimisation. The research utilised Microsoft Excel's Optimisation capabilities in the design of wind turbine foundation and towers. The study also compared the benefit of considering the design of the foundation and tower as an integral system as opposed to designing them independently. To achieve the research outcomes, it was necessary to collect information on the design requirements and parameter values of the wind turbine and foundation. A list of information that was deemed relevant to the study is shown below.

- Maximum deflection at the tower top is limited to 1.25% of the tower height in order to avoid excessive motion (Serviceability Limit State).
- Maximum rotation at the tower top is limited to 5 degrees in order to avoid interference between the turbine blade and the tower.
- Settlement of the foundation is not considered in design as the contact pressure on the soil from the vertical loads are low (50 kPa to 75 kPa).
- Factor of Safety against bearing capacity failure and maximum pressure on the soil is typically from 2 to 3.
- Minimum Values for Rotational and Horizontal Stiffness of the foundation are 50 GN-m/rad and 1000 MN/m respectively.
- For utility scale turbines, operating speeds typically range from 14 to 31.4 rpm (0.23-0.52 Hz) for the smaller turbines and from 6.5 to 17.7 rpm (0.1-0.3 Hz) for larger turbines.



Nicholson concluded, amongst other findings, that considering the tower and foundation as an integral system results in a more expensive design, yet failure to do so may yield inadequate results. He also concluded that, based on the optimisation parameters calculated, the natural frequency controls the tower design and the bearing capacity controls the foundation design. Finally, he added that relaxing or tightening the limit on the natural frequency of the tower will result in the greatest benefit or penalty, respectively on the optimum solution.

### 2.2.3 Henrik Svensson (2010)

Svensson (2010) conducted a study on the design of wind turbine foundations based on three case studies. The case studies involved the design of a foundation for three different founding conditions which could be categorised as strong and stiff soil (gravity spread foundation), 20 m clay layer on top of strong bedrock (end-bearing pile foundation used) and a clay soil with a considerable depth (piled-raft foundation used). It is notable that Svensson used DNV/Riso (2002) (Section 2.2.7) for the geotechnical design which involves sizing of the foundation. Svensson employs beam theory to carry out the structural design of the foundation with regard to the flexural and shear reinforcement according to Eurocode-2 (2004). Fatigue and crack control calculations are also included in the study.

Svensson concluded that foundations on stiff soil were cheaper and easier to construct than on softer clayey soils. The recommended further work from his study is the development of a non-linear 3D model in support of the research, as this research was limited to only linear 2D models.

### 2.2.4 Andrew Way (2014)

Way (2014) carried out a study on the design and material costs of tall wind turbine towers in South Africa. Although the primary focus of his study is on the structural design and costing of various designs of tall wind turbine towers, insight in wind loading on wind turbines is developed and used in FE-Analysis. Way also reports on foundations for wind turbines specifically for South African conditions. His findings indicate that, for the chosen design assumptions; foundations for concrete and hybrid towers are less material intensive and thus cheaper than the ones for steel towers. With regard to the reinforcement design, Way concluded that the reinforcement in the foundation was far below the minimum requirement as stipulated by the Eurocode-2 (2004). Thus according to Way the amount of reinforcement required in the foundation was nominal.

### 2.2.5 Byron Mawer (2015)

Mawer (2015) carried out a study entitled "An Introduction to Geotechnical Design of South African Wind Turbine Gravity Foundations". The focus of his research is built on three representative sites from each of the major wind development corridors and using them as practical examples. Soil properties and site investigation data gathered from the three sites namely the Western Cape, Eastern Cape and Karoo sites are used in the development and design for foundations for each respective site. The locations of the wind farms are shown in Figure 2.8

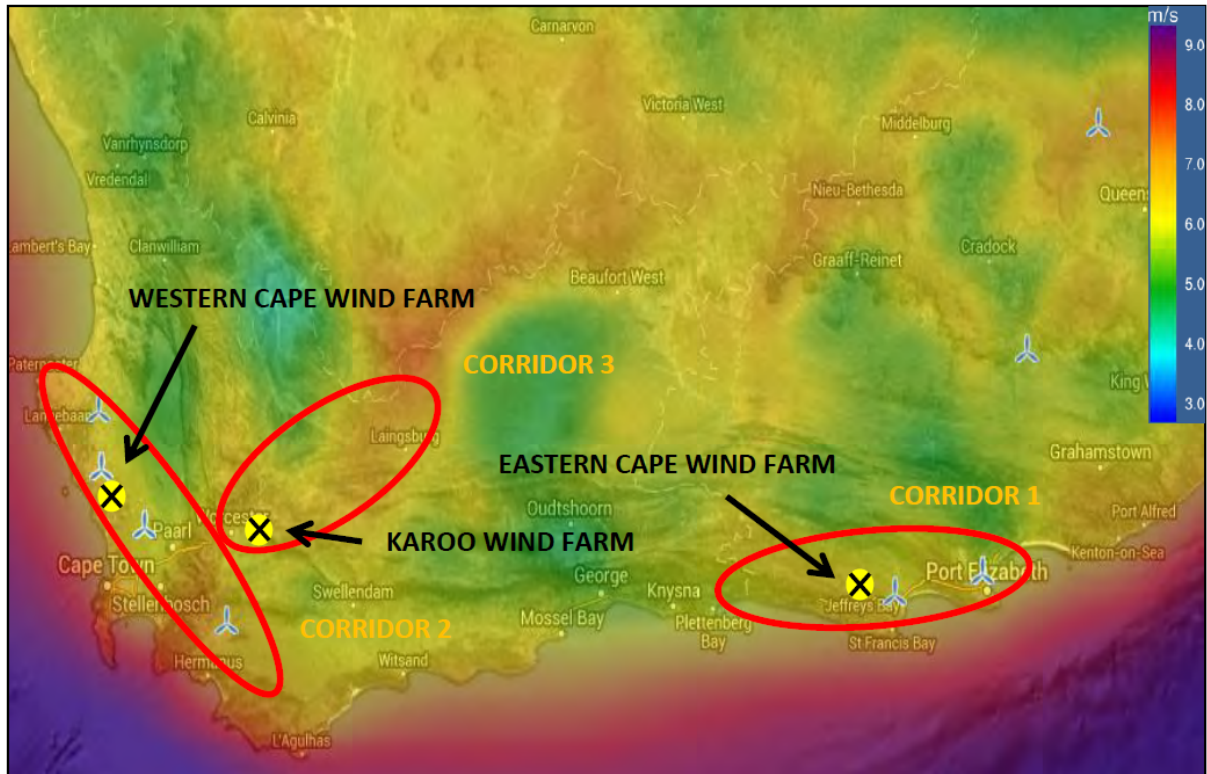


Figure 2.8: Wind Corridor overlain on hybrid topographical map with wind speed. Adapted from Mawer (2015)

Mawer carried out comprehensive research prior to his designs and the information specific to South African soils characteristics is used.

The foundations designed by Mawer are considered to be conservative, and could be optimised. Specific parameters include:

- The eccentricity  $e$  as shown in Figure 2.9 is dependent on the radius of the foundation. However, it is not clear how Mawer increased the radius of the foundation in order to limit  $e < 0.3\text{Radius}$  without recalculating the vertical load that caused by the change in radius. This is a conservative approach to design
- Gapping is limited to 0% for all ULS load cases. This results in conservative designs, as opposed to limiting the gapping only for SLS load cases. Gapping is defined as the lack of contact between the base of the foundation and the underlying soil as a result of a push over moment.
- The sizing of the foundation (geotechnical design) does not include the influence of the backfill as an additional vertical load against overturning.

An example of the conservative design approach is shown in the list below as actual values reported in the thesis for the Eastern Cape foundation design with load applied. The allowable bearing pressure is approximately 6 times the actual bearing load applied.

- Ultimate bearing pressure is calculated as 3803.9 kPa

- Allowable bearing pressure is calculated as 1270 kPa (Factor of Safety = 3)
- Calculated bearing pressure (load on the soil) is 215.97 kPa

### 2.2.6 IEC 61400

IEC 61400 is the international standard for wind turbine design. The document outlines the minimum design requirements for wind turbines and is not intended for use as a complete design specification or instruction manual. There is limited information on the design of wind turbine foundations.

### 2.2.7 Guidelines for Design of Wind Turbines - DNV/RISO

DNV/Riso (2002) is a comprehensive document that can be used as a tool to design wind turbine foundations. Chapter 8 of the DNV/Riso (2002) gives information specific to wind turbine foundations with recommendations on the design of gravity based foundations and piled foundations. DNV/Riso (2002) states that soil investigation should provide soil data needed for a detail design for a particular structure. The soil investigation is divided into three parts namely geological studies, geophysical surveys and geotechnical investigations.

The geological study is needed to establish the basis for site selection and extent of the site investigation. Thereafter the geophysical survey is used to get an understanding of the soil stratification specific to the site. Finally, geotechnical investigations are needed to obtain soil parameters for each soil layer by either soil sampling for laboratory testing or in-situ testing of soil. The investigation is presented as a geotechnical report and it is recommend that a geotechnical report should contain sufficient information about the site and its soil in order to allow for design of the foundation with regard to

- Bearing capacity
- Stability against sliding
- Settlement
- Foundation stiffness
- Need for possible drainage
- Static and Dynamic coefficients of compressibility
- Sensitivity to dynamic loading

The DNV/Riso (2002) was used to understand the design procedure of circular gravity based foundation. To this regard calculations relevant to this study have been focused on and reported in the following subsections.

**Bearing Capacity:** For a gravity based foundation the moments, vertical and lateral forces at the top of the foundation are combined to form resultant forces in the horizontal (H) and vertical (V) direction at the foundation soil interface as shown in Figure 2.9.

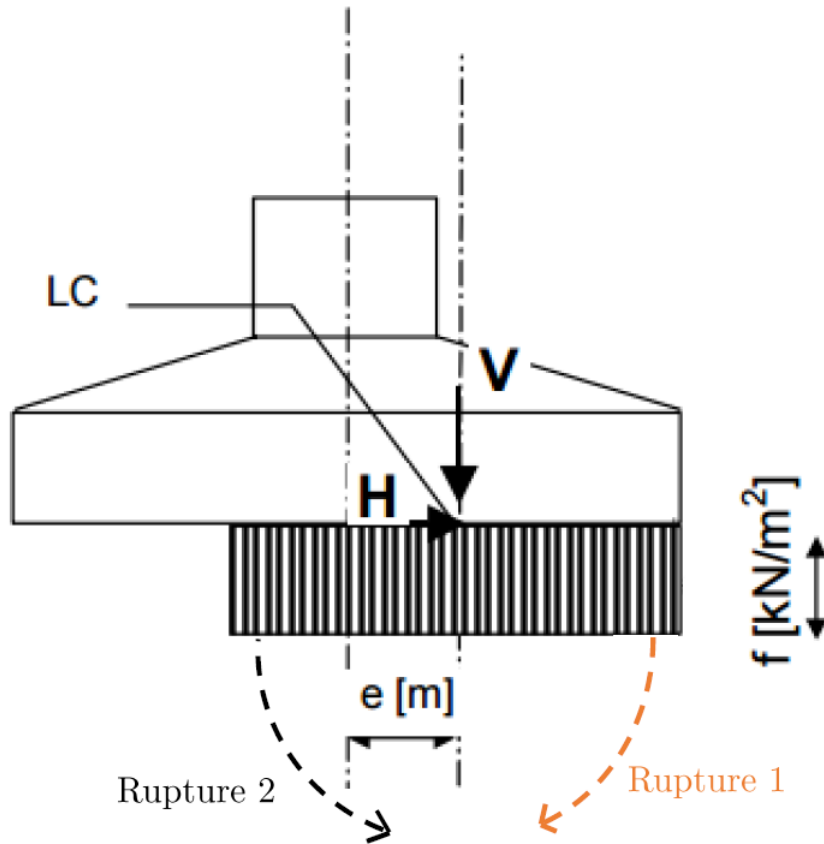


Figure 2.9: Loading of foundation under idealized conditions (DNV/Riso, 2002)

The foundation soil interface is an area with a load center LC where the resultant forces intersect and implies an eccentricity  $e$  of the vertical force relative to the center of the foundation. The effective foundation area with load center LC is used for bearing capacity calculations. For a circular and octagonal footing the effective area is marked out as shown in Figure 2.10.

Where

$$A_{eff} = 2 * [R^2 \arccos(\frac{e}{R}) - e\sqrt{R^2 - e^2}] \quad (2.1)$$

with major axis

$$b_e = 2(R - e) \quad (2.2)$$

and

$$l_e = 2R\sqrt{1 - (1 - \frac{b}{2R})^2} \quad (2.3)$$

$$l_{eff} = \sqrt{A_{eff} \frac{l_e}{b_e}} \quad (2.4)$$

$$b_{eff} = \frac{l_{eff}}{l_e} b_e \quad (2.5)$$

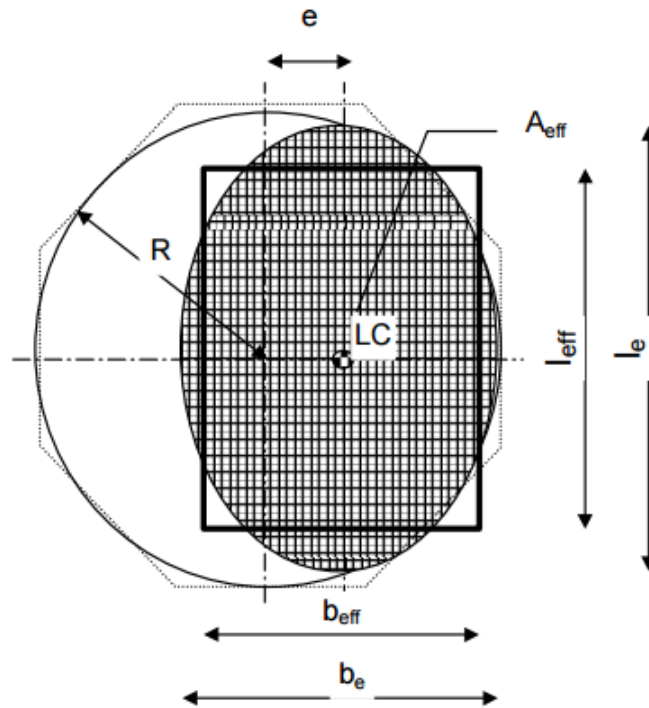


Figure 2.10: Circular and octagonal footing with effective foundation area marked out (DNV/Riso, 2002)

**Stiffness** The founding material has a finite stiffness and thus it cannot be modelled as a rigid solid, i.e. the foundation structure cannot be assumed to have a fixed lower boundary. According to the (DNV/Riso, 2002) the natural frequency is reduced by up to 5% when the fixed boundary condition of the foundation is replaced by a realistic finite foundation stiffness.

In order to model finite stiffness, nonlinear springs should be used, because the soil behavior is nonlinear. However, it is also common to apply linear spring stiffness. Alternatively, the shear modulus of the soil,  $G$  is also used. The equivalent shear modulus  $G$  relates to the initial small strain shear modulus as a function of the shear strain. The shear modulus can be used to calculate the elastic modulus of the soil given the Poisson's ratio.

According to DNV/Riso (2002), induced vibrations by wind loading on the turbine structure are of such a nature that the stiffness determined using "static" load testing is representative of the dynamic stiffness required for structural analysis.

**Resistance of Soil** Although sliding of the foundation is seldom a governing criteria for the design, DNV/RISO stipulates the following requirements for a wind turbine foundation in order to resist horizontal loading:

$$H < A_{eff}c + V \tan(\phi) \quad (2.6)$$

where  $c$  and  $\phi$  are the shear strength and friction angle of the soil respectively and it must also be verified that

$$\frac{H}{V} < 0.4 \quad (2.7)$$

**Pile-supported foundation** Pile foundations consist of one or more piles transferring load from the superstructure to be absorbed by the soil through axial and lateral pile resistance. For design of piles it is common to disregard the possible interaction between the axial pile resistance and the lateral pile resistance due to the argument that the soil near the surface of the soil determines the lateral resistance with minimum contribution to the axial resistance. Figure 2.11 shows the displacements and reaction for a single loaded pile.

The axial pile resistance is a combination of accumulated skin resistance and the tip resistance of the pile or pile group. The DNV/RISO presents equations to calculate the skin friction and tip resistance for piles in cohesive and granular soils. Methods to calculate the tip resistance for both cohesionless and cohesive soils are also given in the DNV/RISO.

For the design of piles, it is important to also consider the installation procedures, as the stress history during pile installation contributes significantly to the fatigue loading and needs to be taken into consideration during design. Another important consideration that needs to be accounted for in the design of piled foundation system is the effect of the pile cap on the foundation stiffness. According to a Australian based company CMW (2015), the pile cap has a significant contribution to the foundation stiffness and it is excessively conservative to ignore its contribution when designing wind turbine foundations supported by piles. The company concluded that, when the pile cap interaction is considered in the design, a piled foundation system becomes cheaper than a gravity based foundation system for Australian conditions.

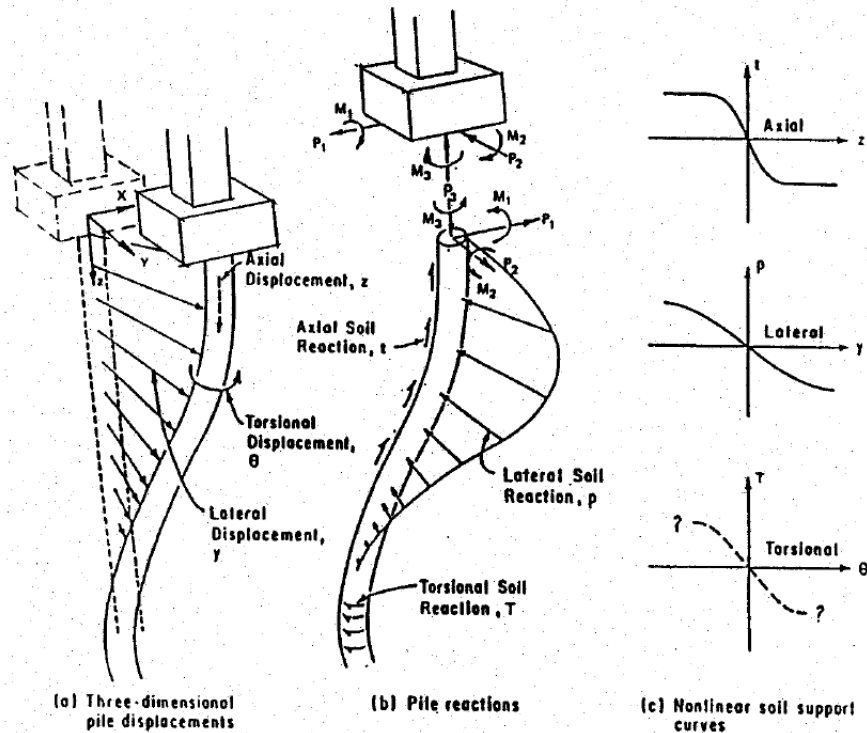


Figure 2.11: Single loaded pile displacement and reactions (DNV/Riso, 2002)

### 2.2.8 Vestas Documentation

Vestas; a Danish manufacturer, seller, installer, and servicer of wind turbines, is the only global energy company dedicated exclusively to wind energy. It was founded in 1945. A considerable number of wind turbines in South Africa have been supplied by the company and their tower design will be used in this study.

Although most of the information supplied by wind turbine manufacturers is proprietary information intended for the client, the information shared in this section was readily available on the internet.

**Foundation Loading Document** The foundation loading document supplied contains load cases for design consideration. The loads are applied at the top of the wind turbine foundation. The foundation design is required to size the foundation as this is usually site dependent. The foundation loads are defined in 3 main categories namely extreme load for normal load cases, extreme load for abnormal load cases and extreme load for normal operation. Fatigue loads are also supplied in terms of a Rain Flow spectrum or Markov Matrices. Rotational and Lateral stiffness requirements for the foundation are also prescribed.

**Description of Standard Gravity Anchor Foundations** This document depicts the reinforcement layout requirements for a gravity base foundation in detail. As mentioned in literature, this is the most critical aspect of the structural design as there are concentrated forces at tower to foundation connection. Figures 2.12 to 2.14 show extracts from the document depicting detailed instructions of how to place the reinforcement steel.

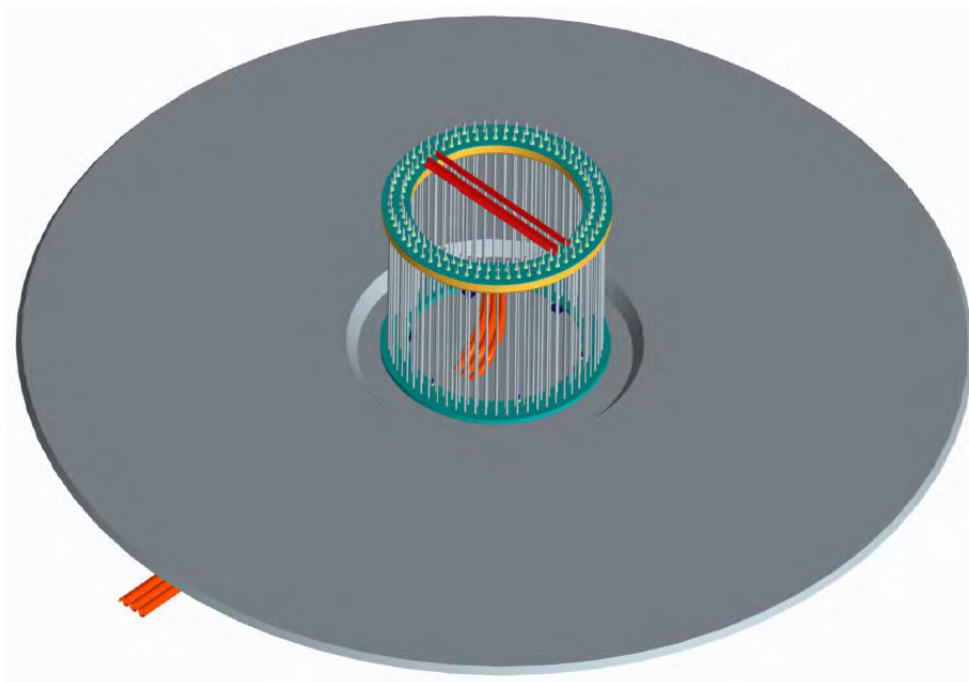


Figure 2.12: Placement of Anchoring Cage (Vestas)

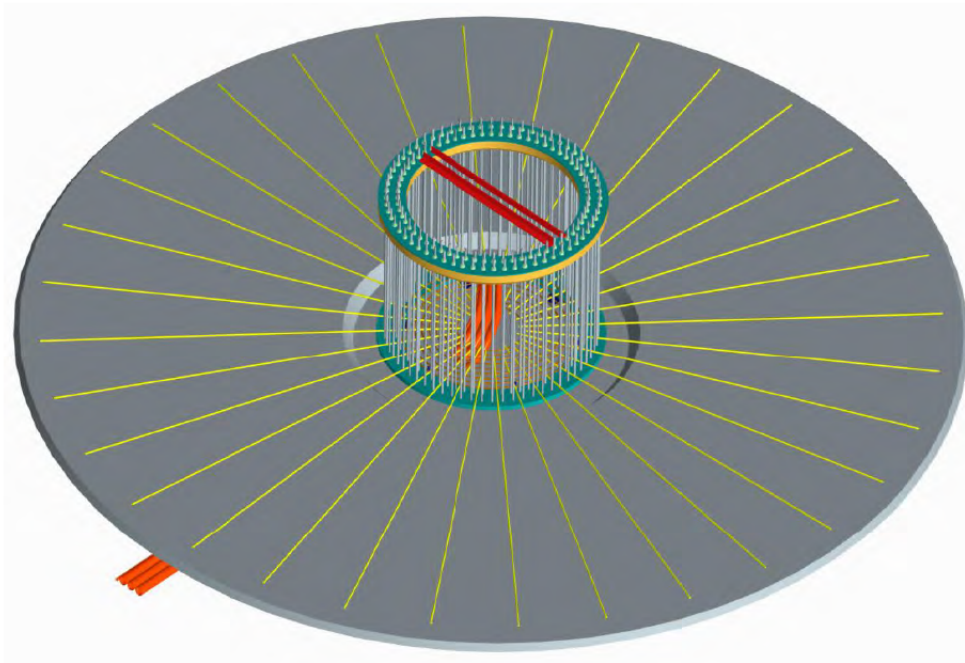


Figure 2.13: Steel Placement Initial (Vestas)

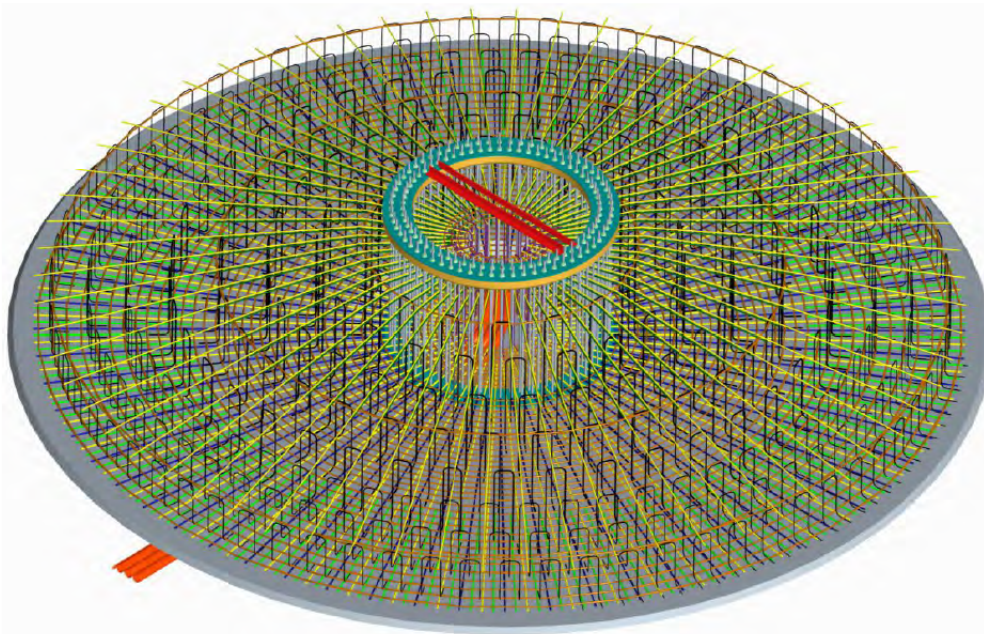


Figure 2.14: Steel Placement Final (Vestas)

The vestas specification standardises the design of gravity foundations. However it limits the foundation designer's ability to be creative. It also prescribes fixed constraints, for example the height of the anchoring cage is fixed, consequently the foundation designer cannot design a foundation shallower than the height of the cage.

It is important to note that this subsection reported on the documentation of Vestas only and this does not necessary hold for all wind turbine suppliers. However, it gave valuable insight in to the practical aspect of wind turbine design in South Africa (Vestas).



### 2.2.9 Discussion and Summary

There are two main considerations required in the design of gravity based wind turbine foundations. Firstly, the geotechnical design which involves the sizing of the foundation radius and depth. Secondly, the structural design which deals with the reinforcement layout and material behaviour of the foundation in terms of cracking, crushing or durability constraints.

Most of the literature reviewed highlights that the size of the foundation is governed by the bearing capacity of the soil for a given load case ((Way, 2014), (DNV/Riso, 2002), (Maunu, 2006) and (Mawer, 2015)). The reinforcement is governed by the connection type or the transfer of loads from the tower to the foundation. It should be noted that some authors, namely Way (2014) and Mawer (2015), did not consider the transfer of the load from tower to the foundation and did not highlight the importance of the connection type or the need for intricate steel reinforcement in this zone. This consideration has in the case of Vestas been dealt with by the wind turbine supplier as stated in Vestas (2011a).

The structural steel reinforcement design noted in literature is based on beam theory ((Svensson, 2010),(Way, 2014), (Maunu, 2006)), the general procedure followed being the establishment of a typical bending moment diagram. The area of steel required is calculated for the maximum bending moment along the bending moment diagram. In the research described here, the beam theory method is deemed conservative due to the following considerations:

- The foundation is represented as a simply supported beam in order to approximate the bending moment diagram whereas the base is founded on soil that offers vertical displacement resistance along the entirety of the foundation base.
- The typical depth of the foundation ranges from 2.7 m to 3.5 m. It is postulated that the behaviour of the foundation is not purely flexural but a combination of flexural and shear resistance. Maunu (2006) also adds that no flexural cracks were identified in the research conducted.

Soil modelling is complex, let alone modelling soil-structure interaction. The literature reviewed on FE-modelling of wind turbine foundations is characterised by the modelling of the soil as springs, the modelling of just the foundation embedded in a linear elastic soil material model or just the modelling of the tower with a fixed foundation support. No literature was found on the effect of cyclic loading of the wind turbine foundation on the soil, or the modelling of the wind turbine foundation embedded in a non-linear material model with the tower connected to the foundation. The aforementioned will be investigated in this study.

## Chapter 3

# Concrete Mix Optimisation

### 3.1 Introduction

A concrete mix design involves the proportioning of construction material to create a paste which can be placed to form a particular concrete structure. The construction materials can be categorised into four main categories namely binder (cement), sand (fine aggregate), stone (coarse aggregate) and water. The proportioning and selection of these materials is dependent on the intended use of the concrete. When designing a concrete mix, numerous considerations need to be taken into account including but not limited to: location and availability of raw materials, transport costs, strength of concrete, placement method and setting time. According to van Mier (1997) there are various scales of observation that can be considered when studying materials and structures. van Mier (1997) outlines the aforementioned scale of observation from the atomic structure of observation to large-scale buildings and civil engineering structures as shown in Figure 3.1.

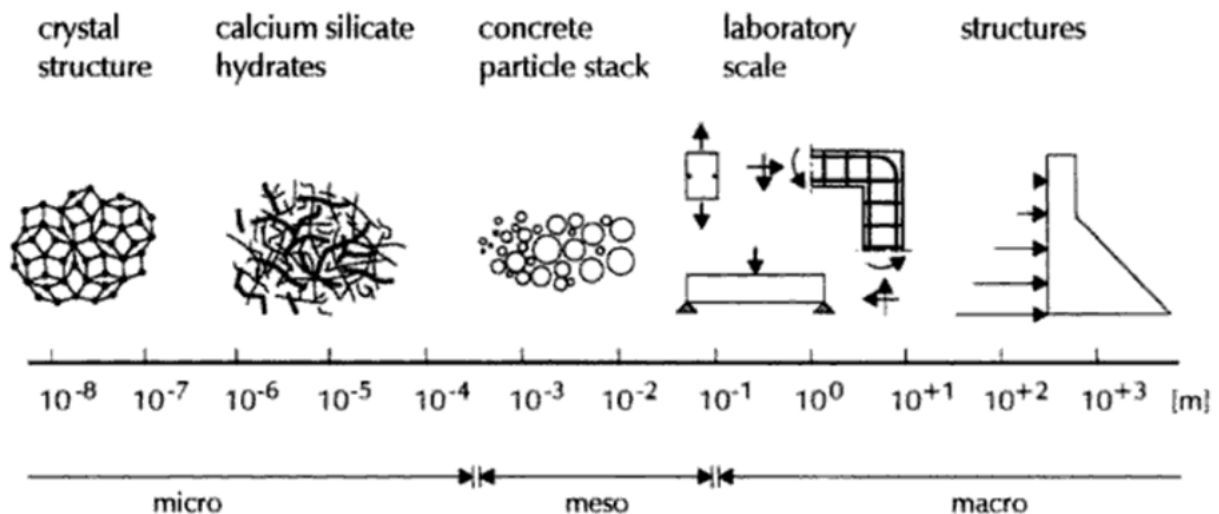


Figure 3.1: Exemplifying the various scales of observation for Civil Engineering Structures (van Mier, 1997)

The optimisation of a reference concrete mix design towards reducing the water required for the construction of a wind turbine foundation is investigated. This investigation is

performed on a "meso" scale. A micro scale optimisation would involve using special admixtures like super plasticisers which are already currently being used in South Africa. Specifically the reference mix used in the investigation included a High Range Water Reducer. After much consideration of various methods which can be used to reduce the water required in the mix, the conclusion was reached to increase the density of concrete towards reducing the required water per foundation. Increase in concrete density results in the reduction of the concrete volume required for each footing and consequently a reduction in the water required per footing. It is important to note that the main purpose of the concrete in the footing is to act as a counter weight to resist the moment induced at the foot of the tower. Thus, reducing the thickness of the concrete whilst maintaining the same radius and weight of the footing will offer the same structural resistance as the reference design. The reference mix design was obtained from the mix used on a wind farm in Nojoli (South Africa).

A comparison was drawn between the aforementioned reference mix (Mix 1) and the optimised mix (Mix 2). The comparison was based on the following criteria :

- Workability
- Setting time
- Compressive and tensile strength
- Coefficient of the thermal expansion
- Water content
- Drying Shrinkage
- Density of hardened concrete

This chapter includes a motivation which serves to outline the need for optimising concrete footings for wind turbines. Thereafter it gives a report of the experimental tests carried out and the results obtained. In conclusion the chapter discusses the results on a comparative basis.

## 3.2 Motivation

There are several water requirements on a wind turbine construction site. The main water requirement is the water required for the concrete mix. Water is also required to construct and maintain the gravel access roads. This is because most wind farms are located in remote areas which require the development of access (gravel) roads in order to allow for delivery trucks to gain access to the site location.

Currently in South Africa and specifically in the Western Cape, the water levels in the dams have reached very low levels. This has led the local government to implement water restrictions. Unmindful use of water might leave the people of South Africa in a very precarious position. During a site visit to Loeriesfontein wind farm, it was learnt that efforts had been made to reduce the water required in concrete mixes by utilising water reducing admixtures. Sustainable development should not just be limited to the end product, in this case being the renewable energy. A cradle to the grave

perspective is required in order to ensure that the overall (environmental and social) cost of a development does not exceed the the overall benefits.

Globally, concrete is the second most consumed construction material next to water. Concrete is the most widely used structural material, exceeding the use of steel by orders of magnitude. This is because it is usually the cheapest and most readily available material. The benefits of concrete include minimum maintenance requirement, fire resistance, resistance to cyclic loading and good composite action with (reinforcement) steel. The optimisation solution investigated in this study does not only reduce the water requirements but also reduces the concrete requirement per wind turbine footing. This is perceived in a positive light with regard to sustainability because of the reduction in carbon footprint. Reducing concrete volume requirements inherently reduces the cement requirement per footing. The production cement (clinker) involves the preheating of limestone and clay (calcining) that releases carbon dioxide into the atmosphere. This has detrimental effects to the environment as release of such gases, normally categorised as green house gases has been the main cause of climate change. Globally, efforts are being made to reduce green house gas emission with an example directly related to this study being wind energy, categorized as renewable, clean or green energy. Observations of the challenges faced on construction sites and restorative efforts by the government lead to the need to investigate ways in which water requirements can be reduced.

Increased concrete density is achieved by using an aggregate of a greater density than the conventional stone aggregate used. High density aggregate is usually iron ore based with the most commonly used aggregate being Barytes, Magnetite, Ilmenite and Galena (Alexander, 2009). With regard to the availability of the iron ore based aggregate; South Africa has one of the largest iron ore reserves in the world. In the Western Cape, ArcelorMittal has a steel manufacturing plant at Saldanha where they receive iron ore via rail. Their plant only uses what they regard as "coarse aggregate" (approximately greater than 19mm). The "fine aggregate"(approximately less than 19mm) is sent back via rail to the Kumba iron ore mine in Sishen. It should be mentioned that by civil engineering definition, their "fine aggregate" is regarded as coarse aggregate (greater than 4.75mm) in concrete mix design (Alexander, 2009). A sample of the aggregate which is not used for steel production at ArcelorMittal was obtained for the purposes of this study.

### 3.3 Design

This section reports on the procedure followed during the design of the concrete mixes used in the investigation. Two mixes are used.

#### 3.3.1 Conceptual

The reference mix is a modification of a mix design acquired as proprietary information. The mix is changed due to the lack of availability of materials. The cement prescribed by the acquired mix is a CEM I 52.5 N cement which is unfortunately unavailable in the Western Cape, hence a CEM II 52.5 N cement is used. The main difference between the two cements is the extender content of the cement. CEM I 52.5 N has less than 5% cement extenders whereas CEM II 52.5 N has between 5% to 35% cement extenders.

The second modification is the stone size, due to the fact that the investigation is primarily based on coarse aggregate replacement. The grading of the aggregate prescribed by the

reference mix differ significantly from the grading of the iron ore sample obtained. In order to establish a comparative study purely based on the density of the aggregate, the coarse aggregate grading prescribed in the reference mix is changed to match grading of the iron ore sample. Initially a 26.5 mm stone size was prescribed. However, due to the aforementioned, 13 mm stone size was used for the purposes of this study. Reducing the stone size would theoretically result in increasing the water requirement of the mix. However, due to the fact that the small stone size improved the packing, it was observed during trial mixes that the change in water requirements was insignificant. The sand content was thus adjusted accordingly to account for the change in stone size. Material properties of the aggregate were tested and compared prior to carrying out the mixes and results are reported in Section 3.5.1.

### 3.3.2 Detail

For the purposes of this study, Mix 1 refers to the reference mix which serves as the control mix with the conventional stone. Mix 2 refers to the optimised mix with 100% of the conventional stone replaced with iron ore. The mix proportions are tabulated in Table 3.1.

Table 3.1: Mix Design

Material	Mix 1	Mix 2
CEM II 52.5 N	245	246
Fly Ash	105	105
Stone	872	1457
Crusher Sand	560	561
Dune Sand	560	562
Water	206	206
OMEGA 134 (High Range Water Reducer)	5.1	6.3

All values in kg. Mix proportions for 1 m<sup>3</sup>

## 3.4 Tests

### 3.4.1 Workability

The required workability or fluidity of concrete is normally dependent on the construction method employed, specifically how the concrete will be placed. For wind turbine foundations the workability is very important. Due to the congestion of the steel in the foundation, especially around the anchoring cage just below base of the tower, the concrete should be designed to minimise the risk of poor compaction. Figure 3.2 shows an example of the reinforcement steel in a typical wind turbine foundation.



Figure 3.2: Fixed Reinforcement Steel



Figure 3.3: Concrete Pouring Method

The selection of the stone (coarse aggregate) size is highly influenced by the steel congestion in the foundation. It is normally recommended to use large stone in concrete mix designs for large concrete elements in order to increase the dimensional stability of the mix as well as reduce the heat of hydration (Alexander, 2009). However, the governing

factor for the choice of stone size for wind turbine foundations is the steel spacing and thus self compacting concrete or concrete with a high slump is normally used. Considering the foundation geometry, the fresh concrete is typically placed by pumping it, in order to reach the full diameter without significant disturbance of the reinforcing steel cages. This requires mix adjustment to high flow-ability without segregation, to be pumpable. Due to the height of the foundation, high lateral pressure is induced at the foot of the foundation. Supporting props are placed and anchored against the interior of the excavations.

Typically, a wind turbine foundation requires a single pour of concrete ranging between 240 m<sup>3</sup> to 450 m<sup>3</sup> of concrete. This is usually done by having ready mix trucks delivering the concrete to a concrete pump that then pumps the concrete as shown in Figure 3.3. The concrete is then compacted using a poker vibrator.



Figure 3.4: Concrete Compaction

The reference mix prescribed a slump of 150 mm. A slump test was thus carried out in accordance with SANS-5862-1 (2006). This was the only workability test carried out with regard to the comparative study in this section. The slump also governed the trial mixes carried out and was used in acquiring an optimum super-plasticiser content required for the mix. A sensitivity analysis was carried and the results were plotted as shown in Figure 3.5. In this regard, it was established that the optimum super plasticiser required for the mix was approximately 1.8% of the binder content.

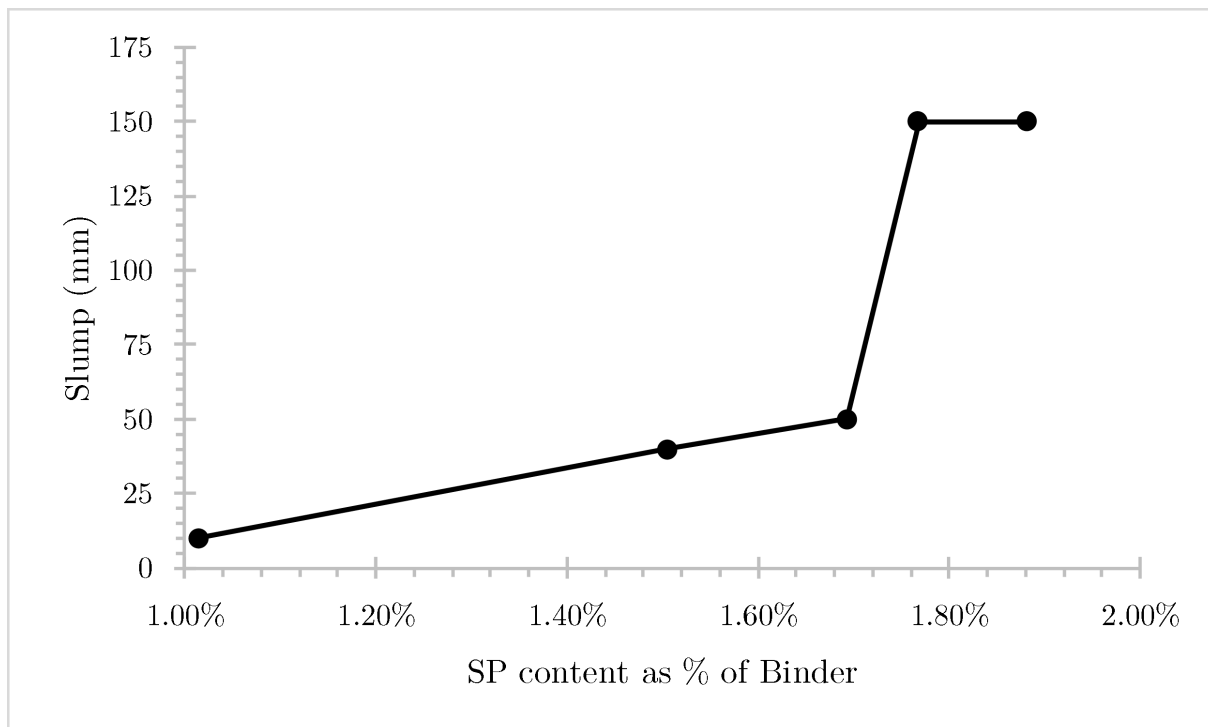


Figure 3.5: Super Plasticiser sensitivity analysis for Mix 1

### 3.4.2 Compressive Strength

The two mixes were tested for compressive strength at 7 days and 28 days after casting in accordance to SANS-5863 (2006). Figure 3.6 shows the test set up. The compressive strength of the wind turbine foundation concrete was prescribed as 35 MPa in the reference mix.

It is important note that

$$\text{target (average) strength} = \text{characteristic strength} + 1.64 * \text{standard deviation}$$

However, the test results reported are for 3 cubes only and do not suffice as a statistical base. Thus it does not accurately reflect the properties of the concrete. This was however accepted for this study because of the lack of sufficient iron ore sample aggregate to cast more concrete cube.

### 3.4.3 Tensile Strength

The tensile strength of the concrete was also tested using the cube splitting method as shown in Figure 3.6 in accordance with SANS-6253 (2006). It was observed in the FEA discussed in Chapter 5 that there are tensile forces induced in the concrete footing due to the moment and axial loading at the foot of the tower. The tensile strength of the concrete mixes was compared to more comprehensively investigate the mechanical properties of the mixes. Equation 3.1 is used to convert the maximum crushing force applied by the



machine to the tensile strength. The Eurocode-2 (2004) prescribes Equation 3.2 in order to convert the splitting force to the tensile strength of the concrete.

$$f_{sp} = \frac{2F}{\pi * l * d} \quad (3.1)$$

$$f_{ct} = 0.9f_{sp} \quad (3.2)$$

Where

**F** is the maximum load at failure

**l** is the loaded length of the specimen

**d** is the cross-sectional depth of the specimen

The average results of three samples is recorded and reported to the nearest 0.05 MPa.

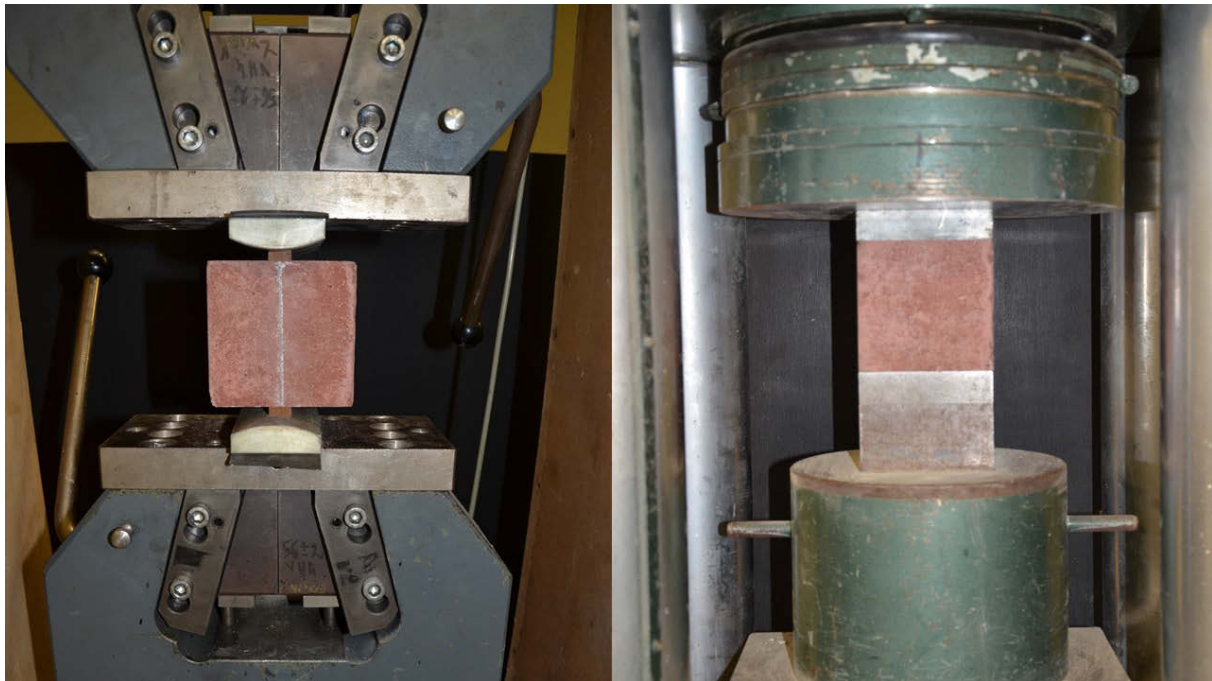


Figure 3.6: Tensile Splitting test (left) and Compressive Strength Test (Right) shown in the Zwick Z250 MTM and Contest 2MN MTM respectively

#### 3.4.4 Stiffness

For FEA the elastic modulus is required. The elastic modulus was tested 28 days after the cylindrical test specimens were cast in accordance with ASTM-C-469 (2014). The cylindrical specimens have a height of 200 mm and a diameter of 100 mm. 3 LVDTs are used to measure the elongation and contraction of the test specimens during the test, as shown in Figure 3.7. The gauge length is 70 mm.

The code prescribes a loading cycle with a nominal upper stress equal to 40% of the compressive strength of the concrete specimen. The specimen is loaded to the the nominal

upper stress value and unloaded. The loading and unloading process is repeated three times. Finally, the stress-strain curves for the third cycle are plotted and used to determine elastic modulus with Equation 3.3

$$E = \frac{S_2 - S_1}{\varepsilon_2 - \varepsilon_1} \quad (3.3)$$

Where

$E$  is the Chord Modulus of Elasticity

$S_2$  is the Stress corresponding to 40% of the ultimate load of the concrete

$S_1$  is the Stress corresponding to a small longitudinal strain of  $\varepsilon_1 = 0.00005$

$\varepsilon_2$  longitudinal strain produced by  $S_2$

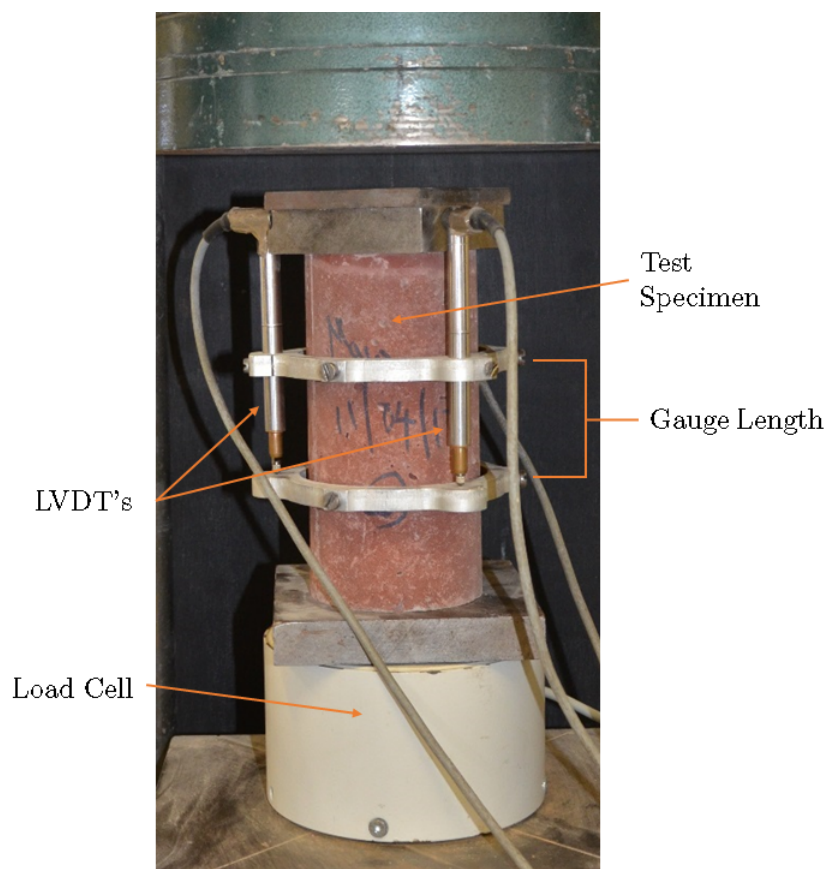


Figure 3.7: Secant Modulus of Elasticity Test Set Up

### 3.4.5 Drying Shrinkage

In normal strength concrete which experiences little autogenous shrinkage, the total measured shrinkage is dominated by drying shrinkage. Drying shrinkage is the shrinkage caused by moisture loss from concrete. For unrestrained concrete, drying shrinkage only results in a volumetric reduction in the structure. However, for most practical applications of concrete the structure is restrained (Alexander, 2009) (Eurocode-2, 2004).

In the case of the wind turbine foundation the reinforcement steel offers some degree of restraint, thus excessive shrinkage may result in shrinkage cracks which should be avoided specifically for wind turbine foundations due to their potential influence on vibrational stiffness, as well as deterioration processes. In order to address this concern, shrinkage tests were carried out to ensure that the optimised mix does not deviate significantly from the drying shrinkage of the reference mix. No standard code was followed for calculating the drying shrinkage of the mixes. However, a method not yet recognised by any standards was used. The apparatus required for the test were :

- Three 500x100x100mm beam moulds
- Vibrating table and trowel
- Shrinkage targets and high strength adhesive
- Mahr Marcator **Length Gauge** with 0.01 mm resolution

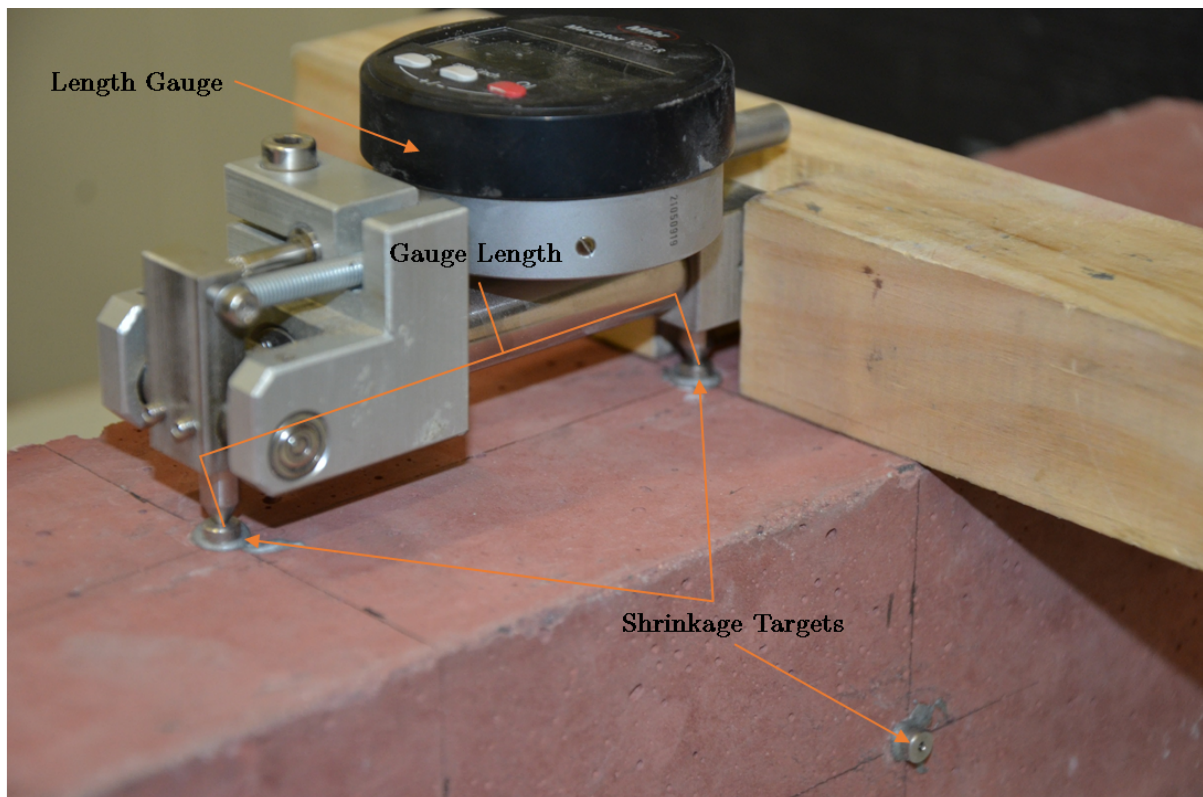


Figure 3.8: Drying Shrinkage Measurement Set Up

Figure 3.8 shows how the readings were taken using a length gauge which was accurate to 0.01 mm. The following procedure was followed to test the shrinkage of each concrete mix:

- The concrete mix was placed in the beam moulds, vibrated into place and surface troweled to a smooth finish.
- Beams were left in the laboratory to set and harden.

- The beams were de-moulded after 24 hours, in order to avoid the influence of temperature on the beams shrinkage, the beams were not placed in curing baths.
- The targets were cleaned and glued (using high strength adhesive) onto three sizes of the beam approximately 100 mm apart (gauge length). No targets were glued on to the casting side of the beam.
- After the glue had set, a reference reading was taken  $L_0$  (initial gauge length at time zero). The beams are then placed in a controlled environment 24°C and 65% humidity.
- Readings are taken on periodic times  $L_t$ .
- The total shrinkage at a specific time  $\varepsilon_T$  is the difference between the initial gauge length and the measured length at periodic times divided by the initial gauge length as shown in Equation 3.4.

$$\varepsilon_T = \frac{L_t - L_0}{L_0} \quad (3.4)$$

## 3.5 Results

### 3.5.1 Coarse Aggregate

Greywacke stone classified as 26.5 mm and 16 mm, available in the concrete laboratory at Stellenbosch University, is compared the iron ore sample supplied Arcelormittal in this section. The comparison is based on the aggregate grading, water absorption, relative density as well as the aggregate crushing value.

**Grading:** The sieve analysis for the coarse aggregate is carried out in accordance with SANS-201 (2008). Results are shown in Figure 3.9.

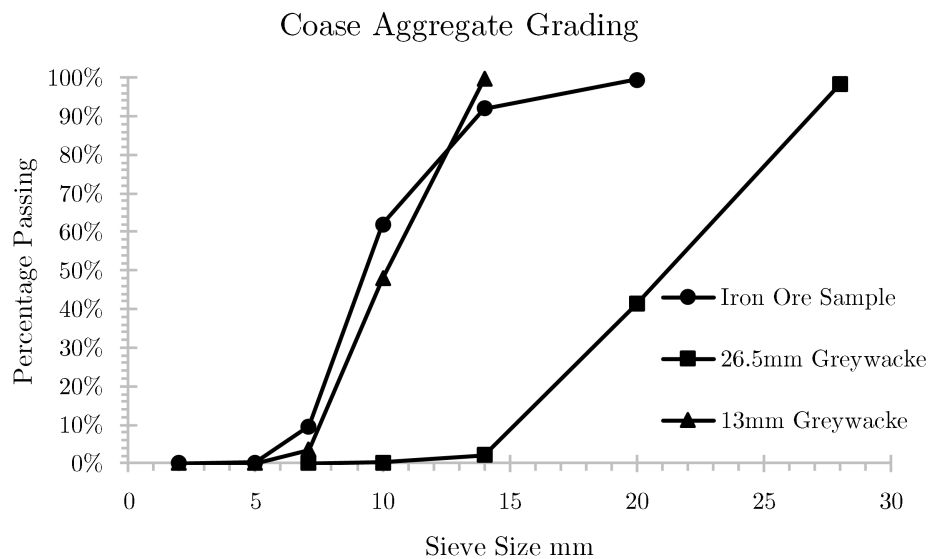


Figure 3.9: Sieve Analysis for Coarse Aggregate

**Relative Density** The relative densities of all the aggregates were tested in accordance to SANS-5844 (2014). This was to insure that the values of the relative densities used in the mix design calculation are specific to the actual materials used in the mix. The results are tabulated in Table 3.2.

Table 3.2: Relative Density

Material	RD
Iron Ore	5.23
Greywacke 26.5 mm	3.14
Greywacke 13 mm	2.98
Dune Sand	2.92
Crusher Dust	2.98

**Water Absorption** Water absorption of the coarse aggregates was tested in accordance with SANS-5844 (2014). The results are tabulated in Table 3.3

Table 3.3: Water Absorption

Material	%
Iron Ore	1.0
Greywacke 26.5 mm	0.5
Greywacke 13 mm	0.8

**Aggregate Crushing Value** The Aggregate Crushing Value (ACV) was calculated in accordance with SANS-3001-AG10 (2012). The 13 mm stone and iron ore mixes were tested and their ACV tabulated in Table 3.4.

Table 3.4: Aggregate Crushing Value

Material	%
Iron Ore	11.4
Greywacke 13 mm	13.3

### 3.5.2 Compressive Strength

The mean 28 day target (average) compressive strength for Mix 1 (reference mix) and Mix 2 (optimised mix) was 38.39 MPa and 41.75 MPa respectively. Both mean values are

greater than the 35 MPa target compressive strength. The results are shown in Figure 3.10. Appendix A gives a detailed report of compressive strength results for each specimen tested.

### 3.5.3 Tensile Strength

The tensile strength achieved for Mix 1 and Mix 2 was 3.93 MPa and 4.45 MPa respectively. Although there was no prescribed tensile strength this is acceptable as it is approximately 10% of the prescribed compression strength. Figure 3.11 shows sectional views of the two mixes after the splitting test. The aggregate to paste distribution was seen to be homogeneous and with an even distribution. Appendix A gives a detailed report of tensile strength results for each specimen tested.

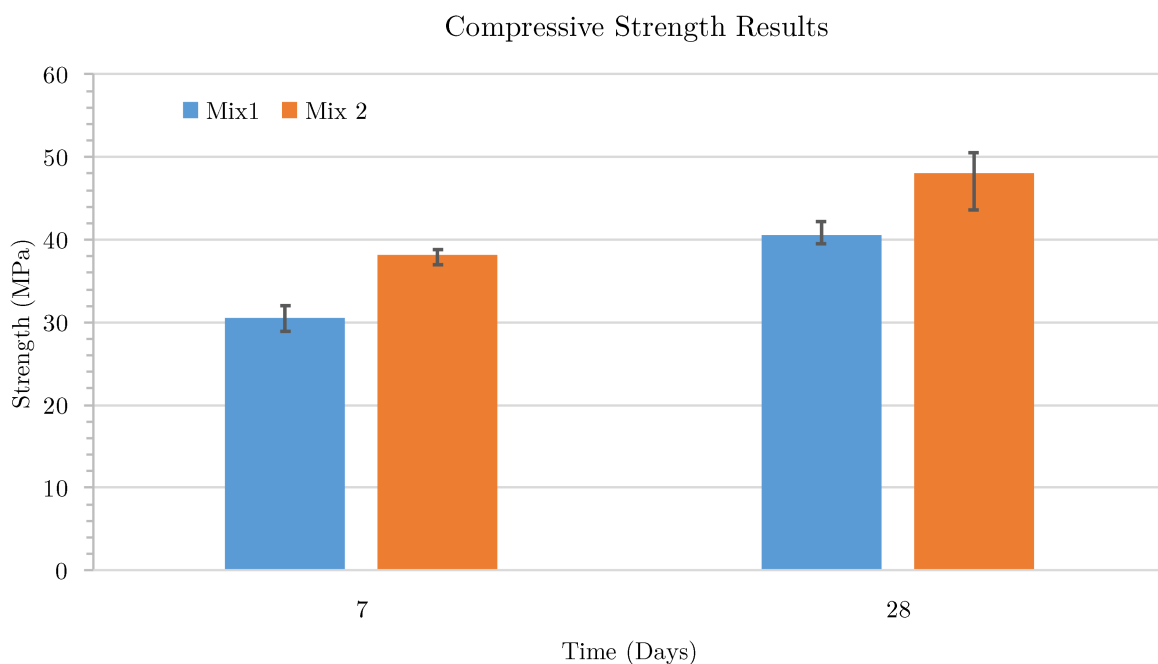


Figure 3.10: Compression Test Results



Figure 3.11: Sectional View of Mix 1 (left) and Mix 2 (right)

### 3.5.4 Stiffness

The elastic modulus achieved for Mix 1 and Mix 2 was 31.0 GPa and 42.06 GPa respectively. The original stress-strain curves plotted were not smooth although they were almost linear. This was due to the loading machine used which did not apply the load in small enough steps to offer a smooth stress-strain curve. To this regard trend-lines were plotted using the measured data to calculate the elastic modulus. The data plots as well as the trend-line are shown in Figure 3.12. Appendix A gives a detailed report of elastic modulus results for each specimen tested.

### 3.5.5 Drying Shrinkage

Figure 3.13 and Figure 3.14 show the shrinkage results plotted for each face of each beam for Mix 1 and Mix 2 respectively. The curves S1, S2 and S3 represent the 3 sides measured for each beam whilst the color coding distinguishes between the different beams. The average shrinkage is also plotted. Figure 3.15 shows the average shrinkage curves for the two mixes in question. Due to the variability of the shrinkage results it is difficult to conclude that the Mix 2 has a greater drying shrinkage than Mix 1 even though the average curve for Mix 2 is higher than the average curve for Mix 1 as shown in Figure 3.15. From Figure 3.15 there is no statistical evidence that can be used to conclude that indeed the shrinkage of Mix 2 is greater than that of Mix 1. This is due to the overlapping error bars in the figure. To this regard, the shrinkage performance for the two mixes is similar for all practical purposes.

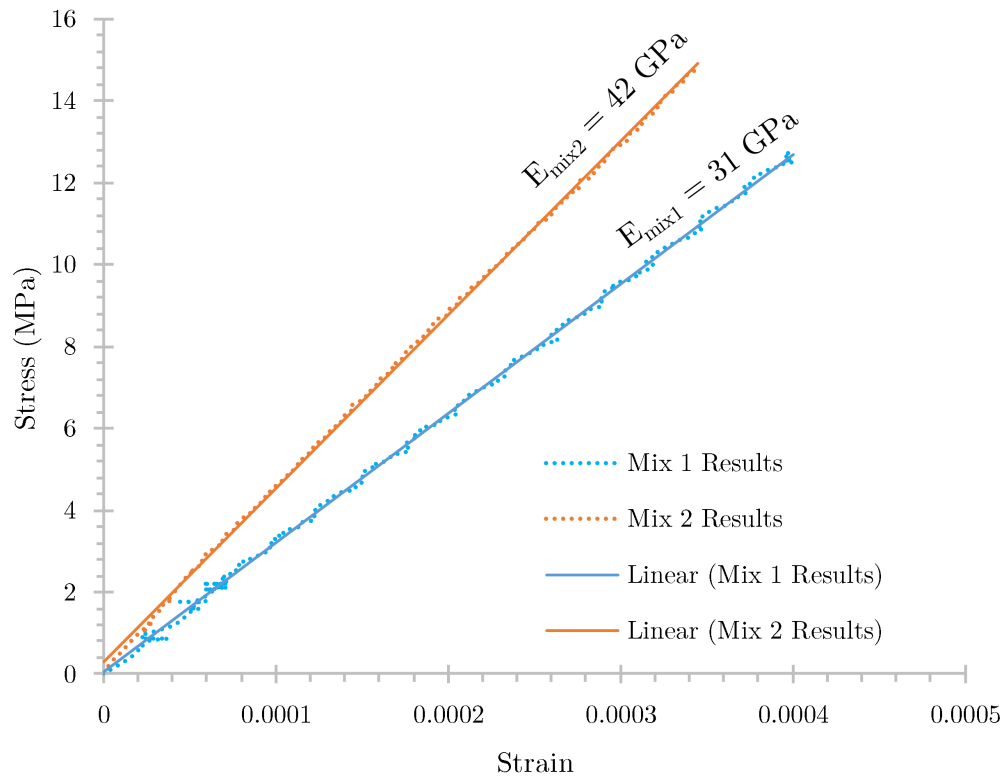


Figure 3.12: Compressive Stiffness Curves

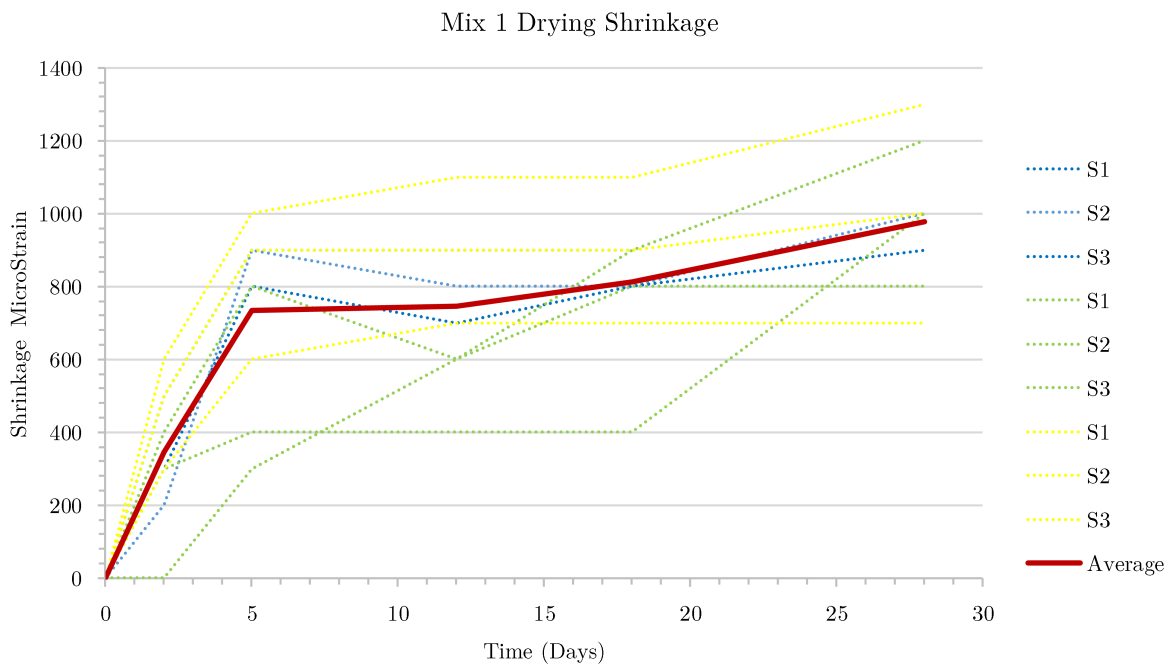


Figure 3.13: Reference Mix Drying Shrinkage Curves



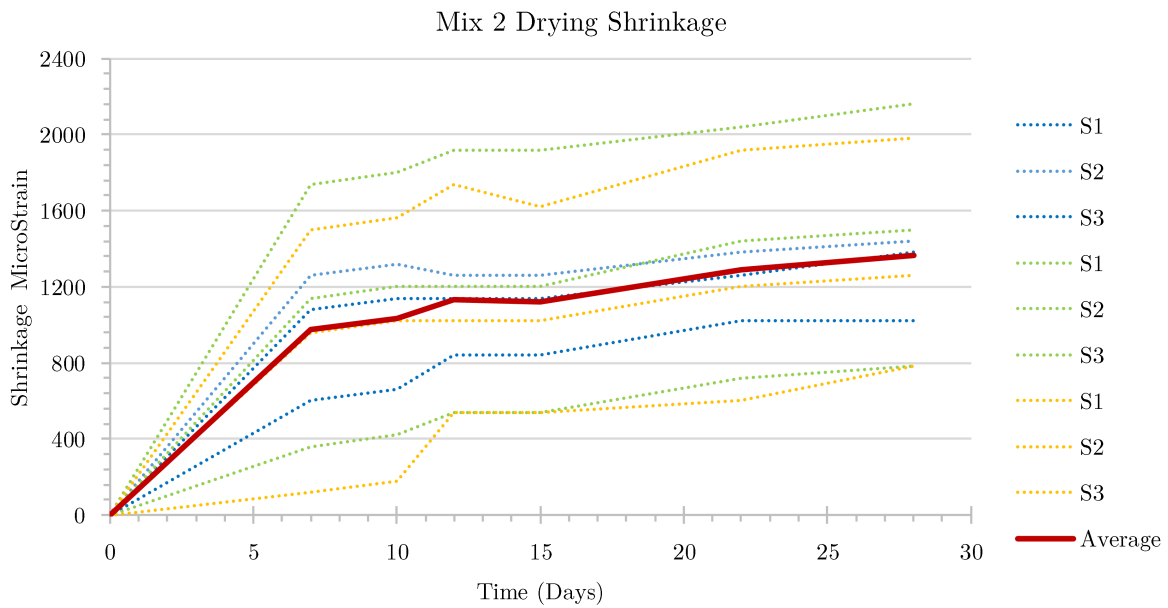


Figure 3.14: Iron Ore Mix Drying Shrinkage Curves

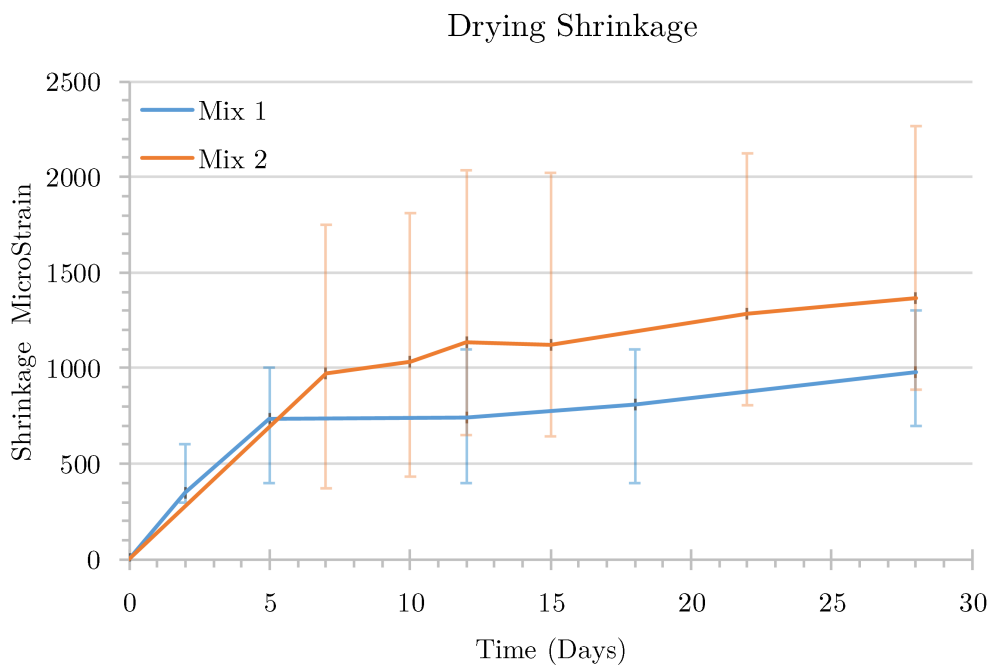


Figure 3.15: Drying Shrinkage Comparative Curves

### 3.5.6 Bleeding

No bleeding occurred with either mixes. This effect has been observed before (Alexander, 2009).

### 3.5.7 Hardened Concrete Density

It was calculated that there was a **25% increase** in density (mass) as a result of the replacement of coarse aggregate with iron ore. The characteristic concrete densities for Mix 1 and 2 are tabulated in Table 3.5.

Table 3.5: Hardened Concrete Density

Description	Density ( $\text{kg}/\text{m}^3$ )
Mix 1	2367
Mix 2	2973

## 3.6 Conclusion and Recommendations

In conclusion, coarse aggregate replacement towards reducing water requirements is a viable solution in terms of the mechanical properties of concrete. The optimised mix (Mix 2) performs better than the reference mix (Mix 1) with regard to strength and stiffness. The iron ore resulted in a 25% mass increase of the concrete. It is envisaged that 20% reduction in concrete used in the construction of a wind turbine foundation will be achieved by using iron ore as a coarse aggregate replacement.

# Chapter 4

## Foundation Design

### 4.1 Introduction

This chapter is intended to provide practising engineers with basic tools and an understanding of how to design wind turbine foundations for South African conditions based on the literature reviewed and industry survey. The sizing of the foundation based on assumed soil conditions and applied loading is presented in the geotechnical design in Section 4.3 as a worked example for the foundation design to be used in Chapter 5. The placement of reinforcement steel and specification of concrete are discussed as the structural design in Section 4.4.

### 4.2 Given Parameters

Although some assumptions are made with regard to the design, the soil parameters are meant to be representative of South African conditions, thus the data below was used. The data was based on an existing wind farm site investigation as reported by Mawer (2015). The soil parameters are tabulated in Table 4.1.

A Vestas 3 MW wind turbine tower is selected. It should be noted that turbine designs are regarded as proprietary information and not readily available. Partial design information on the 3 MW wind turbine is available online and reverse engineering is used together with assumptions in order to establish an acceptable tower design for modelling. The availability of information and the relevance of the turbine size for South African conditions governs the turbine selection. Currently, the turbine sizes range from 2-3 MW. Given the aforementioned information, a wind turbine foundation document, as defined in Section 2.2.8, was available for the V112-3.0 MW HH 119 m wind turbine. The load case used for the purpose of this design is tabulated in Table 4.2

Table 4.1: Soil Parameters

Description	Symbol	Characteristic Value
Bulk Density	$\gamma_{bulk}$	19.2 kN/m <sup>3</sup>
Saturated Density	$\gamma_{sat}$	21 kN/m <sup>3</sup>
Friction Angle	$\phi'$	31.5 degrees
Cohesion	$c'$	12 kPa

Table 4.2: Characteristic Extreme Load for Normal Load Cases

$M_{res}$	$M_z$	$F_{res}$	$F_z$
91100 kNm	-201.5 kNm	784 kN	5130 kN

Vestas (2011b)

$M_{res}$  : Extreme resulting bending moment at the top of the foundation stub

$M_z$  : Simultaneous torsion moment about the axis inline with the tower

$F_{res}$  : Simultaneous resulting shear force

$F_z$  : Simultaneous vertical force

### 4.3 Geotechnical Design

**1 Defined Foundation Geometry:** The generic foundation geometry for a gravity foundation is defined in Figure 4.1 and the specific values for the design to be references as the worked example are tabulated in Table 4.3.

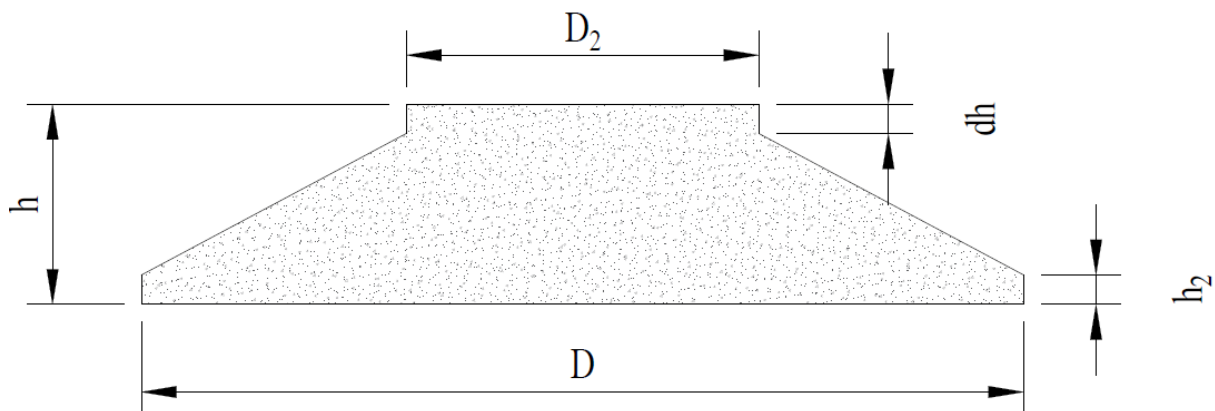


Figure 4.1: Generic foundation geometry (not to scale)

Table 4.3: Design 1 Geometry

Description	Symbol	Value
Base Diameter	$D$	14.74m
Stub Width	$D_2$	6.1m
Total Height	$h$	3.4m
Stub Height	$dh$	1m
Base Height	$h_2$	0.5m

**2 Calculate Vertical Loading:** Equation 4.1 is used to calculate the vertical load contribution by the concrete foundation given the dimension as defined in Figure 4.1. Likewise, the vertical load contribution of the soil directly on top of the foundation is calculated using Equation 4.2. The principle of both equations is multiplying the volume (in  $[\ ]$  brackets) with the unit weights ( $\gamma_s = 19.2kN/m^3$  and  $\gamma_c = 24kN/m^3$ ) of the soil and foundation respectively to equate it to a vertical load.

The weight of the soil above the foundation backfill is significant as shown in the following calculations, and should not be ignored in the design of the foundation unless the foundation will not be covered by soil, which will be a sub-optimal design.

$$V_{concrete} = \left[ \frac{\pi D^2}{4} h_2 + \frac{\pi D_2^2}{4} (h - h_2) + \frac{1}{2} \frac{\pi (D^2 - D_2^2)}{4} (h - h_2 - dh) \right] \gamma_c \quad (4.1)$$

$$V_{soil} = \left[ \frac{\pi (D^2 - D_2^2)}{4} dh + \frac{1}{2} \frac{\pi (D^2 - D_2^2)}{4} (h - h_2 - dh) \right] \gamma_s \quad (4.2)$$

Calculating the specific vertical load contribution for the foundation design tabulated in Table 4.3, the following vertical loads are obtained from Equations 4.1 and 4.2 (positive downward).

$$V_{concrete} = 7304 \text{ kN}$$

$$V_{soil} = 4689 \text{ kN}$$

The total vertical load ( $V_{design}$ ) to be used for the design of the foundation and to check the bearing capacity of the design is the summation of the tower vertical load ( $F_z = 5130kN$ ) prescribed in Table 4.2, and the vertical load contribution of the concrete foundation and soil back fill as shown in Equation 4.3

$$V_{design} = F_z + V_{concrete} + V_{soil} \quad (4.3)$$

$$V_{design} = 17127 \text{ kN}$$

**3 Determine Eccentric Loading Due to Design Moment** The eccentricity ( $e$ ), as calculated in Equation 4.5, is the shift of the design vertical load due to the design moment. Figure 4.2 shows the idealised loading accounting for the moment. There are two possible failure modes based on the eccentricity, namely rupture 1 and rupture 2.

In Figure 4.2, the arrows show the direction in which the bearing failure of the soil will occur for the defined rupture type. Rupture 2 (black arrow) represents the conventional bearing capacity failure mechanism with the soil on which the foundation bears failing towards the outside of the foundation. For Rupture 1 (orange arrow), the soil fails back underneath the foundation into the space formed as a result of gapping.

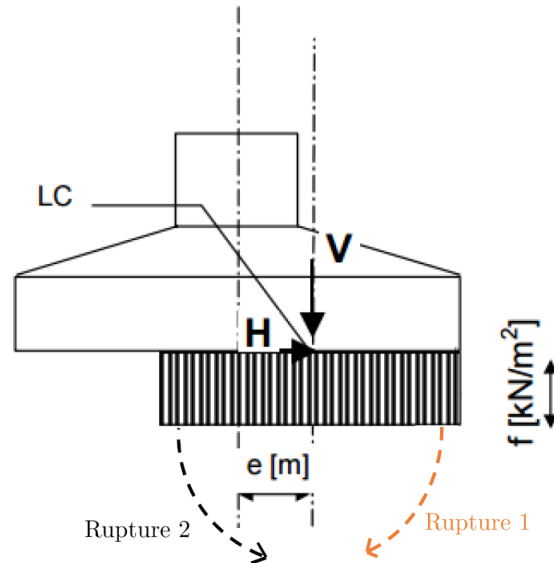


Figure 4.2: Loading Under Idealised conditions (adapted from DNV/Riso (2002))

The design moment  $M_{design}$  is the summation of the following moments:

- $M_{res}$ : Turbine tower induced moment as prescribed in Table 4.2
- $M_{shear} = F_{res} * h$ : the moment contribution of the simultaneous shear force applied at the top of the concrete foundation.

$$M_{design} = M_{res} + F_{res} * h \quad (4.4)$$

$$M_{res} = 91100 \text{ kNm} \text{ Table 4.2}$$

$$F_{res} = 784 \text{ kN} \text{ Table 4.2}$$

$$h = 3.4 \text{ m} \text{ Table 4.3}$$

$$M_{design} = 93800 \text{ kNm}$$

$$e = \frac{M_{design}}{V_{design}} \quad (4.5)$$

$$e = 5.47 \text{ m}$$

According to DNV/Riso (2002), loading is defined as extremely eccentric if  $e > 0.3 * D$ . When this extreme eccentricity loading is exceeded, the foundation failure has the likelihood to follow the Rupture 2 path as defined by Figure 4.2 as opposed to Rupture 1 for an eccentricity less than  $0.3 D$ . The bearing capacity for both failure modes are calculated and the lowest bearing capacity value governs the foundation design. The detailed bearing capacity calculation illustrating this consideration, by way of a worked example, is presented in Appendix B.

It is very important to note that the eccentricity governs the likelihood for gapping. Some suppliers specify 0% gapping as this has a negative influence on the durability of the structure, specifically where the ground water is shallow. For the purpose of this design and to further investigate the influence of gapping, the extreme eccentricity is accepted and used in the FEM to establish the influence of gapping, purely on the structural stability against overturning. However, once a designer chooses to accept gapping of the foundation, it is important to account for it in the bearing capacity design as the distribution of the pressure beneath the foundation ceases to be uniform. This design consideration is shown in the bearing capacity calculation of Step 7.

**4 Calculate the Effective Loaded Area:** As mentioned in Section 2.2.7, the foundation has an effective bearing area due to the moment loading causing an eccentricity. Although the design foundation is circular, the effective area can be calculated and approximated by a rectangular shape as shown in Figure 2.10. Equation 2.1 is used to calculate the effective area of the foundation  $A_{eff} = 25.679m^2$ .

**5 Calculate Bearing Pressure:** The pressure exerted on the soil by the foundation for the given load case is calculated as shown in Equation 4.6

$$q_{gross} = V_{design}/A_{eff} \quad (4.6)$$

$$q_{gross} = 667kPa$$

**6 Calculate Allowable Bearing Capacity:** The allowable bearing capacity is then calculated using a reputable method for the soil condition and parameters listed in Table 4.1. The Terzaghi method and Meyerhof method are two of most used methods to calculate the bearing capacity (Knappett and Craig, 2012). The assumptions made in the development of these methods are:

- Depth of foundation is less than or equal to its width
- No sliding occurs between foundation and soil (rough foundation)
- Soil beneath foundation is a homogeneous semi-infinite mass
- Mohr-Coulomb model for soil
- General shear failure mode is the governing mode (but not the only mode)
- No soil consolidation occurs
- Foundation is rigid relative to the soil

- Soil above bottom of foundation has no shear strength; it is only a surcharge load against the overturning load
- Applied load is compressive and applied vertically to the centroid of the foundation
- No applied moments present

Appendix B thoroughly elaborates the bearing capacity calculations for the design. The Ultimate Bearing Capacity Calculated is  $q_{ult}$ .

$$q_{ult} = 1710 \text{ kPa}$$

Literature does not prescribe a minimum factor of safety for wind turbine designs. It is important to note that in South Africa the geotechnical designs are frequently carried out using working stress design methods, thus characteristic loading values (without partial load factor) have been used thus far for the geotechnical design. It is common practise to include a Factor of Safety (FoS) to the ultimate bearing capacity calculated in order to establish an **Allowable Bearing Capacity**. The FoS defined for the given design was 3 thus the Allowable Bearing Capacity  $q_{allow}$  is calculated as

$$q_{allow} = \left( \frac{q_{ult} - q_o}{FoS} \right) - q_o \quad (4.7)$$

Where

$$q_o = \gamma_{bulk} * h = 65 \text{ kPa Overburden Pressure}$$

$$FoS = 2.73$$

$$q_{allow} = 1261 \text{ kPa}$$

**7 Check Bearing Capacity** The Calculated Bearing Pressure  $q_{gross}$  should be less than or equal to the allowable bearing  $q_{allow}$  otherwise the design does not satisfy the prescribed FoS.

For the given design and soil conditions

$$q_{gross} = 667 \text{ kPa} < q_{allow} = 1261 \text{ kPa}$$

Thus, the design is accepted as safe against bearing and is implemented in the FEM.

**8 Check Torsion** The effect of the torsional load applied on the tower is seldom deemed to govern the design. However, it must be checked. The torsional moment is checked in accordance with the guidelines prescribed by DNV/Riso (2002). In principle, the torsional moment is converted to an equivalent lateral load, which will be added to the shear loading at the top of the foundation.



## 4.4 Structural Design

The reality of the South African wind turbine industry is perceived to limit the foundation designer with regard to the structural design of the foundation, as discussed in Section 2.2.8. The reinforcement steel layout is prescribed by the turbine supplier as this forms part of structural system of connecting the tower to the foundation, using either an anchoring can or cage. The anchoring can/cage has fixed dimensions. Nevertheless, the reinforcement of the foundation is designed in this section from first principles. Two possible design techniques are used; firstly, a strut and tie method and secondly, a beam theory method. Lastly, the two design approaches are compared with the prescribed reinforcement setup.

### 4.4.1 Strut and Tie Method

The Strut and Tie Method (STM) is a lower bound theorem method. The stress fields that satisfy equilibrium in the wind turbine foundation do not violate yield criteria, thus it provides a lower bound estimate of the capacity of elastic-perfectly plastic materials. This implies that crushing of concrete or shear failure must not occur prior to yielding of reinforcement in the ties.

The STM design process is carried out in 5 major steps listed below.

- Establishing the stress distribution in the foundation.
- Sketching a truss in order to determine the ultimate forces and solve for the truss member forces.
- Selecting reinforcing or pre-stressing steel to provide the necessary tie capacity and ensure that this reinforcement is properly anchored at the nodes.
- Evaluate the dimensions of the struts and nodes
- Provide distributed reinforcement to ensure ductile behaviour

**Stress Distribution:** The connection between the tower and foundation is a critical part of the design of the foundation. As shown in Figure 4.5, the interface between the tower and foundation results in complex stress distribution for the assumed connection. Thus, in order to best gain an understanding of the stress distribution, a linear elastic concrete foundation model was developed. Two load cases were considered: Self-weight load case prior to lateral load applied on the tower, and secondly wind load case after the lateral wind load was applied to the tower. Figures 4.3 to 4.6 show the stress distributions for the foundation for the aforementioned load cases. The color contouring gives a visual indication of where the struts and the ties should be placed. The legend shows the stress values with the positive values representing tensile stresses and the negative values representing compressive stresses.

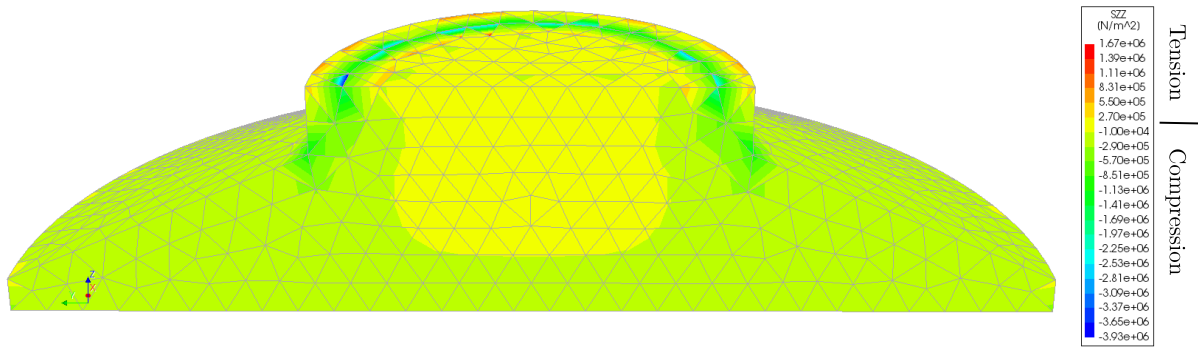


Figure 4.3: SZZ Stresses for Selfweight Load Case

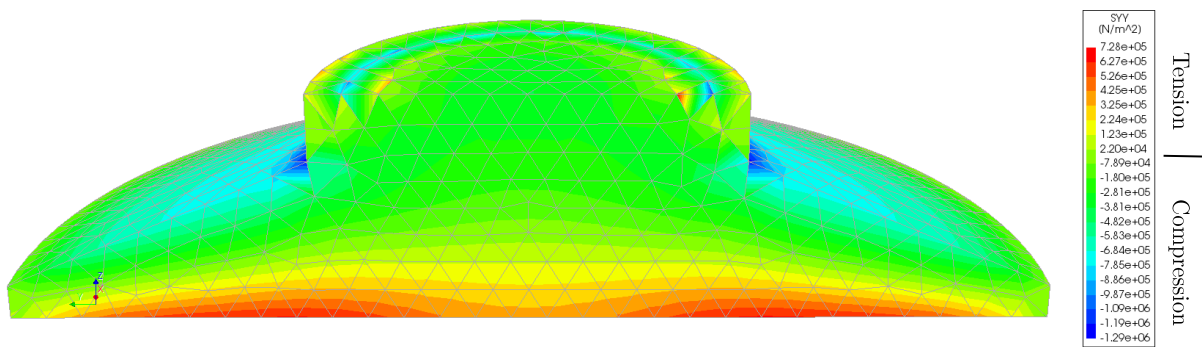


Figure 4.4: SYX Stresses for Selfweight Load Case

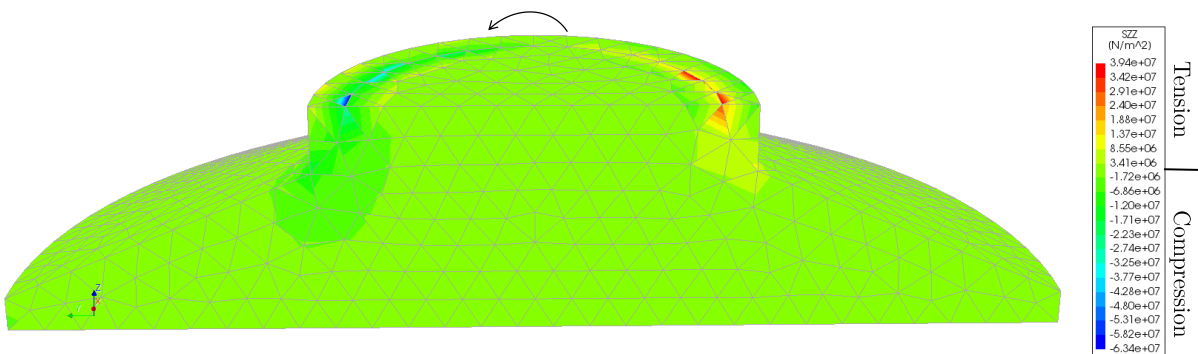


Figure 4.5: SZZ Stresses for Moment Load Case

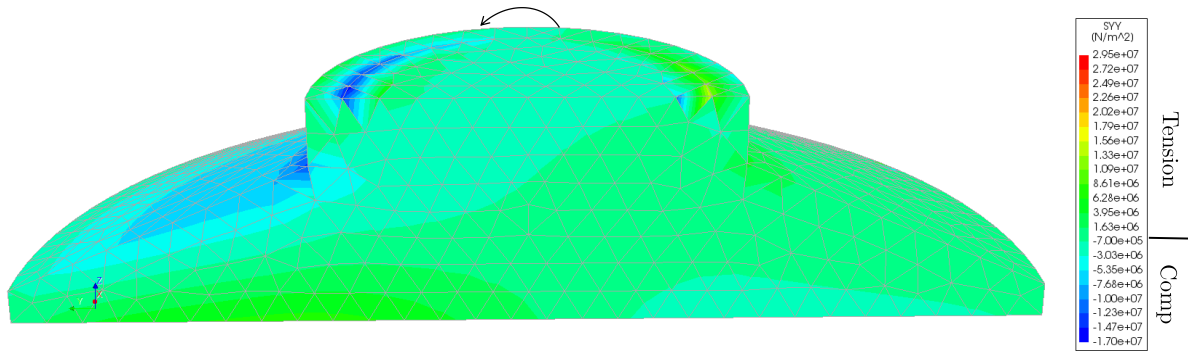


Figure 4.6: SY Y Stresses for Moment Load Case

The Moment load cases is considered for reinforcement and also used for the development of the truss for the STM. Figure 4.5 shows that there are concentrated forces at the connection of the tower and foundation. This was predicted as there is no load transfer system employed (anchoring cage or can). The tower shell elements are connected directly to the foundation solid element. Due to this simplification, the results are hypothetical. However, the results highlight the areas for concern with regard to the steel reinforcement. Similarly, Figure 4.6 highlights the stress distribution in the Y direction for horizontal steel placement.

**Truss Development:** The truss development is designer dependent since there is no unique, workable layout. However, the circular nature of the foundation causes a complexity to the truss development with regard to the thickness of the truss. To overcome this challenge, the following truss development procedure was developed in order to establish a pragmatic approach for reinforcement layout.

Define radial planes as shown in Figure 4.7.

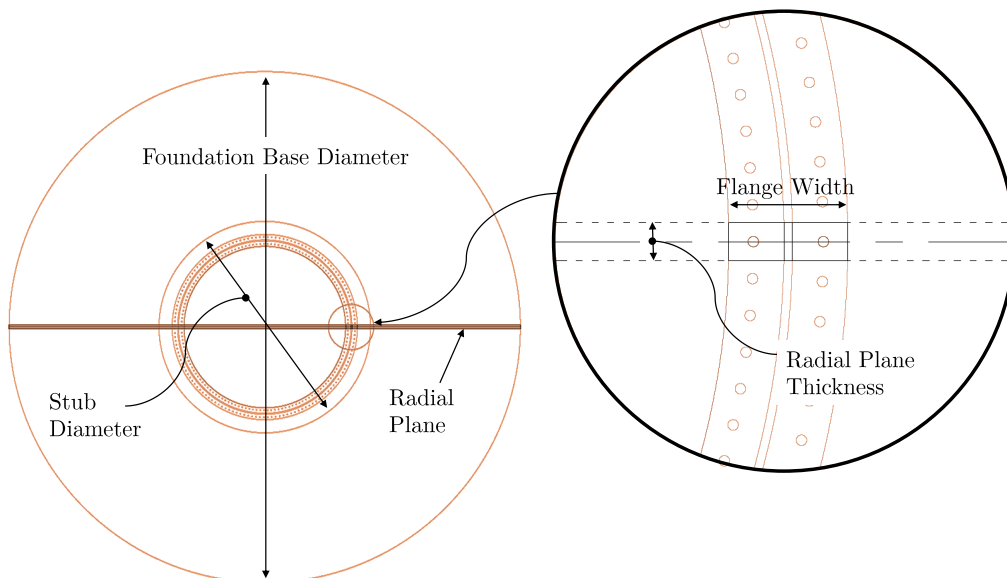


Figure 4.7: Radial plane (RP) for STM truss development

The radial planes have a thickness  $s$ , which is the mean spacing between each pair of the anchoring steel rods. The spacing ( $s$ ) is calculated using the trigonometric equation shown in Equation 4.8.

$$s = r\theta \quad (4.8)$$

Where  $r$  is the radius of the tower at the base and theta ( $\theta$ ) is the angle between the center lines of adjacent radial planes as shown in Figure 4.8. For the purpose of this design the following parameters are defined.

$$\begin{aligned} \theta &= 0.0436\text{rad} (2.5^\circ) \\ r &= 2.5\text{m} \\ s &= 0.11\text{m} \end{aligned}$$

The spacing of the anchors is used to govern the thickness of the radial planes because anchors offer load transfer from the tower flange to the concrete foundation. The anchors are used as struts and ties in the development of the STM truss. For the chosen design, there are 72 radial planes with equal angles of  $2.5^\circ$  between adjacent planes. For illustrative purposes, Figure 4.8 shows an array of some of the radial planes with one of them shaded lightly in blue.

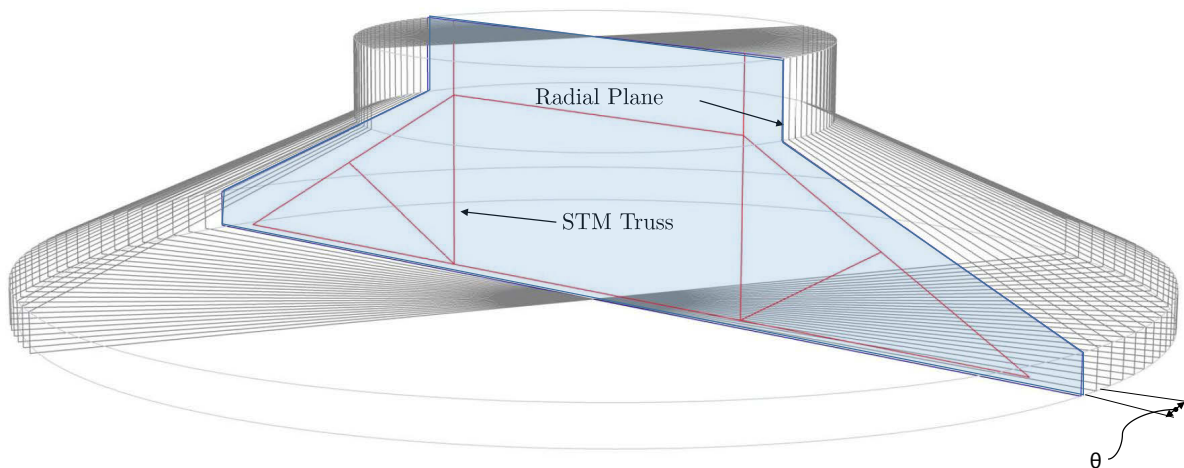


Figure 4.8: 3D schematisation of the radial plane and truss for STM

**Member Forces:** The couple moment methodology is used to transfer the global moment induced by the tower, to a spectrum of couple forces acting on each anchor. Consequently, each radial plane is subjected to a unique couple force. The cumulative couple force results in the total moment applied to the foundation. Vertical load contribution is also added to all the couples as an additional downward force. Figure 4.9 shows the plan view of the tower diameter with couple forces shown as coming out

of the page or going in to the page depending whether the force is on the windward or leeward side respectively. Each couple force is defined according its radial plane ( $RP_i$ ), which is dependent on the angle  $\alpha$ . Figure 4.10 shows the load spectrum for 36 of the 72 radial planes, each couple force as a function of the angle  $\alpha$ . The design moment is 91100 kNm and the vertical design force is -5130 kN, as prescribed by Vestas (2011b).

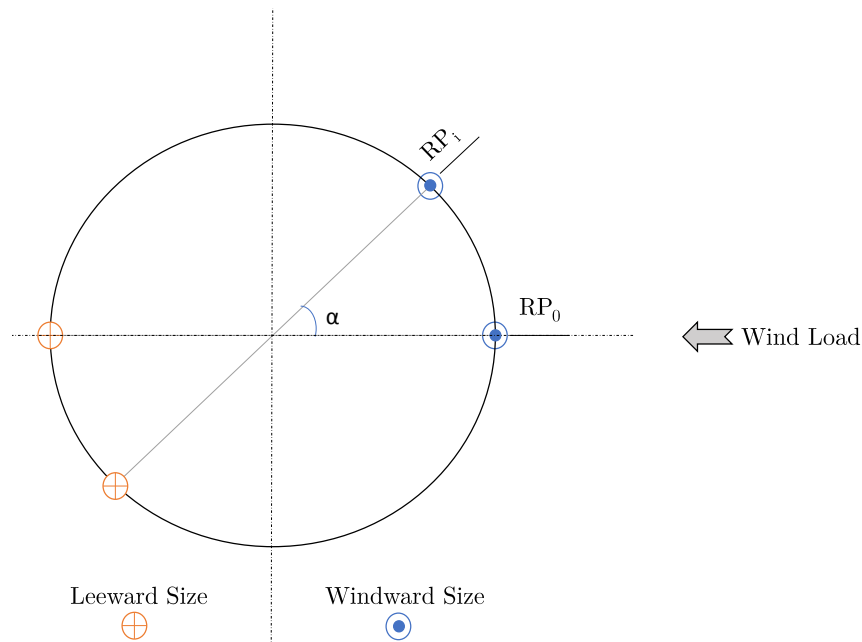


Figure 4.9: Legend for Figure 4.10

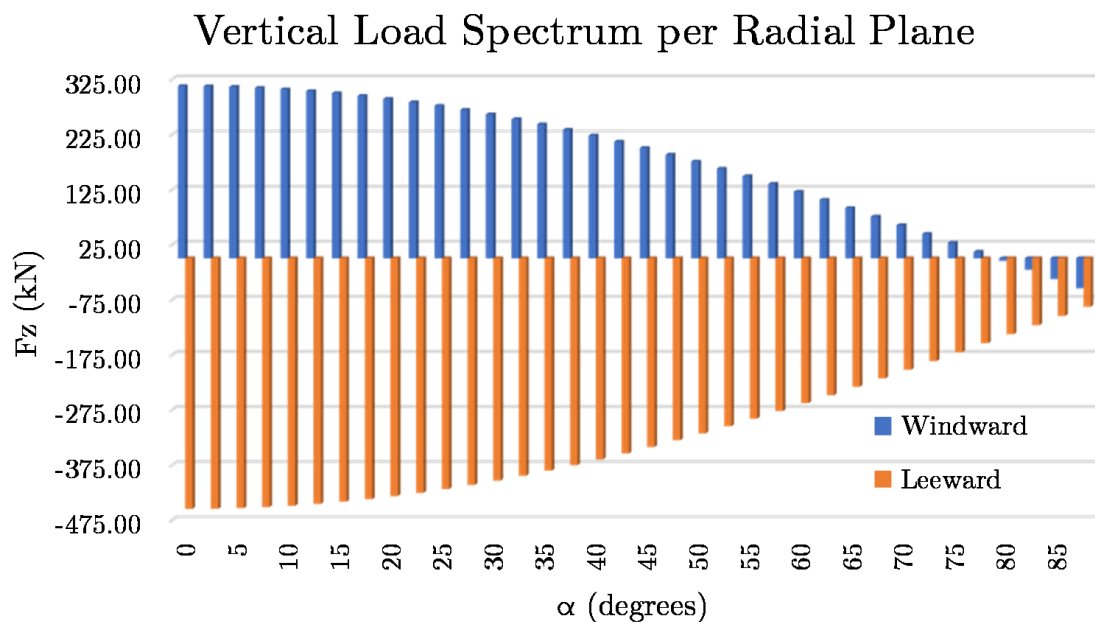


Figure 4.10: Couple forces per radial plane (RP)

The radial plane co-linear to the direction of the wind  $RP_0(\alpha = 0)$ , has the maximum couple forces and thus governs the STM truss development. To perform the next step in the STM, a linear structural analysis model of the truss (Figure 4.8) is built in a locally available software in order to establish the member forces for STM calculations (Prokon, 2010). The loading on the truss is the couple force. The boundary conditions prescribed are two pin supports at the base of the truss. Prior to the chosen truss set-up, the truss initially developed had multiple vertical supports at 1 m spacing along the base of the truss. This was postulated to better represent the soil support. However, the postulation resulted in a convoluted STM truss model without any explicit benefit. The simplified truss was adopted. The results from the final structural analysis of the truss are shown in Figure 4.11. The struts are shown in red and the ties are shown in blue. The member forces are given in kN with the positive values as compression struts and negative values as tension ties. It is important to note that the gapping support condition is not implemented as a simplification here. Appropriate founding for accurate assessment of gapping is described Chapter 5.

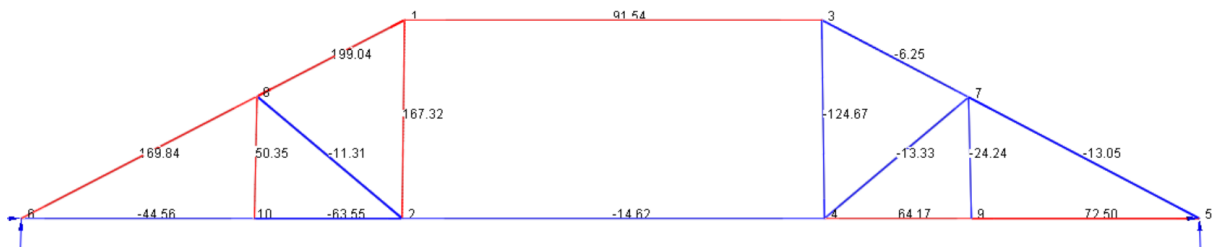


Figure 4.11: Prokon Output for STM Truss

**Reinforcement Selection:** In order to calculate the reinforcement needed, strut and ties member sizes are established for the given member forces. Given Figure 4.11, the truss members tabulated in Table 4.4 are deemed critical to design.

Table 4.4: STM Critical Members

Member	Force (kN)
3-4	-124.67
1-2	167.32
2-10	-63.55
1-8	199.04

Figure 4.12 shows the load transfer for a radial plane utilising the anchors. Figure 4.13 shows the force distribution for the connection labelled 1 and 2 in Figure 4.12. As shown in Figure 4.13, the windward anchors in  $RP_0$  are subjected to a tensile force of  $F_{anchor} = 160$  kN for the selected plane. The applied forces 463 kN (down) and 320 kN (up) are derived from load spectrum in Figure 4.10.

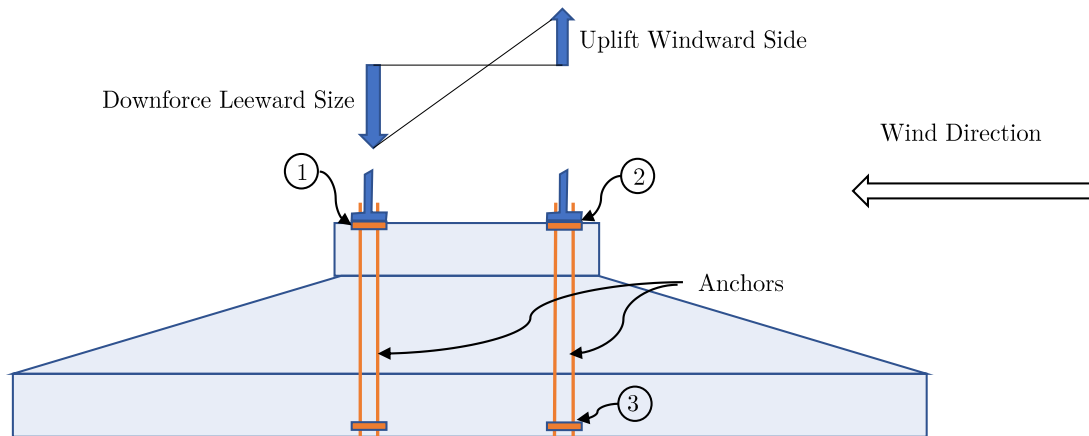


Figure 4.12: Load Transfer Schematisation

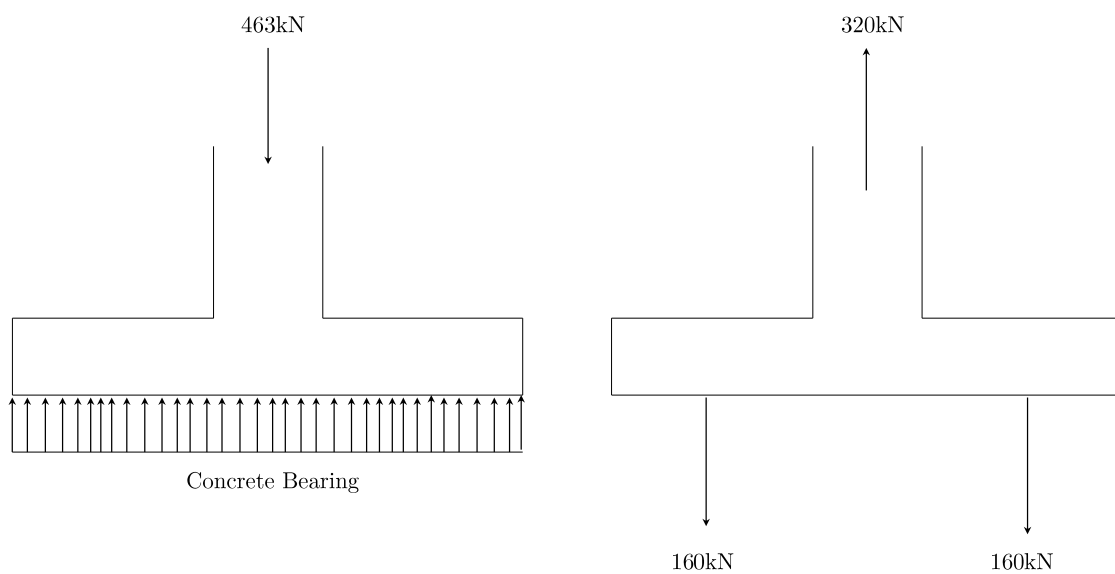


Figure 4.13: Tower Flange Connections 1 (Left) and 2 (Right)

Steel rods of diameter 30 mm are selected as anchor rods. The maximum force that can be applied to each anchor is calculated using Equation 4.9.

$$F_{max} = A_{st} * f_y \quad (4.9)$$

Where

$$\begin{aligned} A_{st}: \text{Area of Tensile Steel} &= 707\text{mm}^2 \\ f_y: \text{Yielding Stress of Steel} &= 450\text{MPa} \\ \therefore F_{max} &= 318\text{kN} > F_{anchor} = 160\text{kN} \text{ [okay]} \end{aligned}$$

The selected anchors have sufficient tensile capacity for the design load of the selected plane  $RP_0$ .

**Member 3-4:** The anchor pair is defined as a tie. From the STM truss developed the anchor pair is a tie and the section of the tie is Member 3-4 with a load of 124.6 kN. From the calculation based on Equation 4.9, it is evident that the tie; Member 3-4, has sufficient tensile capacity for the load.

The connection on the leeward side is also illustrated in Figure 4.13. Assuming that the concrete bears the applied load 463 kN, the loaded concrete area is simplified as the thickness  $s$  of the radial plane multiplied by the width of the flange  $w = 300\text{mm}$  (Figure 4.7).

$$\sigma_{applied} = \frac{463\text{kN}}{A_{concrete}} = 14\text{MPa} \quad (4.10)$$

Where

$$\begin{aligned} A_{concrete}: s * w &= 33000\text{mm}^2 \\ \therefore \sigma_{c,max} &= 35\text{MPa} > \sigma_{applied} = 14\text{MPa} \text{ [okay]} \end{aligned}$$

**Member 1-2** is directly below the applied load as calculated in Equation 4.10. The strut member force from the structural analysis was 167 kN, which is less than the calculated load at the connection (Equation 4.9). The strut Member 1-2 has sufficient compressive resistance for the applied load.

**Member 2-10:** A force of 64 kN acts on the tie Member 2-10. The width of the truss is approximately 110 mm ( $s$ ) for the chosen design. The area of steel required  $A_s$  is calculated as shown in Equation 4.12. 1Y16 reinforcement is sufficient per radial plane.

$$\sigma_{Rd,max} = \frac{f_y}{\gamma_m} = \frac{f_y}{1.15} \quad (4.11)$$

$$A_s = \frac{F_{nt}}{\sigma_{Rd,max}} \quad (4.12)$$

Where

$$\begin{aligned} F_{nt} &= 64\text{kN} \\ \sigma_{Rd,max} &= 391\text{MPa} \\ \therefore A_s &= 163.7\text{mm}^2 \\ \text{Used 1Y16 } (A_{s,1Y16} &= 201\text{mm}^2 > A_s = 163.7\text{mm}^2) \text{ [Okay]} \end{aligned}$$



**Member 1-8:** Figure 4.14 shows the nodal boundary for node 1 as defined by structural analysis output. Once again the thickness of the truss is known to be approximately 110 mm which is the thickness of the radial plane. The width of the strut Member 1-8 is obtained using trigonometry and defining a suitable boundary. For this design the calculated width is 470 mm. The cross sectional area of the strut is calculated using Equation 4.13 and used to check the stress limits in the member. Member 1-8 has sufficient compressive capacity for the applied load.

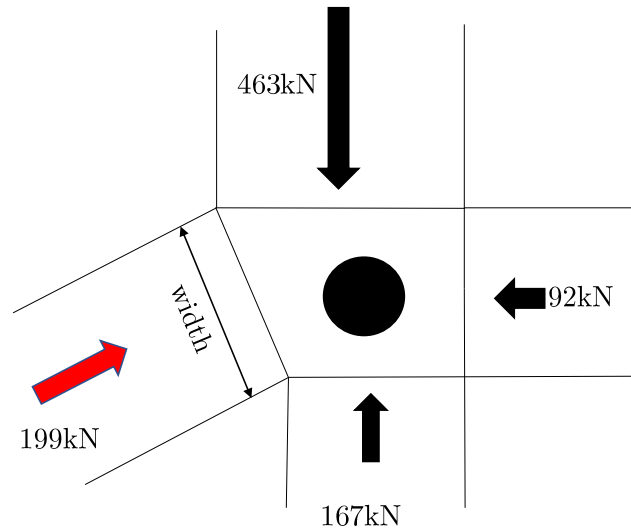


Figure 4.14: Node 1 : Node boundary

$$A_{c1-8} = w * s = 470 * 110 = 51700mm^2 \quad (4.13)$$

$$\sigma_{c,s1-8} = \frac{F_{1-8}}{A_{c1-8}} = \frac{199000N}{51700mm^2}$$

$$\sigma_{c,s1-8} = 3.85MPa < \sigma_{c,max} = 35MPa[\text{Okay}]$$

Only the design of critical members are reported in this section. However, the detailing is essential for construction purposes and is added in Appendix D. The detailed drawings shown in the Appendix are based on the code of practise SABS-0100-1 (2000).

#### 4.4.2 Beam Theory Method

The Beam Theory Method (BTM) is a popular reinforcement steel design method. Literature which included steel reinforcement placement for wind turbine foundations primarily utilises this method. The method is indeed less complicated than the STM. This section reports on the design of the steel reinforcement for the same foundation geometry using the BTM.

#### 4.4.2.1 Conceptual

The section briefly explains the conceptual design process to be followed when designing steel reinforcement for a wind turbine foundation using the BTM. The typical bending moment diagram (BMD) for a wind turbine foundation is shown in Figure 4.15. The diagram is based on a simplification of the foundation modelled as a simply supported beam, with a moment applied as a couple force. A simplification of the load transfer is shown in Figure 4.16. The couple force acts on the centroid of the quarter circle segment. The distance  $d_s$  between the couple force is calculated as shown in Equation 4.14.

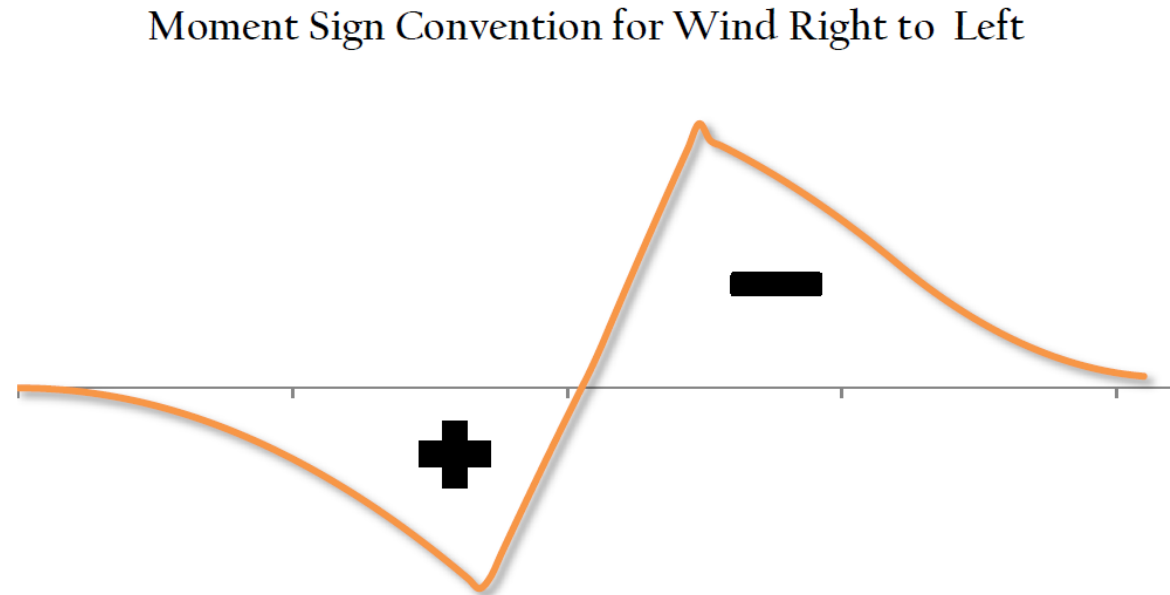


Figure 4.15: Typical bending moment diagram for wind turbine foundation.(Way, 2014)

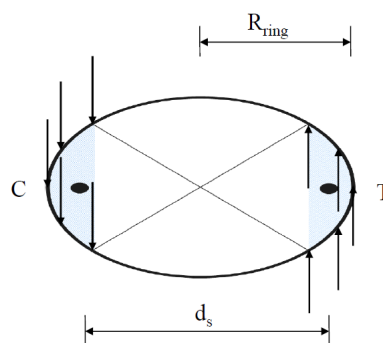


Figure 4.16: Illustration of compression and tension force couple(Way, 2014).

$$d_s = \frac{4 * R_{anchor}}{\pi} \sqrt{2} \quad (4.14)$$

Where

$R_{anchor}$  = Radius of anchor ring (m)

$d_s$  = Distance between couple force

The design moment is divided by  $d_s$  in order to determine the equivalent couple forces. A quarter of the total design vertical force is included in the final forces applied to the beam as shown in Figure 4.16. The final forces are used to establish a shear force diagram (SFD) which is then used to determine a BMD for design. The maximum bending moment on the BMD is used as the design bending moment to calculate the area of steel reinforcement required in accordance with the SABS-0100-1 (2000). The following assumptions are made:

- The depth of the beam is the average height of the foundation.
- The width of the beam is equal to the diameter of the foundation stub at the top of the foundation.
- The influence of the self-weight of the foundation as a distributed load is negligible since the actual foundation is not simply supported but rests on a founding material.
- 30 mm cover.

#### 4.4.2.2 Detailed

This section gives a detailed report of the design. The moment load  $M_{res}$  (91100 kNm) as well as the vertical load  $F_z$  (5130 kN) is prescribed by the turbine supplier and applied at the top of the foundation stub (Vestas, 2011a). The radius of the anchor ring  $R_{anchor}$  is 2.5 m, therefore the distance between the centroid of the quarter circles  $d_s$  is 4.5 m (Equation 4.14). The couple forces  $F_t$  and  $F_c$  for the design load applied to the beam model are calculated as shown in Equation 4.15 and 4.16 respectively. The freebody diagram in Figure 4.17 illustrates the application of the load and the boundary conditions. The statically determinant simply supported beam is solved for the reaction forces  $R_L$  and  $R_R$ , which are 8745 kN and -3615 kN respectively. A SFD is plotted as shown in Figure 4.18. The design bending moment used for the area of steel calculations is derived from the BMD plot in Figure 4.19. It is important to note that the self weight of the beam was not included as a load on the beam.

$$F_t = \frac{M_d}{d_s} - \frac{F_z}{4} = 17679kN \quad (4.15)$$

$$F_c = \frac{M_d}{d_s} + \frac{F_z}{4} = 22809kN \quad (4.16)$$

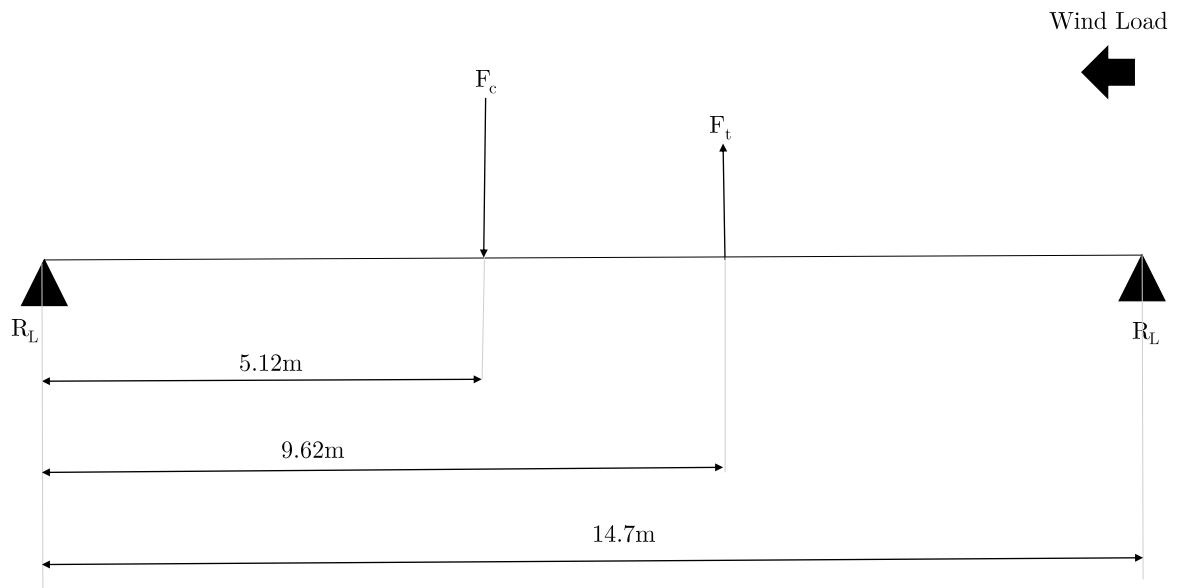


Figure 4.17: BTM Free Body Diagram

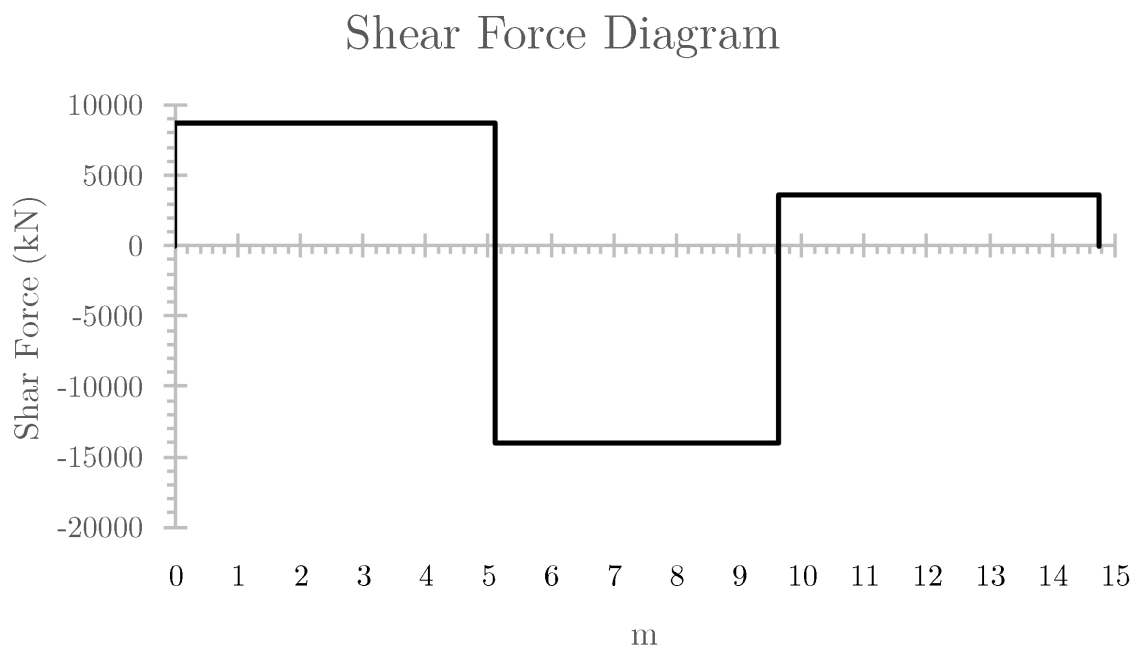


Figure 4.18: Shear Force Diagram for foundation modelled using the BTM

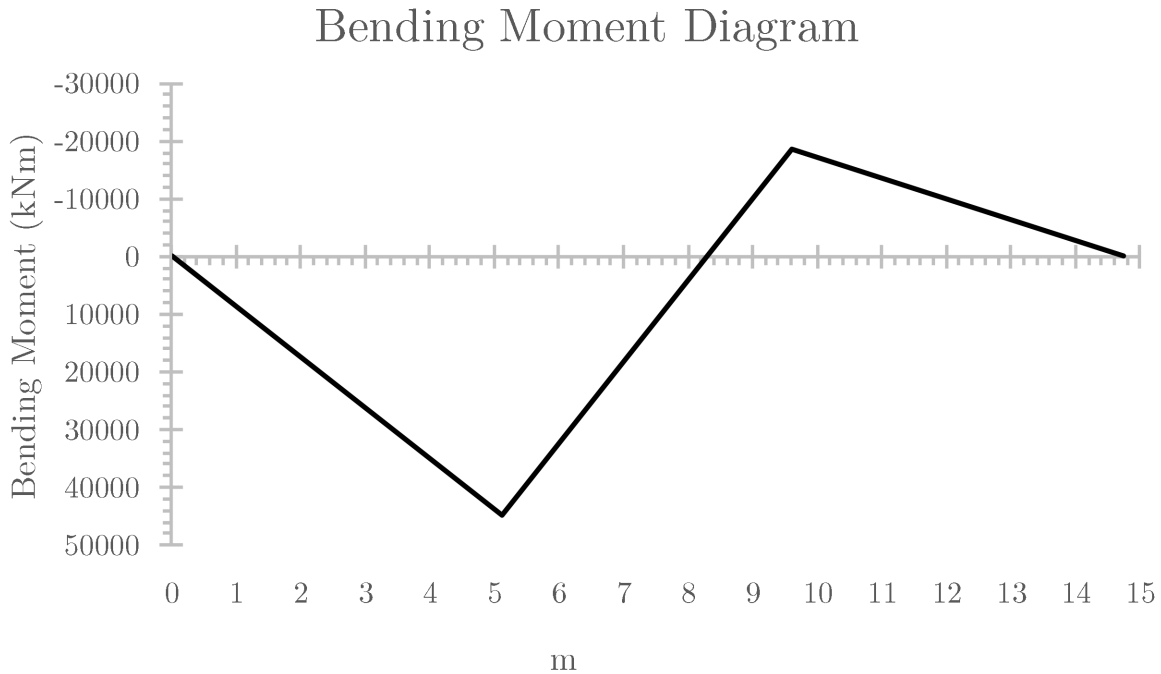


Figure 4.19: Bending Moment Diagram for foundation modelled using the BTM

For the design of the bottom reinforcement steel, the maximum positive moment  $M = 44774$  kN is used to calculate the area of steel required for bottom reinforcement. The design is done in accordance with SABS-0100-1 (2000). The beam width and depth selection is of importance. From the literature review, it was unclear which assumptions were made with regard to the depth and width of the beam because the foundation is circular and tapered as well. For the purpose of this design the beam width chosen is the diameter of the foundation stub ( $b = 6$  m). The beam depth is chosen as the average depth of the foundation ( $d = 2.4$  m). The concrete compressive strength  $f_{cu}$  is 35 MPa.

$$K = \frac{M}{bd^2 f_{cu}} \quad (4.17)$$

$$K = \frac{44774}{6 * 2.4^2 * 35e3} = 0.0403 < K' = 0.156$$

Only tensile reinforcement is required i.e no need for compression steel at the top of the section.

$$z = d \left( 0.5 + \sqrt{0.25 - \frac{K}{0.9}} \right) \leq 0.95d \quad (4.18)$$

$$z = 2.4 * \left( 0.5 + \sqrt{\left( 0.25 - \frac{0.0403}{0.9} \right)} \right) = 2.37 > 0.95d$$

$$\therefore z = 0.95d = 2.28m$$

$$A_{s,req} = \frac{M}{0.87f_y z} \quad (4.19)$$

$$A_{sreq} = \frac{44774e3}{0.87 * 450 * 2.37} = 48255mm^2 \text{ (6 m width)}$$

$$A_{s,req} = 8042mm^2/m$$

Use 10Y32 - 100

$$A_s = 8042mm^2/m = A_{s,req} \text{ (Okay)}$$

The same calculation is used to determine the top steel for the top section of the windward side of the foundation. The  $A_{st,req} = 3325 mm^2/m$ . Therefore 10Y25 - 100 is prescribed.

### 4.4.3 Comparison

A qualitative and quantitative comparison is drawn between the STM and BTM for steel reinforcement design.

#### 4.4.3.1 Quantitative

The flexural steel reinforcement comparison per 1 m strip of the foundation is made. Table 4.5 shows the area of steel calculated from the two design methods.

Table 4.5: Area of Steel Comparison

Method	Area of Steel ( $mm^2/m$ )
Strut and Tie	1809
Beam Theory	8042

#### 4.4.3.2 Qualitative

A significant variation is observed in Table 4.5. Although best practise is used in the calculation of the area of steel, the BTM yields more conservative results by a factor of approximately four. Various assumptions and simplifications were made in both methods.

The BTM is a popular design tool as it is fairly easy to use with design code implementation. However, it has the disadvantage that it is overly conservative, specifically for wind turbine foundation design. This is primarily because:

- The design procedure of the BTM is strain distribution on a beam section. However, the strain condition in the wind turbine foundation does not obey the Bernoulli's hypothesis of straight line strain profiles across the foundation section.

- The geometry of the wind turbine foundation has abrupt changes offering discontinuities, for example, between the stub and the base. The BTM is based primarily on the assumption that the beam is not discontinuous.
- It is an over simplification to assume that a strip (e.g. 6 m) of the circular base offers the rotational resistance of the entire base. This simplification is a conservative and uneconomical assumption.
- Equation 4.18 calculation shows that for the given section  $z > 0.95d$ . This means that the beam has a small compression block, which supports the hypothesis that the wind turbine foundation of 3.5 m depth does not behave as a purely flexural beam but carried much of the load in shear.

The STM offers a more realistic methodology to design wind turbine foundations and is emerging as a code-worthy methodology. This study introduced design novelties by incorporating "radial planes" as the basis to define trusses and truss widths for the STM as well as distributing the tower moment as unique couple forces applied to the defined radial planes.

Two design methodologies were compared in this section. Other design methodologies like FEM and empirical design methods can also be use. It should be noted that the BTM is not a recommendable design methodology considering the over-conservative results yielded by this model.

#### 4.4.4 Crack Width Control

The STM and BTM can be used to compute the flexural steel reinforcement required to resist the design moment and vertical load. However, it is important to note that the crack width design governs the reinforcement spacing. Crack propagation in the foundation changes the foundation's vibrational response. The crack width is limited to 0.2 mm, which is regarded as a minimum crack width, similar to water retaining structures. A crack width design check is considered. Vestas (2011a) prescribes a crack width limit of 0.2 mm - 0.3 mm. It is postulated that the foundation rotational stiffness is reduced with crack propagation. This section shows how reinforcement spacing compliance is achieved for the given foundation design to adhere to the crack width limit. The member forces from the structural analysis of the STM (Figure 4.11) are used in this section. Two critical surfaces are checked as they pose the greatest potential for crack propagations. The first surface check is on the base of the foundation with the tensile stress caused by the design load. The second surface check is on the stub surface as the maximum tensile stress in the foundation is present there.

Member 2-10 is subjected to a tensile load  $T_{2-10} = 63.55$  kN and reinforced with 1Y16 steel reinforcement bar with a yielding stress of 450 MPa. The width of the member is 110 mm and the depth is 76 mm. The depth is chosen as the bar diameter  $\phi$  plus twice the cover depth. The spacing  $s$  between each member is 110 mm and the cover is 30 mm. The surface crack width for this member is calculated as,

$$w = 3a_{cr}e_m \quad (4.20)$$

Where

$$a_{cr} = \sqrt{\frac{s^2}{2} + \left(\text{cover} + \frac{\phi}{2}\right)^2} - \frac{\phi}{2} = 58.9\text{mm}$$

$$e_m = e_1 - e_2 \quad (4.21)$$

$$e_1 = \frac{T}{A_s E_s} = 0.001592 \text{ (Strain at Surface)}$$

$$e_2 = \frac{2bh}{3E_s A_s} = 0.0009 \text{ (Accounting for tension stiffening)}$$

The average surface strain is  $e_m = 0.001453$ .

The crack width is calculated to be

$$w = 3 * 58.9 * 0.001453 = 0.26\text{mm} > 0.2\text{mm} \text{ (Not OK!)}$$

The surface check shows that the flexural steel prescribed using the STM does not satisfy the crack width limit of 0.2 mm. To overcome this challenge, a smaller rebar is used and the spacing between them reduced. The final steel used was 2Y12-65 per radial plane. Due to the radial nature of the reinforcement placement, the spacing increases with distance away from the center. This is also checked and complies with the crack width limit. The detailed drawings of the final reinforcement layout are shown in Appendix D.



# Chapter 5

## Finite Element Modelling

### 5.1 Introduction

Diana FEM software DIANA (2016) was used to develop all the Finite Element Models discussed in this chapter. The chapter firstly describes the material models used and motivates their choice. Thereafter, elements used for FE modelling of the various components in the FEM are explained and their selection motivated. In the first section of the chapter, the analyses carried out and the intended objective for each analysis type are explained, and finally the results are shown in the last section of the chapter. Figure 5.1 shows the generic schematisation of the models developed. Three dimensional (3D) modelling was carried out to include all vibrational modes. Symmetry modelling was used to limit computational time of push-over analyses, and for ease of visualisation along the symmetry plane. The symmetry proportion was half symmetry, with symmetric boundary conditions along the plane through the center of the foundation parallel to the wind direction.

### 5.2 Material Models

Finite element modelling facilitates numerical simulation of the behaviour of structural materials. Each structural material behaves in a way which is unique to its material properties. Material behaviour is simulated in various ways depending on how the material deforms under loading conditions. Some materials experience permanent or irreversible deformations. Other materials experience reversible deformations. These two types of behaviour are attributed to plasticity and cracking material behaviour and elastic material behaviour respectively. Often, reversible deformation is dependent on the intensity of the load applied to the structure. Usually, at low stress levels, a material behaves elastically and only at a particular stress state (yielding condition) plastic behaviour or cracking is initiated. Consequently, material behaviour can be a combination of both plastic and elastic behaviour.

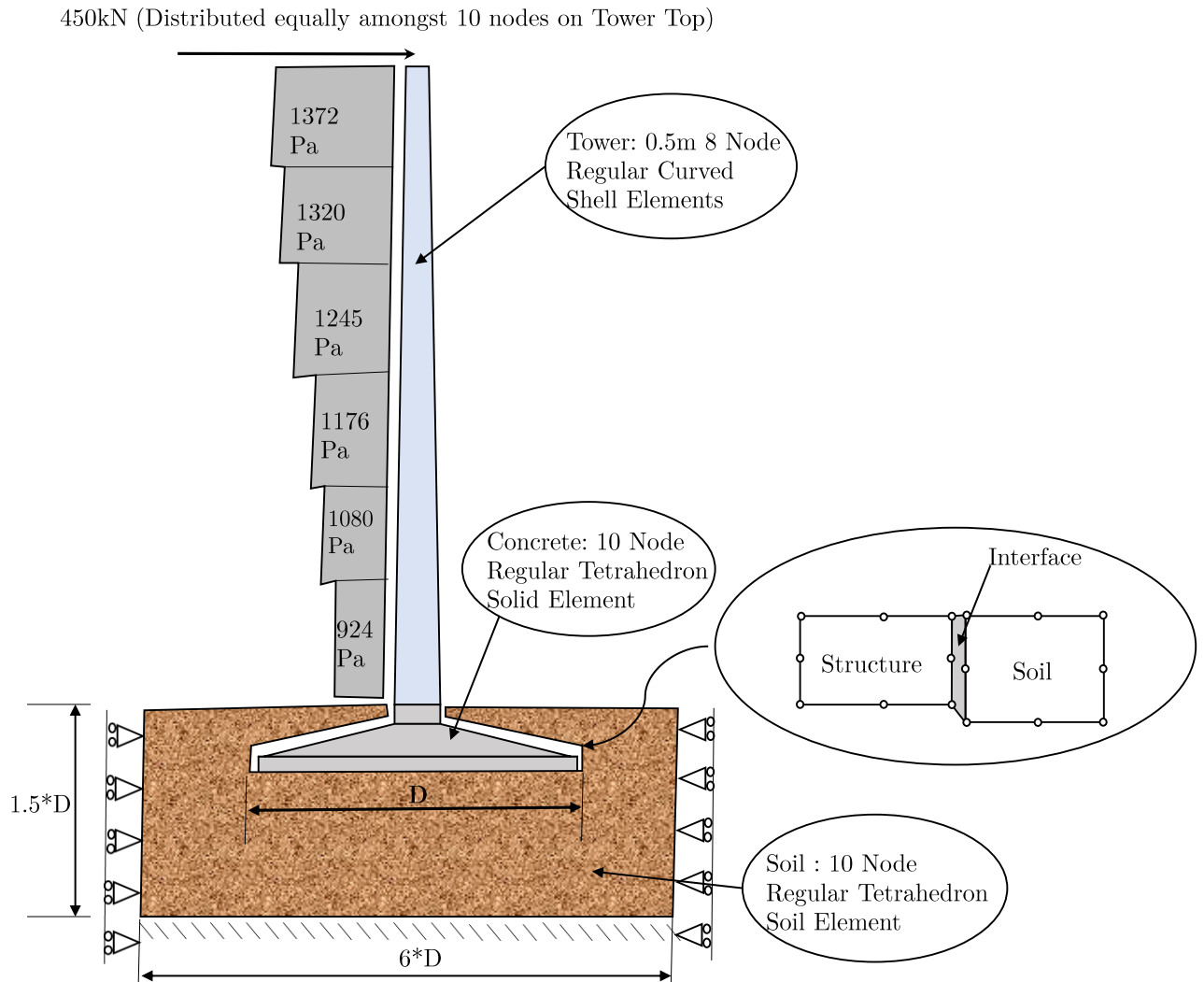


Figure 5.1: Model Schematisation *Illustration not drawn to actual modelling scale*

### 5.2.1 Soil

This section discusses the material modelling of soil in finite element analyses. Finite element modelling of soil is specifically challenging as soils are not continuum materials but discrete materials. Generally, structural engineers and geotechnical engineers work closely together in most projects as they share information that allows the other to carry out their required design. However, when it comes to structural response and soil structure interaction there is occasionally a misunderstanding because geotechnical engineers are used to defining their materials based on strength parameters, and structural engineers define their materials based on stiffness parameters. Another challenge, specifically in South Africa, is that many geotechnical engineers use factor of safety design yet structural engineers use limit state design.

Computational plasticity allows for realistic and accurate modelling of inelastic phenomena in structural and soil response. In this thesis, various models formulated in computational plasticity are used. According to DIANA (2016), the following assumptions are made with regard to plasticity of materials:

- An initial linear elastic stress-strain relation
- A yield condition which specifies the state of stress when the plastic flow is initiated
- A flow rule which specifies the plastic strain rate vector as a function of the state or stress
- A hardening hypothesis

For the purposes of this study, the DIANA Modified Mohr-Coulomb model was used to define Soil Material behaviour.

### 5.2.1.1 Modified Mohr-Coulomb/Soil Hardening Model

The Modified Mohr-Coulomb model is a combination of a non-linear elastic model and a plasticity model. The non-linear elasticity is based on experimental observations showing that during elastic swelling or reloading the compression modulus  $K$  is governed by the void ratio and the current hydrostatic pressure according to:

$$K_t = \frac{1 + e}{k} p' \quad (5.1)$$

in which the  $e$  is the void ratio,  $k$  is the material parameter,  $p'$  is the current hydrostatic pressure and  $v$  is the volume calculated as  $1 + e$ . Figure 5.2 assumes elastic behaviour indicating the material parameter.

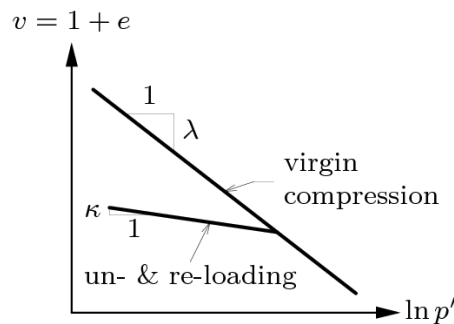


Figure 5.2: Soil response in compression  
(DIANA, 2016)

The model includes soil dilatancy, introduces a yield cap and distinguishes between two types of hardening, namely: shear hardening and compression hardening. Total strains are calculated using stress dependent stiffness, which are also different for both virgin loading and un-/reloading. The Modified Mohr-Coulomb model as the name suggests, is the modification of the Mohr-Coulomb by use of a double stiffness model for elasticity in combination with isotropic strain hardening.

### 5.2.1.2 Mohr-Coulomb Model

The Mohr-Coulomb model is the combination and generalisation of Hooke's law of linear elasticity for describing soil behaviour under working loading conditions and Coulomb's law of perfect plasticity for describing soil behaviour under collapse state. It is chosen for its simplicity in application, yet reasonable simulation of the physical phenomena of friction and adhesion in soils. According to Ti *et al.* (2009), Mohr-Coulomb is a simple and applicable model to use for 3D modelling and analysis of the stability of shallow foundations. The model captures failure well in drained conditions. The failure criterion for the model is shear failure with a small tension cut-off (Ti *et al.*, 2009). Furthermore, the yield condition of the Mohr-Coulomb model is an extension of the Tresca yield condition which is a maximum shear stress condition used for metals. The Tresca yield condition can be expressed in the principal stress space. An important difference between standard Tresca and Mohr-Coulomb is pressure dependence, as required for soils.

### 5.2.1.3 Motivation of Selected Soil Model

The plastic and non-elastic behaviour is captured by the Modified Mohr-Coulomb which is expected of Soil/Sand material behaviour. The Modified Mohr-Coulomb model has stiffness dependent on virgin loading, unloading and reloading, which is required for founding material under a dynamic structure like a wind turbine. The failure surface of the Modified Mohr-Coulomb model is a so-called double hardening model in which the shear failure and the compressive failure are uncoupled (DIANA, 2016). For the purposes of this research, it was concluded that the Modified Mohr-Coulomb material model should be used.

## 5.2.2 Soil Structure Interaction

The process by which the response of the structure affects the response of the underlying soil, and vice versa is known as Soil-Structure Interaction (SSI). According to Fitzgerald and Basu (2016), when a structural element is in contact with the ground, the displacement of the element is dependent on the displacement of the ground. For the purpose of this study, it is important to accurately define the boundary/interface between the concrete foundation and the founding material as this influences both the static response and the dynamic response of the models. Interfaces can exhibit de-lamination, leading to the loss of continuity in the mechanical and kinematic response of the structure. In this regard, the ability to transfer loads can control the stability and deformation of the structure (Selvadurai and Yu, 2005).

Figure 5.1 shows a schematic drawing of the model highlighting the interface between the concrete foundation and the foundation material. For the purposes of the model developed in this study, 3D interface elements were used to model the SSI. The interface is modelled to replicate 3 main interface phenomena, namely:

- High compressive stiffness in order to avoid overlapping/penetration of the concrete element and the soil elements.
- Zero tensile stiffness in order to allow for gapping.
- Shear strength reduction based on normal interface tractions.

The influence of the SSI on wind turbine foundations was studied by Fitzgerald and Basu (2016). They concluded that SSI does not affect blade vibration. However, they showed that by accounting for SSI, the natural frequencies of the nacelle/tower can be affected significantly. Thus, it can be deduced that the SSI offers energy dissipation or damping of the tower and nacelle. This phenomenon was also supported by Way and van Zijl (2015). Murtagh *et al.* (2005) carried out a study on the vibration response of wind turbine towers when SSI effects are incorporated into the structural model. They found that incorporating the compressibility of soil into the model introduces a considerable amount of damping into the system. They suggested that natural frequency calculations that do not consider damping due to SSI will be unrealistic and may lead to uneconomical designs (Nicholson, 2011). Contrary to the aforementioned research, Muzofa *et al.* (2017) report that the influence of including the SSI in modelling of wind turbine towers has an insignificant effect on the natural frequency of the tower for stiff founding material. The founding material modelled by Muzofa *et al.* (2017) simulates a soil with a friction angle of 32 degrees, which can be regarded as typical medium dense or granular soil. This led to the hypothesis that the dissipation of energy by the founding material is dependent on stiffness of the founding material. While less stiff soils lead to reduced structural natural frequency, stiff soils allow less energy dissipation and consequently do not lower the natural frequency of the tower.

### 5.2.3 Concrete

Chapter 3 addresses the concrete properties required for a typical wind turbine foundation. The results from Chapter 3 are used in the definition of the concrete material models in the analysis. For the purposes of this research, two concrete models are used; Linear elastic and Total Strain Based Crack Model (DIANA, 2016).

#### 5.2.3.1 Linear Elastic

The linear elastic material model is used primarily to optimise the modelling by reducing the computational time and the size of the model. It is important to note that depending on the connection of the turbine to the foundation, the concrete can be subjected to strains that will result in the cracking of the concrete, which is a source of non-linearity for the foundation. However, for the analyses discussed in Section 5.4.2 and 5.4.3, the results are independent of the cracking. Section 5.4.2 depicts the Cyclic Loading analysis. The analysis involves loading of the model repeatedly within the elastic region. Section 5.4.3 describes the Eigen frequency analysis, which also does not require cracking as a form of non-linearity.

#### 5.2.3.2 Total Strain Based Crack Model

The Total Strain Based Crack Model is used in order to establish the cracks that would occur in the concrete foundation as a result of tensile strains. Whilst linear material properties are defined for the compressive behaviour, inelastic tensile behaviour was considered. The bi-linear tensile curve (Figure 5.3) is defined as a Linear - Crack Energy curve with the tensile strength and the Mode-I tensile fracture energy as input parameters.

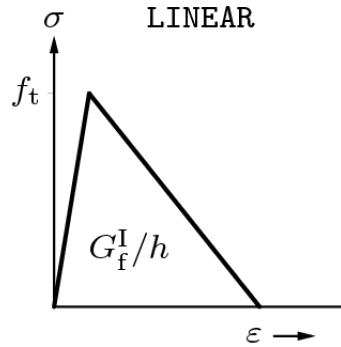


Figure 5.3: Concrete Tensile Curve  
(DIANA, 2016)

### 5.2.4 Steel

A linear elastic steel material is used in the modelling of the tower and reinforcement steel. The failure mode of the tower was beyond the scope of this research. The yielding of the reinforcement in concrete is indeed of concern. However, during the modelling it was discovered that the ultimate stresses induced on given reinforcement arrangement fell within the elastic region of stress strain curve of the steel. Due to the aforementioned, a linear elastic material behaviour was deemed adequate for the purposes of the research.

## 5.3 Elements

The FEM is influenced by the size and type of elements selected. Knowledge of the behaviour of the elements selected is important in order to accurately build a model as close to reality as possible. This section explains the elements selected from the DIANA element library and also motivates the selection of the size and type of elements used for the steel tower, concrete foundation, founding soil and SSI.

### 5.3.1 Steel Tower

Eight noded, regular, curved (Figure 5.4) elements were used to model the tower. Due to the thickness to surface area ratio of the tower, solid brick elements are uneconomical. Alternatively, the tower may be modelled as a lumped mass connected with beam elements. The disadvantage of this lumped mass and beam model is primarily the connection between the tower the concrete foundation. Depicting the behaviour of the node on the surface of the concrete foundation based on one node on the base of the tower would have counteracting degrees of freedom and would not accurately capture the transfer of stress.

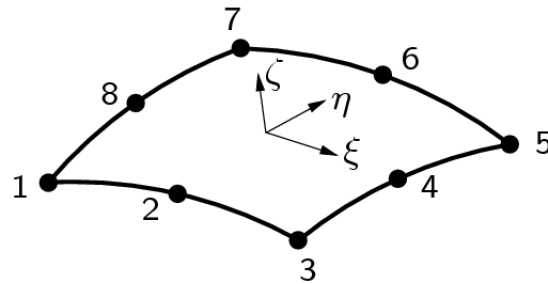


Figure 5.4: 8-node Regular Curved Shell Element Used to Model Tower (CQ40S (DIANA, 2016))

### 5.3.2 Concrete and Soil

Tetrahedron elements, with four sides and ten nodes (Figure 5.5) are used to model the concrete foundation and the founding soil. Due to the circular shape of the foundation and soil, the tetrahedron elements offer the best mesh. Solid brick elements result in a sensible mesh when smaller element sizes are used. This is uneconomical as the founding soil requires a considerably large number of elements.

The concrete foundation element size is dependent on the tower size. The founding soil element size is dependant on the computation time required without detrimentally reducing computational accuracy. It is important to note that the element size for the soil is adaptive. This implies that the elements sharing nodes with the foundation have the same size as the foundation element and the size increases with increase in distance away from the foundation. Nevertheless, a soil element size is prescribed in order to limit the maximum size of the element.

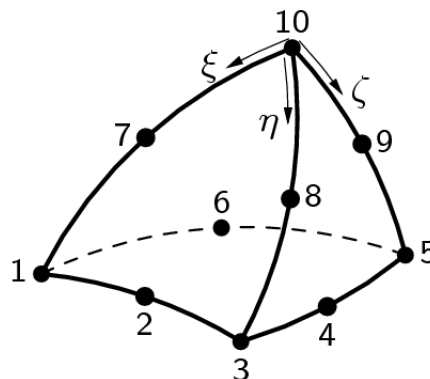


Figure 5.5: 10-node Regular Tetrahedron Solid Element Used to Model Concrete and Soil (CTE30)

(DIANA, 2016)

### 5.3.3 Soil Structure Interaction

The DIANA element library offers an interface element shown in Figure 5.6. The element size is dependant on the foundation element size in order to best capture the relative displacement and interface tractions precisely between the concrete foundation and the soil.

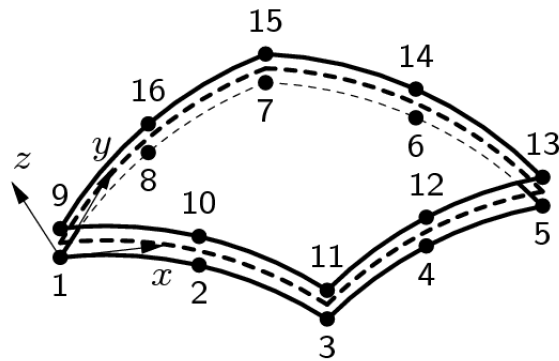


Figure 5.6: Plane Quadrilateral, 8+8 nodes, 3-D Interface Element (CQ481)  
(DIANA, 2016)

## 5.4 Analysis

Three different types of analyses are carried out, namely: Static Push Over, Cyclic Loading and Eigen Frequency Analysis. The main objective of each analysis carried out is described in this section. In instances where a comparative study is required, more than one model is developed for the same analysis. For all models developed, geometric non-linearity and physical non-linearity were activated.

The soil stress initialisation is carried in order to model the foundation as realistically as possible. To achieve this, a phased analysis approach is used. Four phases are defined. The first phase is the stress initialisation phase, with the self weight load applied for the in situ soil prior to excavations or construction. The phase activates the soil stress distribution for the in situ soil. The second phase is the excavation phase where the overburden pressure caused by the weight of the excavated material is removed and the concrete foundation is placed, and stresses activated simultaneously. The third phase is the stress activation of the backfill material. The last phase is the stress activation of the superstructure (tower, turbines and platforms) in the start step and the lateral wind load applied in the loading step(s). The analysis procedures used are as follows:

- For stress initialization in all phases  
Load incrementation : Explicit  
Iterative solution method : SECANT BROYDE  
Convergence criteria : FORCE or ENERGY with default tolerances
- Execution of "Wind loading"  
Load incrementation : Explicit  
Iterative solution method: NEWTON REGULA  
Convergence criteria : ENERGY with default tolerance

The phased analysis procedure is used for both the Static Push Over analysis and the Cyclic Loading analysis. Figures 5.7 to 5.10 show the various meshing for the phases and the included members of the models for each phase. The first phase is not shown because



it includes the same elements as the backfill phase with the difference being the change in the material properties of the concrete for ease of modelling.

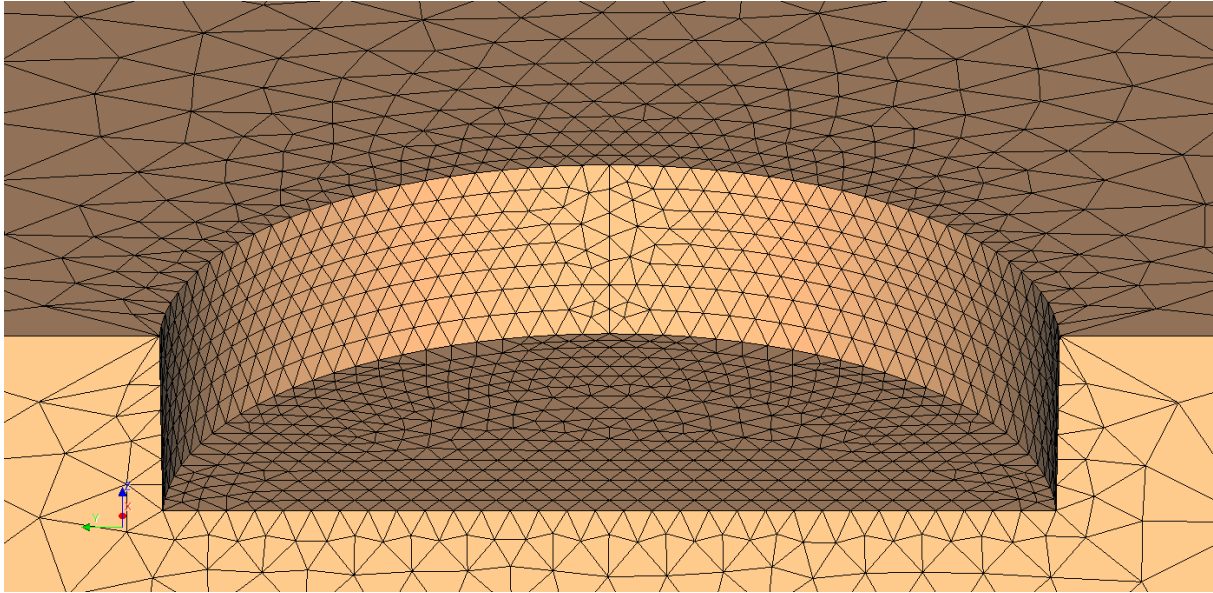


Figure 5.7: Excavation mesh: Second Phase

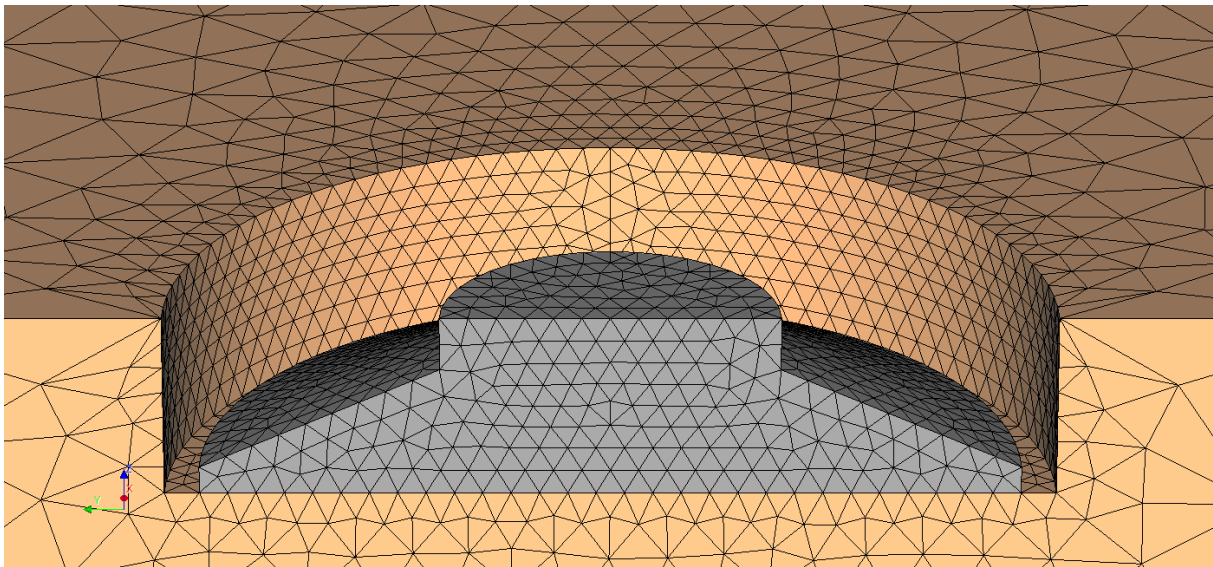


Figure 5.8: Excavation and concrete foundation mesh : Second Phase

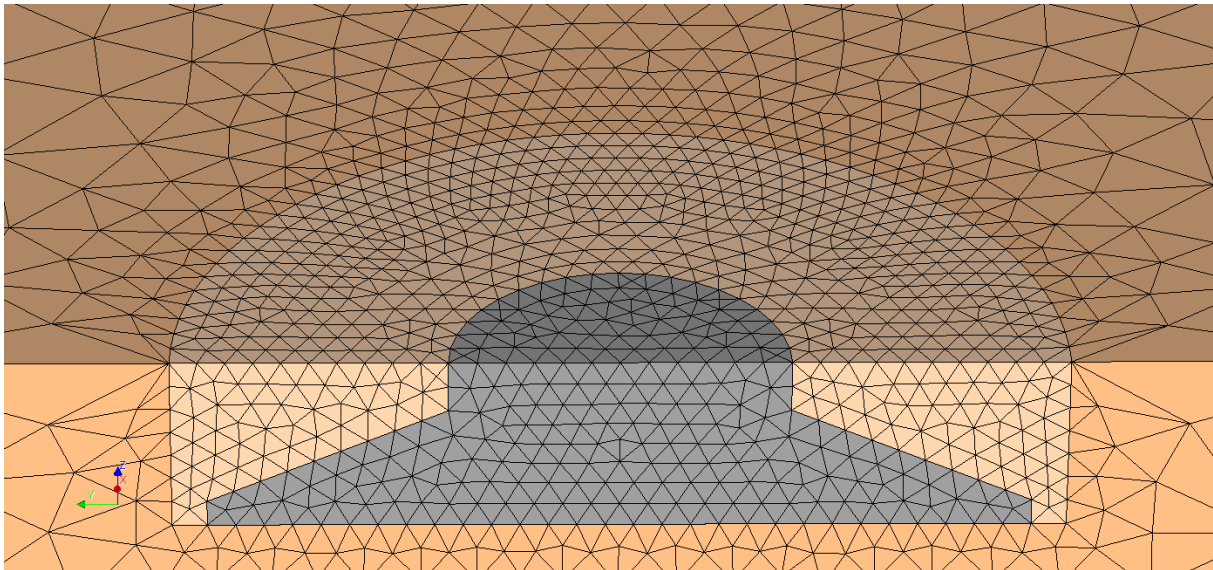


Figure 5.9: Foundation backfill mesh : Third Phase

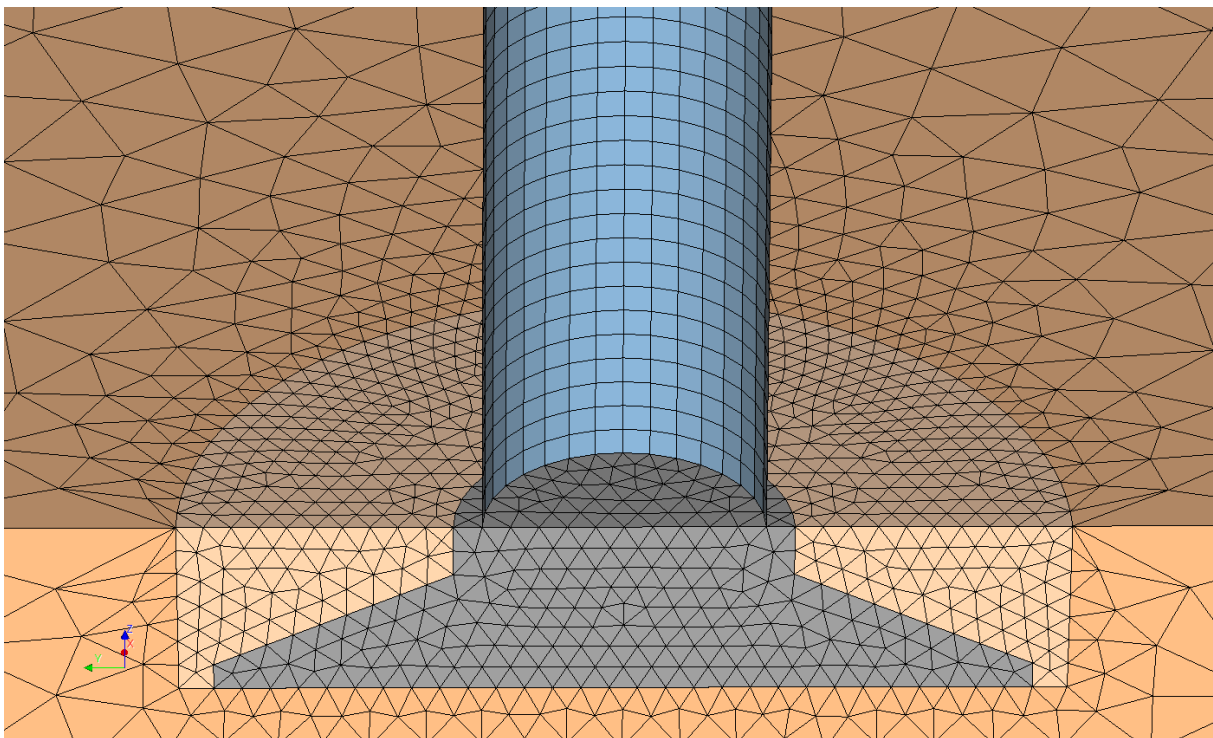


Figure 5.10: Tower on founded concrete foundation mesh : Fourth Phase

### 5.4.1 Static Push Over

One of the main objectives of the research is to consider back fill material as a structural material thereby reducing the concrete required in a wind turbine foundation. To this end, two models are built in order to establish a comparison. The first model is a conventional gravity base foundation footing named Model 1. The second model utilises back fill materials as a concrete replacement in areas of the foundation where the concrete only serves as a counterweight and offers no structural contribution; Model 2. Due to the

size of the models developed and computation time required, it is deemed economical to develop only one side of the models and apply symmetrical boundary conditions. The plane of symmetry is the vertical plane of symmetry of the wind tower structure. The mesh for both models is shown in Figure 5.11.

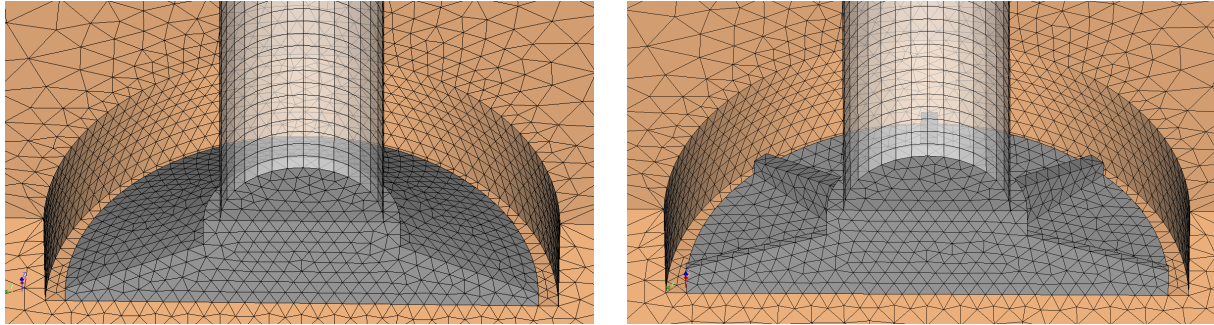


Figure 5.11: Model 1 (Left) Model 2 (Right)

Upon carrying out the analysis, it was established that the foundation has two possible causes of non-linear behaviour based on rotation of the foundation: 1) Lack of contact between base of the foundation and the soil on the windward side (gapping) and 2) concrete non-linear material behaviour due to cracking would result in a non-linear response. For the given model, it is important to identify which of the aforementioned modes of non-linearity occur first and also their influence on the structure. Thus, as an additional study, a reinforced concrete foundation with a total strain based crack model is developed and compared to a foundation with a linear elastic concrete material model. The two models are also subjected to a static push over analysis.

### 5.4.2 Cyclic Loading

A wind turbine foundation supports a tower that is not statically loaded. The development of a model subjected to a dynamic wind load history is beyond the scope of this research. Nevertheless, there is need to investigate the behaviour of the underlying soil when subjected to cyclic loading. The model is characterised by applying a wind load initially in one direction, unloading the structure in order to apply the load in the other direction. Finally, the same load is applied in the initial direction. Figure 5.12 illustrates the cyclic loading procedure in a visual manner. The same geometrical and material properties assigned to Model 1 (Figure 5.11) are used for the cyclic loading analysis.

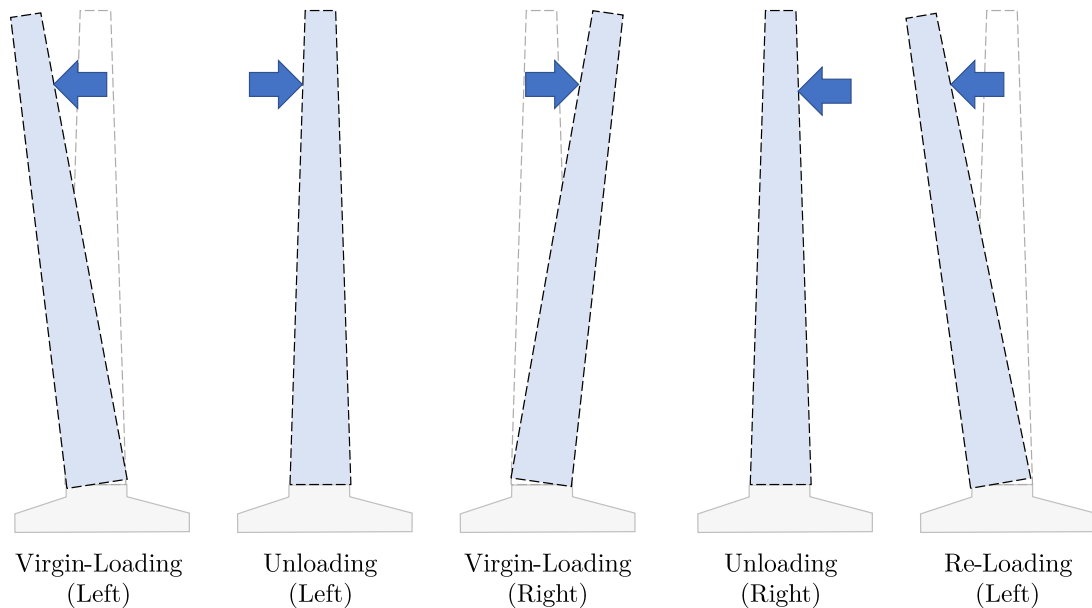


Figure 5.12: Cyclic loading procedure depicted in an exaggerated sketch

### 5.4.3 Eigen Frequency Analysis

A wind turbine tower supports a dynamic turbine with two main frequencies induced. The first is the blade rotation frequency (1P) and the second is the blade passing frequency (3P). Figure 5.13 shows the aforementioned frequencies. The tower should be designed with a natural frequency in the frequency range 1.1P and 2.7P for the specific turbine. A working frequency in this range yields the most economical design.

Energy dissipation or damping of wind turbine towers by the founding material has been postulated by numerous authors in literature. The main objective of the structural eigenvalue analyses carried out is to investigate this postulation further and most importantly, offer a numeric threshold to what could be regarded as founding material that offers significant damping to the structure. In order to achieve this, 9 different soil types, ranging from gravel to clay are investigated. The soil types are modelled as founding material in the FEA. The turbine and foundation geometry used for the push over analysis is maintained for the eigenvalue analysis. It is important to note that for the varying soil types modelled, there is need to model a different foundation size for each soil type in order to ensure a FoS against bearing. This is not done as this offers more degrees of freedom to the model comparative study. Therefore, the only difference prescribed to the varying models is the material properties of the founding material. A structural eigenvalue analysis is carried out for each soil condition and the natural frequency of the structure is obtained.

In order to verify the results from the FE eigenvalue analysis, a Single degree of freedom (SDOF) model is developed. The schematic illustration of the model is shown in Figure 5.14.

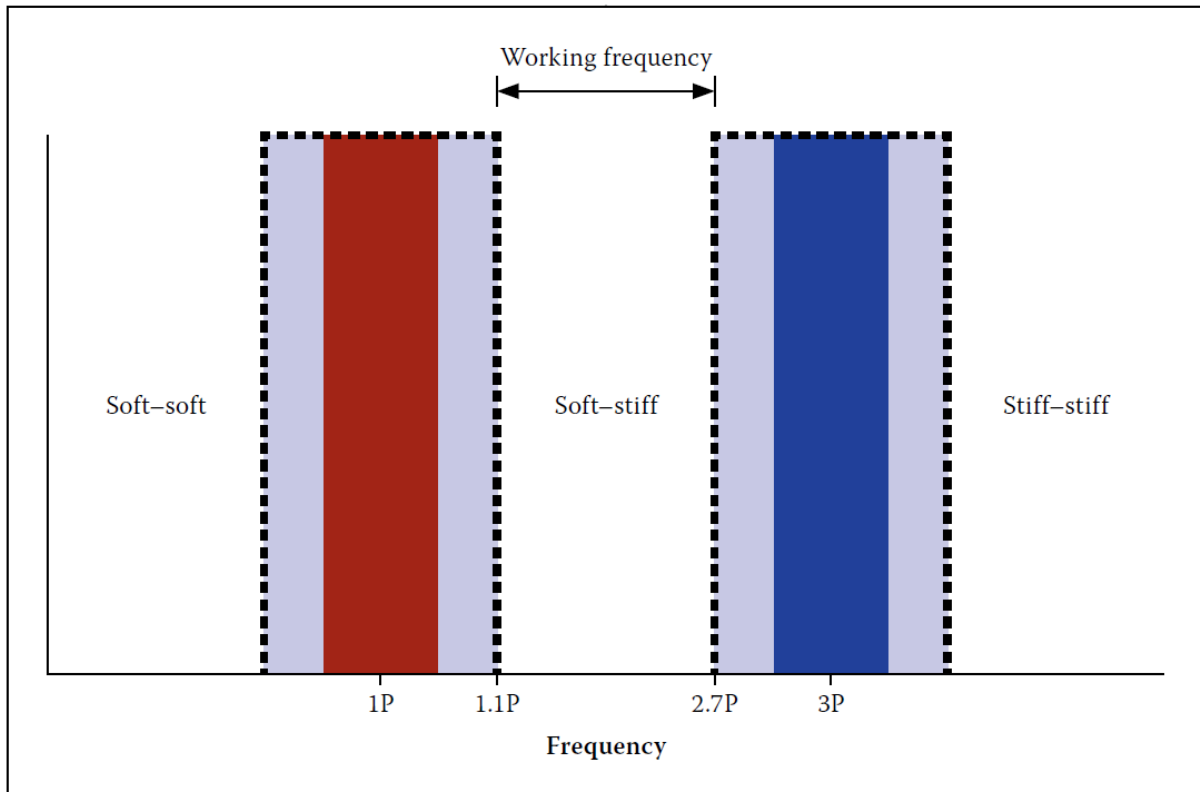


Figure 5.13: Working frequency for wind turbine foundation (Way, 2014)

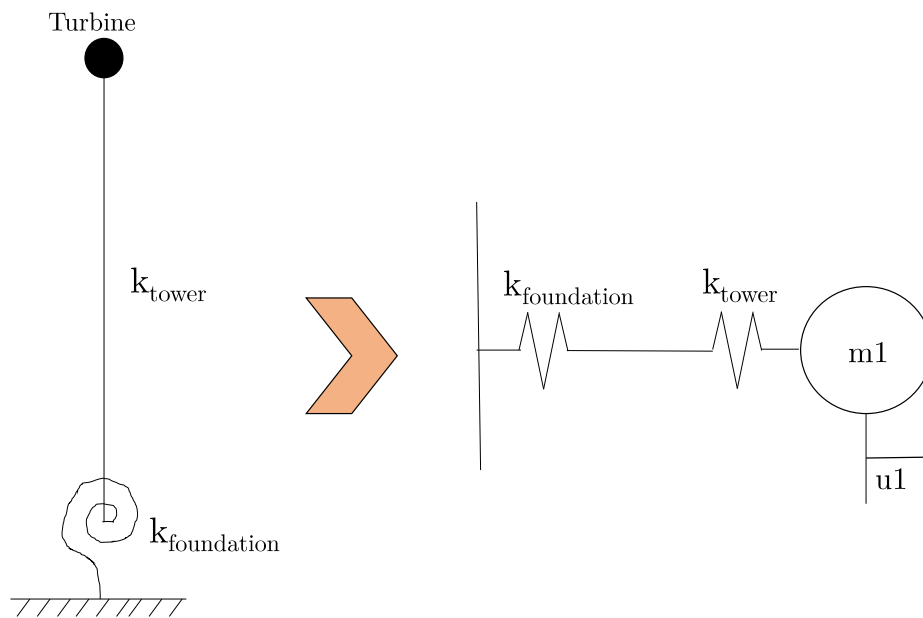


Figure 5.14: Single Degree of Freedom Simplification sketch

The rotational stiffness of the tower  $k_{tower}$  is calculated using the cantilever beam force-displacement relationship shown in Equation 5.2. The tower is tapered, so it does not have a constant moment of inertia  $I$ . However, the average radius of the tower was

used to calculate the moment of inertia for the SDOF problem calculation.

$$k_{tower} = \frac{3EI}{L^3} \quad (5.2)$$

DNV/Riso (2002) prescribes an equation to calculate the rotational stiffness of a circular foundation based on the radius of the foundation, the Poisson's ratio of the founding material and the stiffness of the material. The rotational stiffness  $k_{foundation}$  is calculated in accordance with the DNV/Riso (2002) as shown in Equation 5.3

$$k_{foundation} = \frac{8GR^3}{3(1-\nu)} \quad (5.3)$$

Where

$$G = \frac{E}{2(1+\nu)}$$

E is the unload/reload modulus of elasticity of the soil (derived from static tests),  $\nu$  is the Poisson's ratio of the soil and R is the foundation radius.

Figure 5.14 shows that the stiffness of the tower and the foundation are in series, therefore the effective stiffness used for the calculating the natural frequency of the SDOF problem is shown in Equation 5.4

$$K_{eff} = \frac{1}{\frac{1}{k_{tower}} + \frac{1}{k_{foundation}}} \quad (5.4)$$

Accounting for the mass distribution of the tower in the SDOF was done by modifying the natural frequency equation for cantilevered wind turbine towers, according to DNV/Riso (2002). The natural frequency calculation prescribed by the document is shown in Equation 5.6. From the equation it is evident that mass is added to the tower by a factor of 0.23. The same factor will be used in the SDOF problem.

$$f_n = \frac{1}{2\pi} \sqrt{\frac{3EI}{(0.23m_{tower} + m_{turbine})L^3}} \quad (5.5)$$

The natural frequencies for all 9 founding conditions are computed using Equation 5.6.

$$f_{SDOF} = \frac{1}{2\pi} \sqrt{\frac{K_{eff}}{M_{eff}}} \quad (5.6)$$

Where

$$M_{eff} = 0.23m_{tower} + m_{turbine}$$

# Chapter 6

## Results

This chapter reports and discusses the results obtained from the analyses described in Chapter 5. Section 6.1 reports on the Static Push Over analyses, Section 6.2 on the Cyclic Load analysis and Section 6.3 reports on the Eigenvalue analyses.

### 6.1 Static Push Over

#### 6.1.1 Gapping

Gapping, defined as the loss of contact between the foundation base and the founding soil, was observed in the Static Push Over analysis. Reference is made to Model 1 (conventional concrete foundation) in order to provide insight on the gapping observed.

Figure 6.2 shows the stress distribution beneath the base of the foundation. The stresses were captured by querying the vertical stress SZZ in each element (soil) along the base of the foundation. Figure 6.1 illustrates the elements queried for the acquisition of results. The querying was done for each load case, however, only three load cases are plotted for ease of interpreting the results. For the purposes of this study and of Figure 6.2, the following terminology will be used to interpret the results.

- **Initial Condition:** The load case that represents the stress initialisation of the soil and the application of the self weight prior to the lateral wind load.
- **Initial gapping:** The load case where the first 0 MPa SZZ stress is observed at a soil element directly beneath the concrete foundation.
- **Ultimate Load:** The load case where the maximum lateral load applied to the model.

Figure 6.2 shows the vertical stress distribution of the initial condition prior to the lateral load applied. It is seen that indeed that the stress distribution beneath the foundation is not entirely uniform, however, the achieved stress distribution for the **Initial Condition** agrees with the stress distribution reported by (Maunu, 2006) in Figure 2.7. In addition, Nicholson (2011) states that settlement for wind turbine foundations is not considered, as the contact pressure on the soil from the vertical loads are low. The results obtained in the **Initial condition** agree with the range proposed by Nicholson (2011) [50 kPa; 75

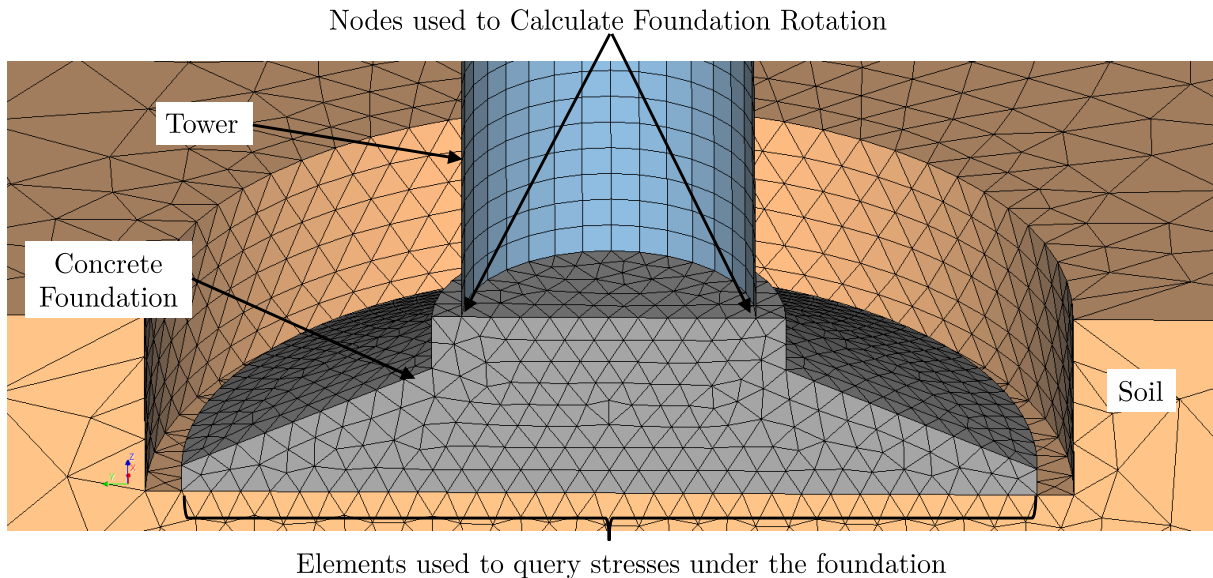


Figure 6.1: FEM Nodes and Elements queried for Results Calculation

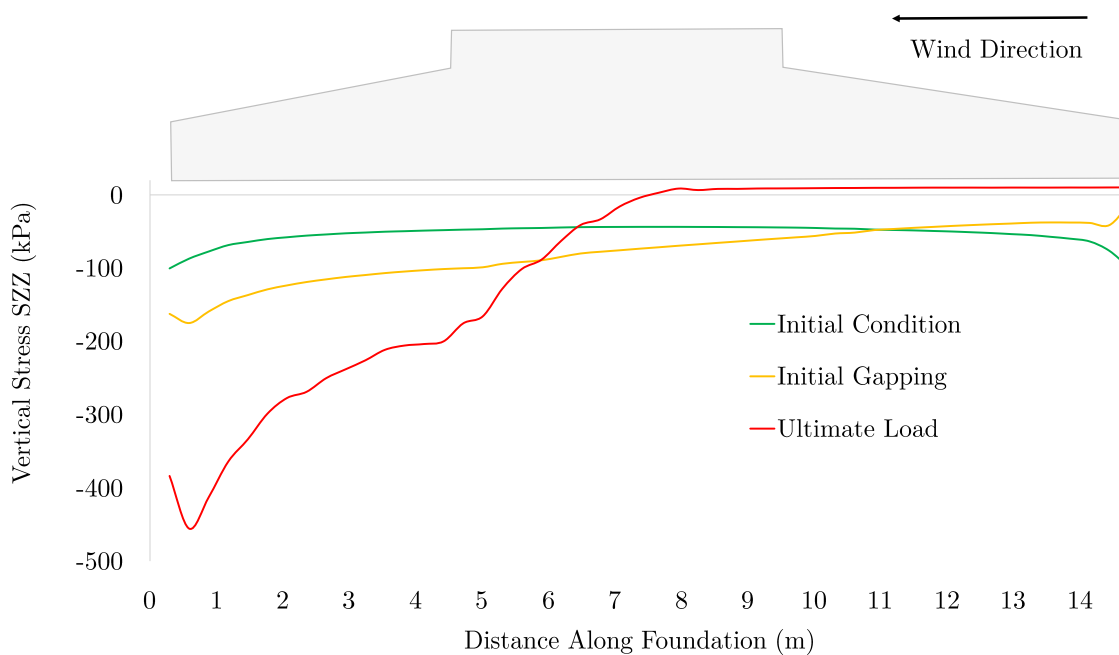


Figure 6.2: Stress Envelope for soil directly below the concrete foundation [kPa]. These consideration give confidence in the phased analysis approach used with soil stress initialisation and aid as a form of validation of the results.

At the **Ultimate Load** approximately 50% gapping is observed. 50% gapping is defined as the gapping that results in 50 % of founding soil directly below the foundation being unloaded ( $SZZ = 0$  MPa). To best illustrate this, screen shots of the gapping observed in analysis Model 1 are shown with corresponding load factors in Figures 6.3 to 6.5. Each figure also shows the relative interface displacement which is the vertical displacement between the soil and concrete foundation where gapping is achieved. The color contour



legend is used in conjunction with the top view for each load case as shown in the figure. Wind direction is from the right to the left in the y direction. From the Figures 6.3 to 6.5, it is seen that the uplift gradually occurs at the right toe (windward) of the foundation.

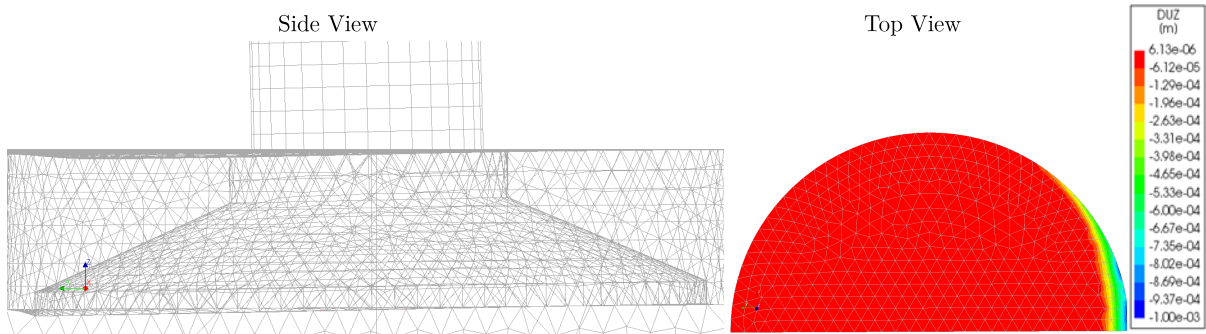


Figure 6.3: Initial Gapping at load factor 0.3

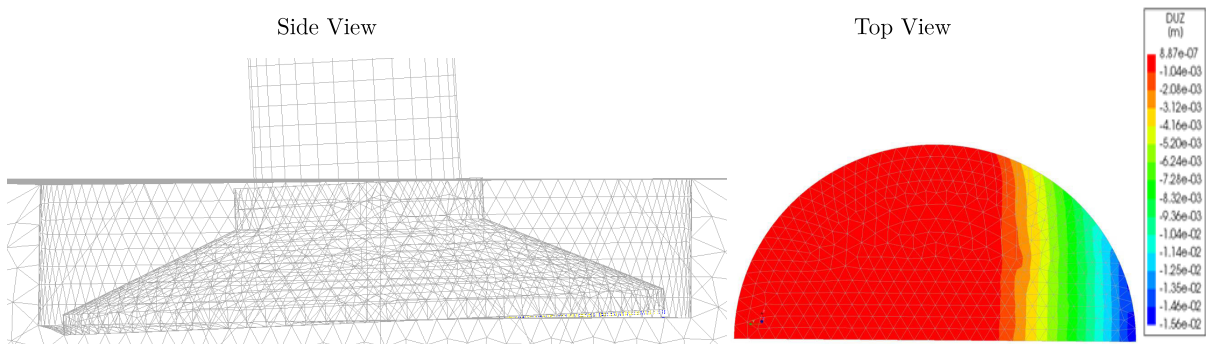


Figure 6.4: 25% Gapping at load factor 0.6

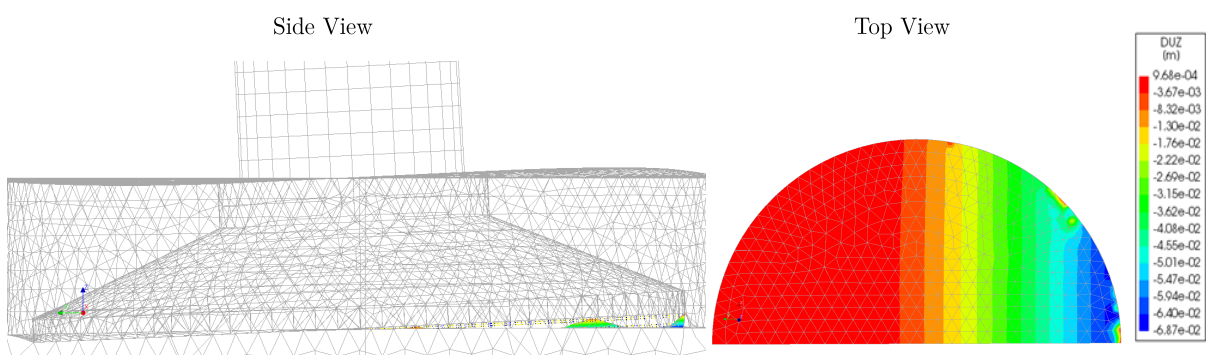


Figure 6.5: 50% Gapping at Ultimate Load

The foundation geometry for Model 1 was designed for a factor of safety (FoS) of 2.5 in Chapter 4. The FoS is based on the ratio between the allowable bearing capacity and the ultimate bearing stress over the affected area. The foundation does not fail with regard to the bearing capacity at the Ultimate (Wind) Load. However, the foundation experiences gapping, increasing the foundation rotation to a state where the limit to the

lateral displacement of the tower is reached for the model developed (1.25 % of Tower Height).

In principle, the geometry sizing explained in literature in Section 2.2.7 is based on an effective area calculation which inherently allows for gapping when a moment is applied. Figure 2.10 shows how only part of the foundation geometry transfers vertical bearing to the underlying foundation. The results shown in Figure 6.3 to 6.5 agree with this design approach, however at the detriment of the rotational stiffness of the foundation.

## 6.1.2 Conventional Foundation vs Reduced Concrete Foundation

The basis of comparison between foundation types modelled is primarily the rotational stiffness, but the stress distribution also receives attention.

### 6.1.2.1 Foundation Rotation

The rotation of the foundation is calculated by dividing the vertical displacement difference between nodes on the top of the foundation stub (Figure 6.1) by the horizontal distance between the nodes. Due to the small angles, the calculated values are converted from radian to degrees for each load case without any trigonometry functions used. Figure 6.6 shows the foundation rotation as well as the tower top displacement as a function of the load factor for the two foundation types. Model 1 and Model 2 refer to the conventional foundation and reduced concrete foundation respectively.

The concrete material model used is a linear elastic material. Thus the non-linearity shown in Figure 6.6 is purely due to the non-linearity of the SSI resulting in gapping. Figure 6.3 shows that the initial gapping is achieved at a load factor of approximately 0.3 and this is consistent with the foundation rotation curve for Model 1. For a load factor less than 0.3 the curve approximates a linear curve.

The lateral displacement at the top of the tower is also plotted. Nicholson (2011) recommends a limit to the lateral displacement of the tower. The limit is given as 1.25 % of the height. For the 117 m tower modelled this limit approximates a lateral displacement of 1.5 m. The lateral displacement limit is violated for both Model 1 and Model 2 at a load factor of 0.62 and 0.58 respectively. Although not shown in Figure 6.6, the tower top rotation is also limited to 5 % in order to avoid the blades from coming in contact with the tower. The maximum tower top rotation observed was 2.25 % at a load factor of 0.9.

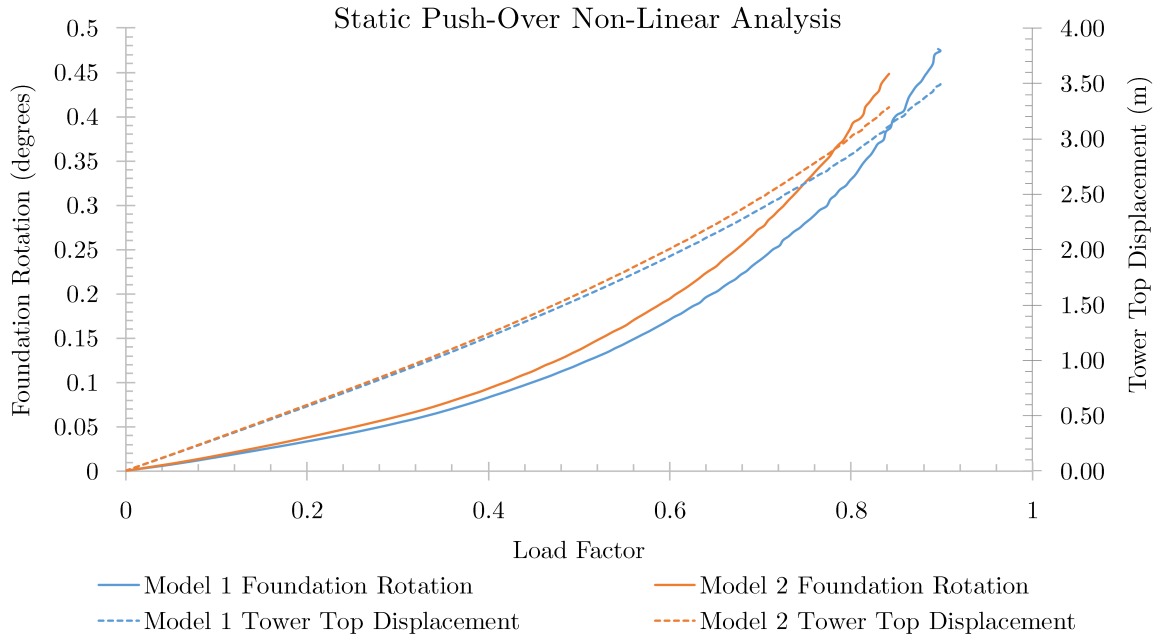


Figure 6.6: Foundation Rotations and Tower Top Displacement for Static push over analysis; Model 1 and 2

### 6.1.2.2 Stress Distribution

An important parameter to compare is the stress distribution in the foundation because the concrete replacement with backfill reduces the structural material in the foundation. To best illustrate this, the vertical normal stresses  $SZZ$  in the foundation are compared for the two foundations. Likewise, a comparison is also drawn in terms of the lateral normal stresses  $SYY$ . Granted that the analysis uses a linear elastic soil model with no tensile stress limits or steel reinforcement, the stress distribution in the foundation at the ultimate load exceeds the tensile limits of realistic concrete. However, a comparison purely based on the stress redistribution according to Saint Venant's principle is used. Saint Venant principle states that the stress and strain produced at points in a body sufficiently removed from the region of load application will be the same as the stress and strain produced by any applied loading that have the same statically equivalent resultant, and are applied to the body within the same region (Hibbeler, 2014). In Model 1 and 2, the connection of the tower and the concrete is a tower shell element (0.0235 m thick) connected to the solid concrete element. This connection results in stress concentrations that are not realistic at the connection because realistically the load transfer method is employed e.g. anchoring cage. However, the influence of the concentrated stress is insignificant at a distant away from the connection. The stress distribution results compared for Model 1 and 2 are at a distance of 1 m and 2.9 m away from the tower to foundation connection.

Figures 6.7 and 6.8 show the  $SZZ$  and  $SYY$  stress distributions for the foundation respectively. For both Models 1 and 2, the concrete foundations experience concentrated stresses of up to 35 MPa in tension and 56 MPa in compression at the tower to foundation connection. This is obviously not a representation of the actual foundation but hypothetical illustration of the stress distribution.

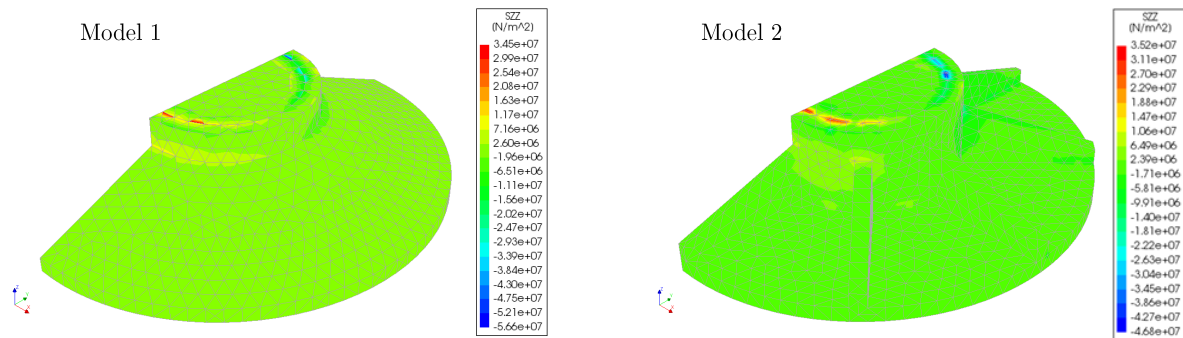


Figure 6.7: Normal Stress SZZ

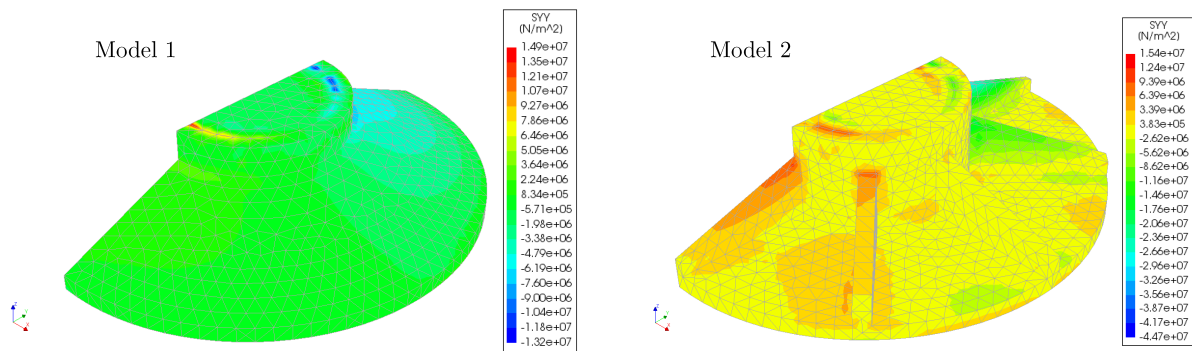


Figure 6.8: Normal Stress SYX

A cutting plane is used to section the foundation at 1 m below the tower base. This plane attempts to investigate the stress distribution at the geometrical discontinuity from the stub to the base of the foundation. It is postulated that this is a sufficient distance from the connection to allow for Saint Venant's principle to hold. Figures 6.9 and 6.10 show the stress distribution at the cutting plane 1 m away from the base. Evidently, the maximum SZZ stresses observed in Model 1 are 6.7 MPa and -12 MPa. In the case of the Model 2, higher SZZ stresses are observed 9.4 MPa and -32 MPa. DIANA sign convention regards negative stresses as compression and positive stresses as tension. For all practical purposes the observed stresses as shown in Figures 6.9 and 6.10 are a fair representation of the stress distribution in the concrete foundations. Indeed the tensile stresses exceed the conventional concrete limits (2 MPa to 4 MPa), however this is sufficient to aid a designer with insight for steel placement.

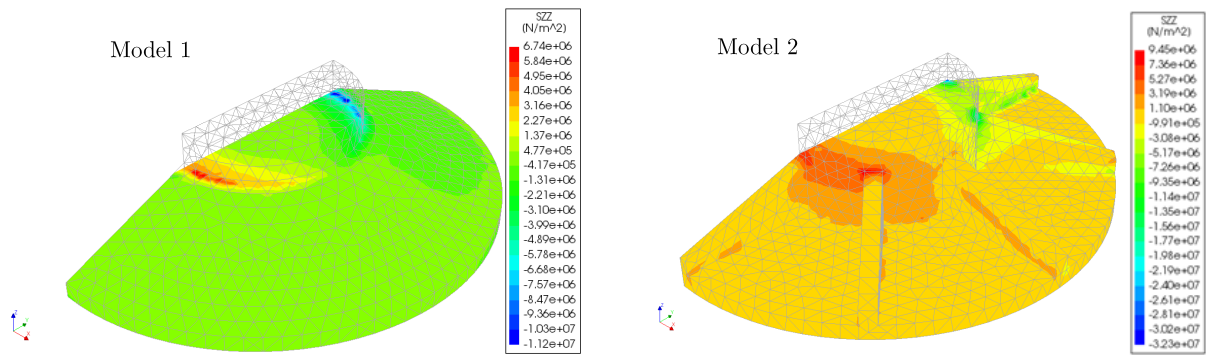


Figure 6.9: Normal Stress SZZ : Sectional View 1 m below Tower Base

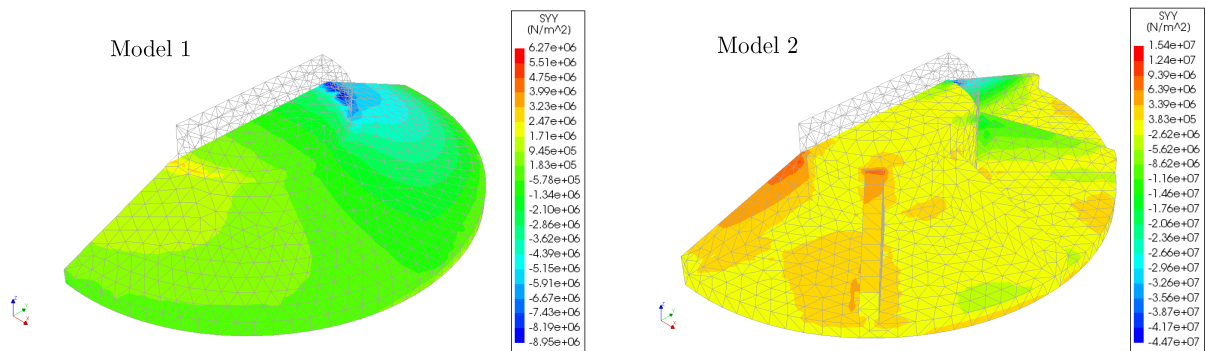


Figure 6.10: Normal Stress SYY : Sectional View 1 m below Tower Base

The final cutting plane is applied at a distance 2.9 m below the tower base. The purpose of this plane is to establish stress distribution near the base of the foundation. Chapter 4 highlights in the STM design method that the base is a critical component for flexural steel design. Figures 6.11 and 6.12 show the stress distribution at the cutting plane 2.9 m below from the base. The maximum SZZ stresses observed in Model 1 are 0.4 MPa and -2.5 MPa. From Model 2 the maximum SZZ stresses observed are 3.5 MPa and -12 MPa as shown in Figure 6.11. A worms view is used to best show the SYY stress distribution. Figure 6.12 shows the maximum tensile SYY stresses for Model 1 and 2 as 6.27 MPa and 15.4 MPa respectively. As expected there are high lateral stresses, resulting in the need for flexural steel in a radial placement.

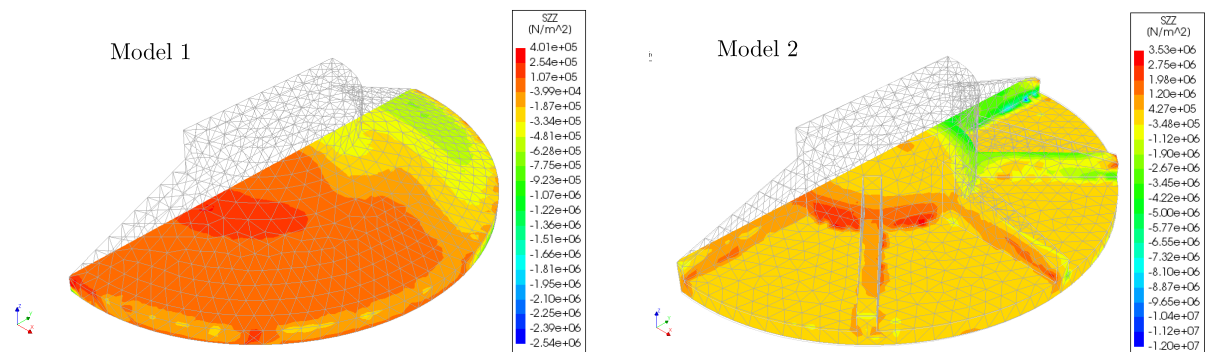


Figure 6.11: Normal Stress SZZ :Sectional View 2.9 m below Tower Base

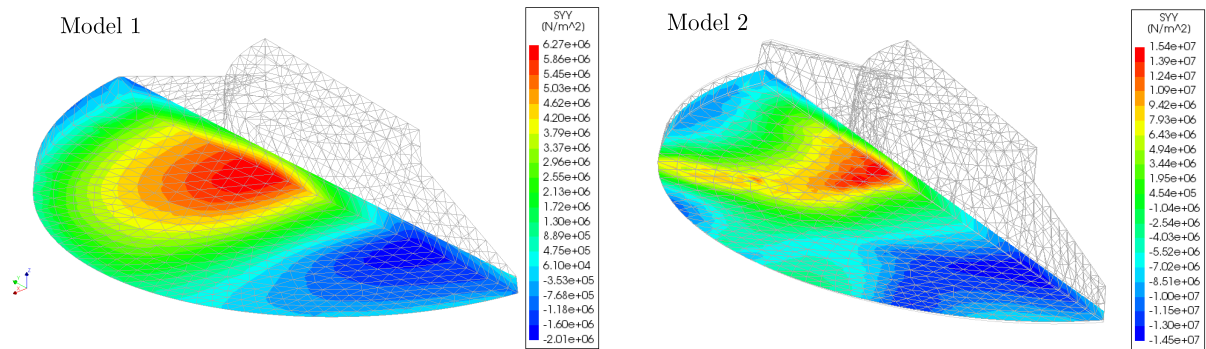


Figure 6.12: Normal Stress SYY :Sectional View 2.9 m below Tower Base (Worm's Eye View)

Figures 6.9 to 6.12 agree with the postulation that there are higher stress concentrations in Model 2 than Model 1. This is because Model 2 has more geometric discontinuities. However, one of the research objectives is to investigate the feasibility of concrete replacement by backfill. In the foundation regions where the concrete is removed, it is seen in Model 1 that there is certain under-stressed concrete and that the critical structural concrete is directly below the tower and also at the base of the foundation.

### 6.1.3 Linear Elastic Concrete vs Total Strain Based Crack Model Concrete

Model 1 is used to establish the influence of the material non-linearity in the concrete. Two models are compared, one with a Linear Elastic (LE) material behaviour and the second model with a Total Strain Based Crack (TSBC) material behaviour. Both models consist of the same concrete geometry. The model with the Total Strain Based Crack Model (DIANA, 2016) also included embedded reinforcement steel as designed in Chapter 4 and the anchoring cage as the connection method between the tower and the foundation. Figure 6.13 shows the foundation rotation in degrees for two foundation models developed. The two models behave similarly between the load factor 0 to 0.27 which approximately coincides with the loading prior to the **Initial Gapping**. There is no evidence to assert that the material non-linearity (cracking) occurs prior geometric non-linearity (gapping).

From Figure 6.13 it is seen that the additional non-linearity due to cracking of the concrete reduced the foundation rotational stiffness.

From Section 6.1.2 and 6.1.3 it seen that there are two sources of non-linearity in the foundation rotation stiffness; gapping and cracking of concrete.

This section also reports on the crack distribution in the wind turbine foundation. From the linear elastic model the stresses that exceeded the typical tensile strength of concrete are seen on the connection between the foundation and the tower. From the reinforced concrete model with TSBC material model, it is observed that the crack propagation emanated from the tower to foundation connection. At a load factor of approximately 0.28 initial gapping is observed and the associated initial cracks and crack width results are shown in Figure 6.14. It is important to note that the reinforcement modelled was the main flexural reinforcement steel as calculated in Chapter 4. The stresses in the reinforcement are also queried and reported in Figure 6.15. It was seen that the stress

stress concentration was at the anchor rods of the tower foundation connection. Due to the mesh size of the foundation (0.5 m), the pair of rods are modelled as one rod with twice the rod diameter.

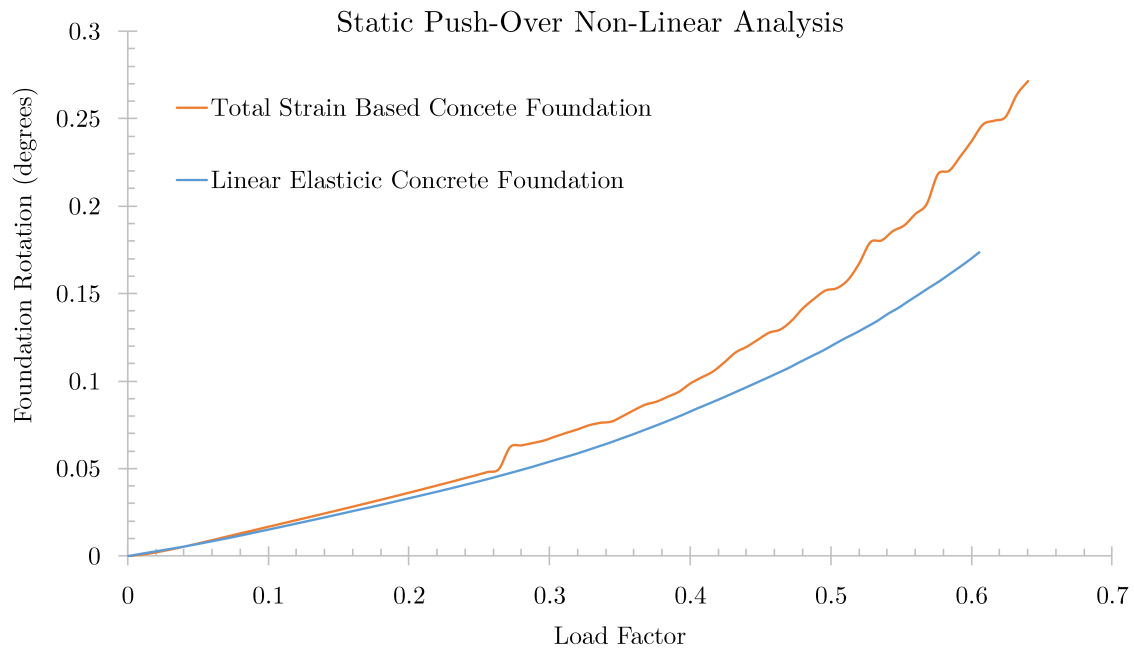


Figure 6.13: Linear Elastic Concrete Foundation vs Total Strain Based Crack Model Concrete Foundation

From Figure 6.14 and 6.15, it is concluded that the connection between the foundation and tower is critical and should be well reinforced and grout provided under the tower flanges as this region experiences high tensile and compressive stresses. The main tensile cracks propagated from the connection which is also dependant on the connection method employed.

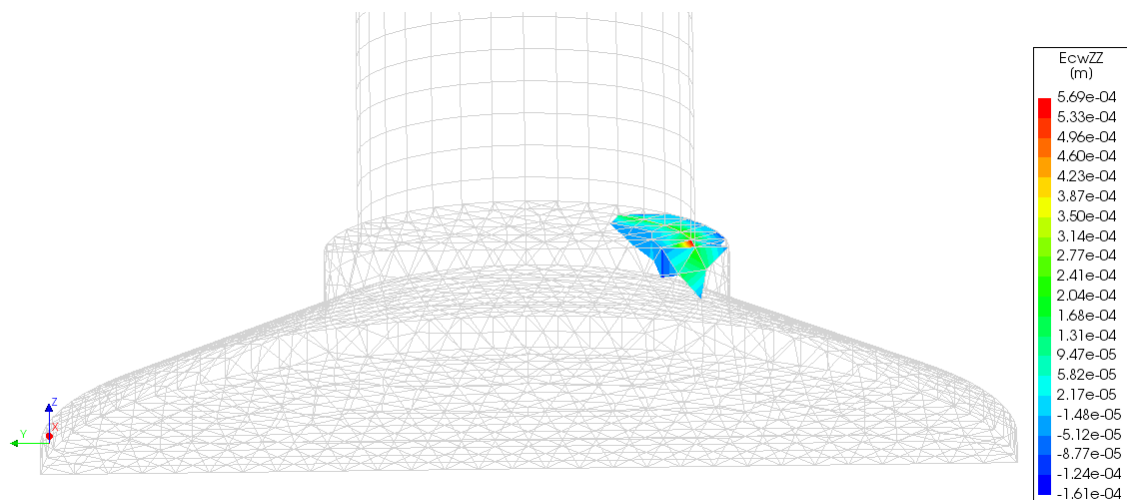


Figure 6.14: Crackwidth at initial gapping

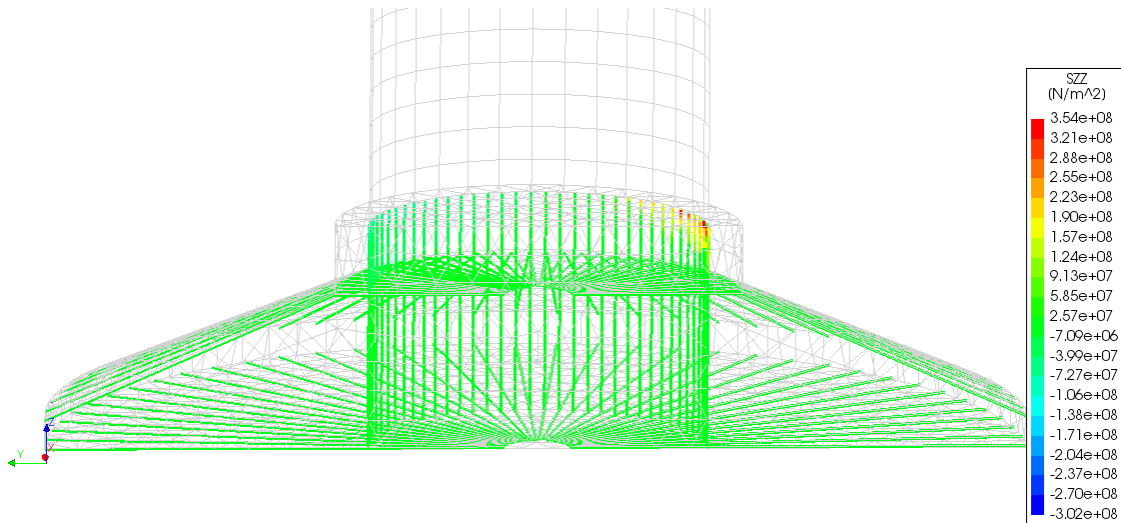


Figure 6.15: Stress distribution in Reinforcement

## 6.2 Cyclic Loading

Figure 6.16 shows the response of the foundation under a cyclic load. The response shows that the loading stiffness (rotation) varies from the unloading stiffness. The graph also shows that the re-loading stiffness is greater than the virgin loading stiffness. This response was postulated after an oedometer test was modelled in DIANA to analyse the soil behaviour in compression loading and unloading. Specifically, the stiffness of the soil under reloading was similar to the unloading stiffness within the stress range that was previously achieved in the virgin loading. Beyond the previously achieved loading the stiffness of the soil is the same as the virgin loading stiffness as shown in the oedometer results in Figure 6.17. The maximum wind load applied for the cyclic load analysis is less than the load factor of 0.3 for the static push over analysis. Thus, the cyclic load analysis was conducted in the linear region for both the material and geometry i.e no material non-linearity or gapping occurred.

From both Figures 6.16 and 6.17 it is seen that the unloading stiffness is approximately equal to the re-loading stiffness.



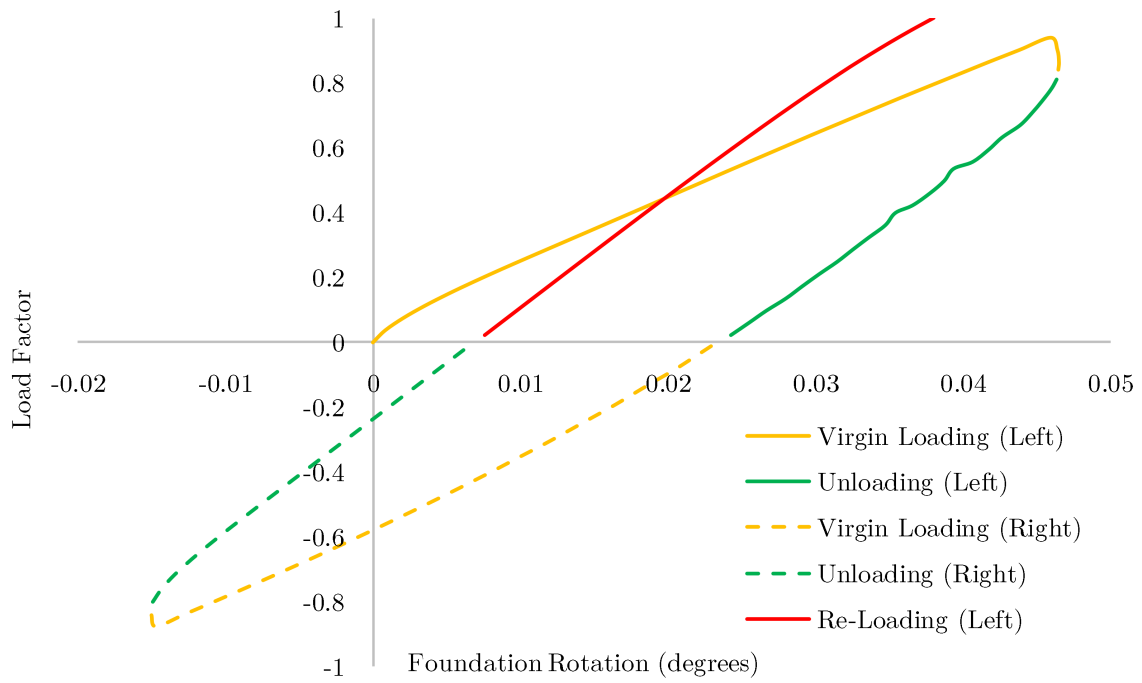


Figure 6.16: Cyclic Loading Results

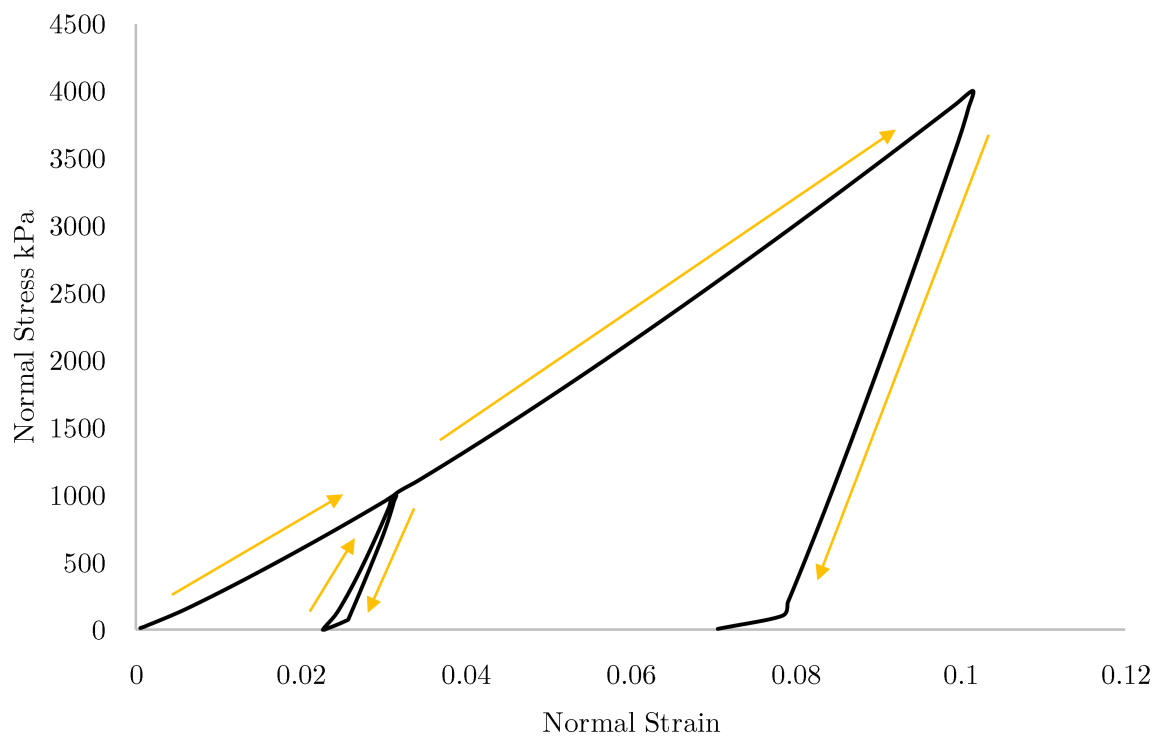


Figure 6.17: Oedometer Test Results

### 6.3 Eigen Frequency Analysis

The eigenvalue analysis is carried out with symmetrical boundary conditions. Therefore the non-symmetrical mode shapes are lost. Figure 6.18 shows the mode shapes obtained for the fine sand founding material, which is also the soil type used for the push over analysis and the cyclic load analysis.

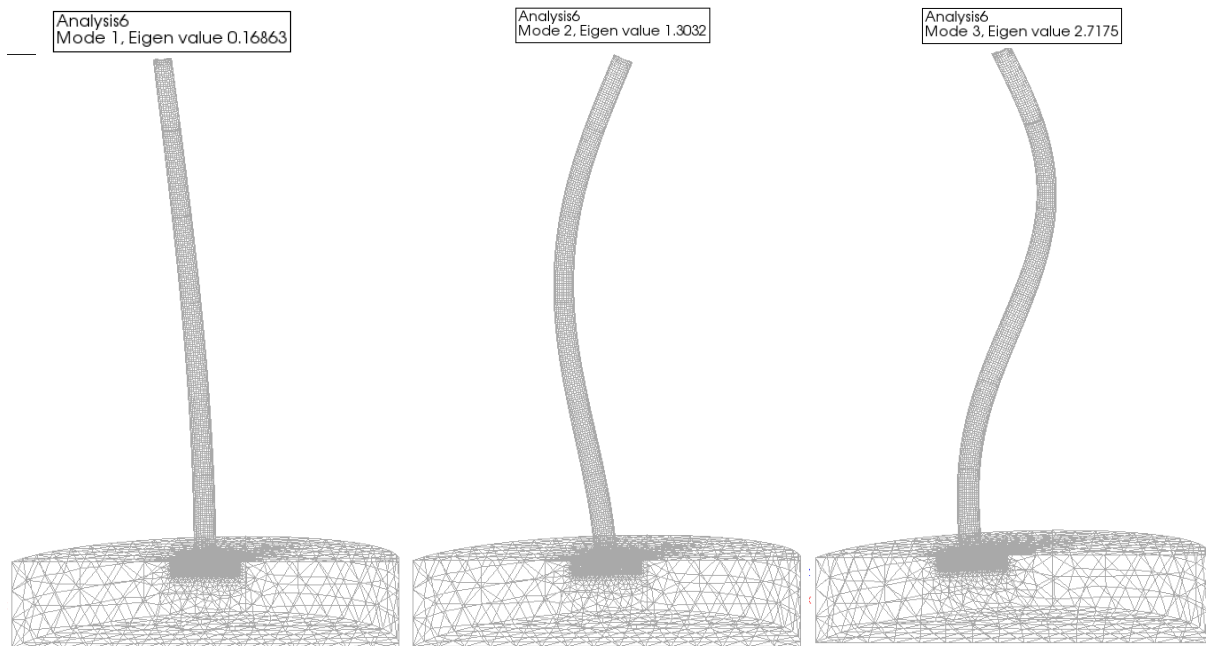


Figure 6.18: First 3 mode shapes for the structural eigenvalue analysis for fine sand soil type category

The wind turbine tower used in this research has a working frequency range of [0.165 Hz; 0.182 Hz]. The results from the 9 soil types modelled are tabulated in Table 6.1. The shading red highlights the natural frequencies that do not fall in the working frequency range.

It is evident that the natural frequency of the structure is dependent on the stiffness of the soil. Increase in stiffness results in increase in the natural frequency and in turn a decrease in stiffness results in the decrease in natural frequency. It was observed that soft soils offer more energy dissipation to the foundation than stiff soils. It is important to note that towards achieving a variable parameter in the soil types, a sensitivity analysis was conducted on the influence of friction angle on the natural frequency. It was observed that the friction angle does not influence the natural frequency in any way as it is a strength parameter and not a stiffness parameter.

It is also important to note that the variation in the natural frequency based on the SDOF calculation is minimal. This is because the foundation rotational stiffness is orders of magnitude larger than the tower rotational stiffness. Table 6.2 shows the rotational stiffness of the foundation for each soil type as calculated by Equation 5.3 as well as the effective stiffness (Equation 5.4) used for the natural frequency calculation (Equation 5.6).

Table 6.1: First Eigenvalue results: Natural frequency

Soil Type	$E_{Stat}$ [MN/m <sup>2</sup> ]	$E_{Dyn}$ [MN/m <sup>2</sup> ]	Natural Frequency Hz	
			Diana FEM	SDOF Calc
Sand, Fine	30	170	0.16863	0.1763701
Sand	55	250	0.17047	0.1763708
Sand, Coarse	70	400	0.17148	0.1763709
Gravel	100	600	0.17172	0.1763711
Clay, Soft	5	70	0.14857	0.1763625
Clay	10	140	0.15981	0.1763670
Clay, Stiff	20	280	0.16629	0.1763693
Sandy clay, soft	8	80	0.1568	0.1763659
Sandy clay, stiff	15	120	0.16405	0.1763685

Table 6.2: Rotational stiffness values used for SDOF Eigenvalue analysis

Soil Type	$E_{Stat}$ [MN/m <sup>2</sup> ]	$G_{Stat}$ [MN/m <sup>2</sup> ]	$k_{foundation}$ [Nm/rad]	$k_{tower}$ [Nm/rad]	$K_{Eff}$ [Nm/rad]
Sand, Fine	30	10.7	1.91E+10	3.14E+05	3.14E+05
Sand	55	19.6	3.49E+10	3.14E+05	3.14E+05
Sand, Coarse	70	25.0	4.45E+10	3.14E+05	3.14E+05
Gravel	100	35.7	6.35E+10	3.14E+05	3.14E+05
Clay, Soft	5	1.9	3.04E+09	3.14E+05	3.14E+05
Clay	10	3.7	6.08E+09	3.14E+05	3.14E+05
Clay, Stiff	20	7.4	1.22E+10	3.14E+05	3.14E+05
Sandy clay, soft	8	3.0	4.87E+09	3.14E+05	3.14E+05
Sandy clay, stiff	15	5.6	9.12E+09	3.14E+05	3.14E+05

It is also observed in the results tabulated in Table 6.1 that the SDOF natural frequencies calculated are larger than the FEM natural frequency calculations. This is primarily because the SDOF, as the name states has one degree of freedom and does not incorporate the geometrical non-linearities or second order effects of the tower hence resulting in a "stiffer" approximation of the tower stiffness.

# Chapter 7

## Cost Comparison

### 7.1 Introduction

This chapter reports on the cost comparison of implementing alternative wind turbine foundations. Acknowledging that there are parameters like distance and man hours not included in this comparison, it is deemed necessary to report on cost comparison based purely on the material quantities. The cost estimates are based on current rates in South Africa. The rates reported on in this chapter are supplied by an industrial source and, although the rates vary from supplier to supplier, a reasonable cost estimate is drawn.

### 7.2 Typical wind energy project in South Africa

The wind energy industry in South Africa is based on a public-private partnership under the program called the Renewable Energy Independent Power Producer Procurement Program (REIPPPP). This program has successfully channelled substantial private sector expertise and investment into grid-connected renewable energy in South Africa at competitive prices. By March of 2016 the commulative capital investment in to wind energy was approximately R192 billion of which 28 % was foreign investment. Each wind energy project consists of various stakeholders from financial service providers, project managers, developers, engineers and many others; resulting in economic growth and job creation (Eberhard *et al.*, 2014).

With regard to the construction of each wind turbine structure, the wind turbine supplier also supplies the tower which is designed specifically for each turbine. Thereafter design loads are given to the foundation designer who is responsible for designing a foundation that is sufficient to support the given tower. As envisaged, there is interdisciplinary collaboration for each project requiring team work as each role player's success is dependant on the other.

### 7.3 Wind energy project cost breakdown

Way (2014) reports on the costing for wind turbine structures as motivation for the need to optimise the turbine tower. Table 7.1 shows the cost breakdown of a typical South African wind energy project. Although it is seen that the foundation cost percentage relative to the project cost is 5 %, Way reports that the foundation costs vary from 4 % to 15 % of the cost of some projects encountered in his research. Table 7.1 provides

a cost breakdown by percentage, this study attempts to quantify the relative cost of the foundation.

Table 7.1: Cost breakdown of a typical South African wind energy project (Way, 2014)

Component	% of total cost
Grid Connection	12
Civil Works	4
Other Capital Costs	8
Tower	19
Electrical and Mechanical Constituents	14
Rotor, Blades, Rotor Accessories	18
Gearbox	9
Generator	2
Foundation	5*

## 7.4 Foundation Cost Comparison

Tables 7.2 and 7.3 show the cost breakdown of foundations used in the two models developed for this research. A cost comparison of the two foundation is drawn. A 37% concrete volume reduction is achieved by the implementation of the foundation in Model 2 design (reduced concrete foundation).

Table 7.2: Material cost for Model 1

Description	Unit	Quantity	Rate (R)	Cost (R)
Excavate for bases	$m^3$	580.00	160.23	92 933.40
Back filling material	$m^3$	275.00	82.88	22 792.00
Excess material for carting away	$m^3$	304.00	259.68	78 942.72
Concrete 35MPa in base	$m^3$	304.00	1 460.60	444 022.40
Mass concrete blinding under base 15mpa	$m^3$	13.00	1 328.00	17 264.00
Formwork to side of bases	$m^2$	66.16	189.10	12 511.42
Steel rods $80kg/m^3$	t	30.40	12 004.42	364 934.37
Total				1 033 400.31

Table 7.3: Material cost for Model 2

Description	Unit	Quantity	Rate (R)	Cost (R)
Excavate for bases	$m^3$	580.00	160.23	92 933.40
Back filling material	$m^3$	389.20	82.88	32 256.90
Excess material for carting away	$m^3$	190.80	259.68	49 546.94
Concrete 35MPa in base	$m^3$	190.80	1 460.60	278 682.48
Mass concrete blinding under base. 15mpa	$m^3$	13.00	1 328.00	17 264.00
Formwork to side of bases	$m^2$	184.85	189.10	34 955.14
Steel rods $80kg/m^3$	t	19.08	12 004.42	229 044.33
Total				734 683.19

From Table 7.2 and 7.3 it is seen that there is a 29 % saving in cost per foundation for the given models. It should be noted that the cost estimation does not account for the difference in man hours between the construction of the two foundations as it is envisaged that the foundation in Model 2 might require two pours of concrete unlike the foundation in Model 1. The complexities of accounting for the time loss are unique to each project thus for the purposes of this study a comparison purely based on material quantities is conducted. Thus the implementation of a reduced concrete model like model 2 type foundation could potentially yield a significant cost saving and is worth considering during the project's design phase.

From the Loeriesfontein wind farm as a case study; the project consists of 61 wind turbines. Implementation of concrete replacement by backfill for each and every wind turbine would result in a cost saving of approximately R 18 million. This is a significant amount when economies of scale are taken into account.

In conclusion, although the foundations cost by percentage is approximately 5 % of the wind energy project cost, there is potentially a significant economic cost benefit to implementing concrete replacement by backfill. Added to that the reduced carbon footprint is also important.

# Chapter 8

## Conclusions and Recommendations

### 8.1 Conclusions

This section reports the conclusions drawn from the research. Firstly, conclusions based on design approaches are made in terms of the geotechnical and structural design, followed by conclusions based on the concrete volume reduction by aggregate replacement or concrete replacement by backfill. Lastly, general conclusions are made based on the research experience and limitations.

#### 8.1.1 Geotechnical Design

A comprehensive approach to designing gravity based wind turbine foundations was reviewed. From literature it was discovered that the main geometrical design approach for wind turbine foundation sizing is based on the guidelines provided for wind turbine design by (DNV/Riso, 2002). This design approach was used and applied in a finite element model. This study concludes that the bearing pressure distribution assumed in this design approach implies that gapping will occur. Nevertheless the gapping can be reduced by increasing the foundation size and thus reducing the ratio of the eccentricity  $e$  to the width of the foundation  $D$ . This increases the effective area used in the bearing capacity calculation and also increases the rotation stiffness. In summary the study concluded that:

- The FoS design approach does not necessarily ensure sufficient rotational stiffness of the foundation, although it is sufficient to ensure safety against shear failure of the bearing soil.
- In principle, the geometry sizing explained by (DNV/Riso, 2002) is based on an effective area calculation which implies gapping will occur when a moment is applied.

#### 8.1.2 Structural Design

In light of the structural design involving steel reinforcement placement the study concluded that:

- The Beam Theory Method (BTM) yields conservative results as opposed to the Strut and Tie Method (STM) for flexural reinforcing steel design.

- Assumptions on which the BTM rely are violated when used for wind turbine foundation design because of the geometric discontinuities and thickness of the foundation. The geometry of the wind turbine foundation has abrupt changes creating discontinuities for example between the stub and the base. This results in both static discontinuities and geometrical discontinuities. The BTM is based primarily on the assumption that the beam is not discontinuous and that shear deformation is small compared to flexural deformation.
- Shear reinforcement is not crucial in gravity base foundations. However, reinforcement stools used to aid the placement of the reinforcement offer shear reinforcement.
- From Chapter 4 it is concluded that the crack width compliance governs the foundation steel spacing.
- From the Total Strain Based Crack model it is concluded that the connection between the foundation and tower is critical and should be well reinforced and grout provided under the tower flanges as this region experiences high tensile and compressive stresses. The main tensile cracks propagate from the connection which is also dependent on the connection method employed.

Another structural parameter is the dynamic behaviour of the structure. The following was concluded with regard to the wind turbine foundation influence on the superstructure natural frequency.

- Soil offers damping / energy dissipation to wind turbine foundations.
- The stiffness of the soil determines the influence a soil has on the natural frequency of the superstructure; High stiffness results in higher natural frequency and lower energy dissipation whilst lower stiffness results in a lower natural frequency and a high energy dissipation.
- The simplified natural frequency calculation by SDOF problem results in a higher estimate of the foundation stiffness. The SDOF calculation does not rigorously account for the effect of non-linear soil stiffness on the natural frequency.
- The rotational stiffness of the foundation is larger than the rotational stiffness of the tower by several orders of magnitude.
- The stiffness of the soil has a larger influence on the natural frequency of the structure than the strength of the soil.

### 8.1.3 Concrete Volume Reduction

Concrete volume reduction was achieved by use of denser aggregate in the concrete mix of the foundation and concrete replacement by backfill material. This was done in an attempt to firstly reduce the carbon footprint of wind turbine foundations and secondly to reduce the water usage resulting from the construction of wind turbine foundations. The following conclusions are made:



- Feasible concrete volume reduction methods are presented namely, using high density aggregate and utilising backfill as a mass replacement for concrete. The methods offer 21% and 37% reduction in concrete volume respectively.
- Increase in density of concrete by volumetric replacement of aggregate by a denser aggregate is a feasible solution to reduce foundation size.
- The foundations' cost by percentage is approximately 5% of the wind energy project cost, however, implementing concrete replacement by backfill is expected to reduce the cost of foundations by approximately 29%.

### 8.1.4 General

The wind industry in South Africa is a niche industry. Academic development of wind energy is suppressed by the lack of initiative from industrial role players to collaborate with academia in South Africa. Proprietary information and trade secrets characterise the wind industry in South Africa, this limited the study as it was unable to acquire a detailed wind turbine tower design to model for academic purposes.

## 8.2 Recommendations

The following recommendations based on the conclusions are made:

- FE modelling is recommended for optimized designs of wind turbine foundations. There is simply no other known method to accurately determine the foundation rotational stiffness without neglecting the effects of the founding soil of the SSI.
- For steel reinforcement design, it is recommended to use the STM method as well as the radial plane simplification developed and reported in Chapter 4. The BTM is perceived as a conservative and uneconomical design approach.
- DIANA is recommended for modelling SSI as it was found to best simulate geotechnical properties and structural properties. Other FE software considered had a bias to either the geotechnical or the structural component.

## 8.3 Future Study

- This research was conducted primarily on gravity based foundations. The design approaches available currently result in a design that has sufficient bearing capacity as well as acceptable natural frequency. However, the design investigated here has insufficient rotational stiffness although taking care of the bearing capacity and natural frequency. For future study it is recommended that a study is conducted on how to increase the rotational stiffness without increasing the size of the foundation.
- Alternative foundations like piles are not popular in South Africa but should be investigated and compared to the current gravity based foundation with regard to cost and carbon foot print.

- Iron Ore was used as an aggregate replacement. The availability and cost of iron ore is uncertain. However, a study is recommended to investigate other high density aggregate which can be an economic aggregate replacement for use in wind turbine foundations or any other counter-weight structures.
- The connection between the tower and the foundation was found to be a critical aspect of the design. The only connection method used in this study is the anchor cage connection method, thus alternative connection methods should be investigated.
- Thermal cracking as a result of heat of hydration was not covered in the scope of this study however is recommended for future study.

# Appendices

# Appendix A

## Concrete Strength and Stiffness Detailed Results

This Appendix reports on the detailed results for the calculations carried out for the compressive strength, tensile strength and compressive stiffness of the concrete mixes performed in the study. 2 main mixes we made, namely Mix 1 which included a **Greywacke 13 mm** stone aggregate and Mix 2 which included **Iron Ore** stone aggregate. For the purposes of Table A.1 to A.8 Greywacke 13 mm and Iron Ore refers to Mix 1 and Mix 2 respectively.

### A.1 Compressive Strength

Table A.1: Iron Ore 7 Day Compressive Strength

Specimen	Mass (kg)	Area ( $mm^3$ )	Force (kN)	$f_{cu}$ (MPa)
1	2950	10000	387.6	38.76
2	2980	9900	382.6	38.65
3	2990	10000	369.5	36.95
Average				38.12
Standard Deviation				1.01

Table A.2: Iron Ore 28 Day Compressive Strength

Specimen	Mass (kg)	Area ( $mm^3$ )	Force (kN)	$f_{cu}$ (MPa)
1	3008	10000	436.3	43.63
2	2967	10000	504.9	50.49
3	2976	10000	501.7	50.17
Average				48.10
Standard Deviation				3.87

Table A.3: Greywacke 13 mm 7 Day Compressive Strength

Specimen	Mass (kg)	Area ( $mm^3$ )	Force (kN)	$f_{cu}$ (MPa)
1	2387	10000	310.8	31.08
2	2356	10000	289.2	28.92
3	2358	9900	311.1	31.42
Average				30.48
Standard Deviation				1.36

Table A.4: Greywacke 13 mm 28 day Compressive Strength

Specimen	Mass (kg)	Area ( $mm^3$ )	Force (kN)	$f_{cu}$ (MPa)
1	2415	10000	401.2	40.12
2	2406	10000	395.8	39.58
3	2393	10000	421.6	42.16
Average				40.62
Standard Deviation				1.36

## A.2 Tensile Strength

Table A.5: Iron Ore Tensile Strength

Specimen	Force (kN)	$f_{sp}$	$f_{ct}$ (MPa)
1	63100	4.02	3.62
2	75500	4.81	4.33
3	71500	4.55	4.10
Average		4.46	4.01
Standard Deviation		0.40	0.36

Table A.6: Greywacke 13 mm Tensile Strength

Specimen	Force (kN)	$f_{sp}$	$f_{ct}$ (MPa)
1	63700	4.06	3.65
2	56100	3.57	3.21
3	65700	4.18	3.76
Average		3.94	3.54
Standard Deviation		0.32	0.29

### A.3 E-Modulus

Table A.7: Iron Ore E-Modulus Results

Specimen	$\sigma_1$ (MPa)	$\sigma_2$ (MPa)	$\epsilon_1$	$\epsilon_2$	E-Modulus (GPa)
1	2.32	15.26	0.00005	0.00039	38.40
2	2.66	15.29	0.00005	0.00031	48.69
3	2.70	15.29	0.00005	0.00037	39.10
Average					42.06
Standard Deviation					5.75

Table A.8: Greywacke 13 mm E-Modulus Results

Specimen	$\sigma_1$ (MPa)	$\sigma_2$ (MPa)	$\epsilon_1$	$\epsilon_2$	E-Modulus (GPa)
1	2.17	13.00	0.00005	0.00040	30.54
2	1.48	13.02	0.00005	0.00041	31.98
3	2.17	13.03	0.00005	0.00041	30.37
Average					30.96
Standard Deviation					0.88

## Appendix B

# Detailed Bearing Capacity Calculation

### B.1 Introduction

This appendix gives report of the bearing capacity calculation in the form of an excel spreadsheet with explanations. The design is based on the development of a spreadsheet which incorporates the sizing of the foundation based on a generic foundation geometry , the effective area calculations by DNV/Riso (2002) and lastly bearing capacity calculation.

The first sheet calculates the mass of the foundation input as well as the over laying back fill. Equations B.1 and B.2 are used and results represented in Table B.1. Figure B.1 show the variables used in the calculation.

$$V_{concrete} = \left[ \frac{\pi D^2}{4} h_2 + \frac{\pi D_2^2}{4} (h - h_2) + \frac{1}{2} \frac{\pi (D^2 - D_2^2)}{4} (h - h_2 - dh) \right] \gamma_c \quad (\text{B.1})$$

$$V_{soil} = \left[ \frac{\pi (D^2 - D_2^2)}{4} dh + \frac{1}{2} \frac{\pi (D^2 - D_2^2)}{4} (h - h_2 - dh) \right] \gamma_s \quad (\text{B.2})$$

Table B.1: Foundation dimensions and equivalent vertical load

Definition	Symbol	Value	Unit
Radius	R	7.37	m
Diameter Bottom	D	14.74	m
Diameter Top	$D_2$	6.10	m
Bottom Height	$h_2$	0.50	m
total Height	h	3.40	m
Stub Height	dh	1.00	m
Unit Weight of Concrete	$\gamma_c$	24.00	kN/m <sup>3</sup>
Unit Weight of Backfill	$\gamma_s$	17.00	kn/m <sup>3</sup>
Weight of Concrete	$V_{\text{concrete}}$	7307.60	kN
Weight of Backfill	$V_{\text{soil}}$	4689.45	kN
Total Weight	V	11997.05	kN
Concrete Volume	$C_v$	304.48	m <sup>3</sup>
Back fill Volume	$B_v$	275.85	m <sup>3</sup>

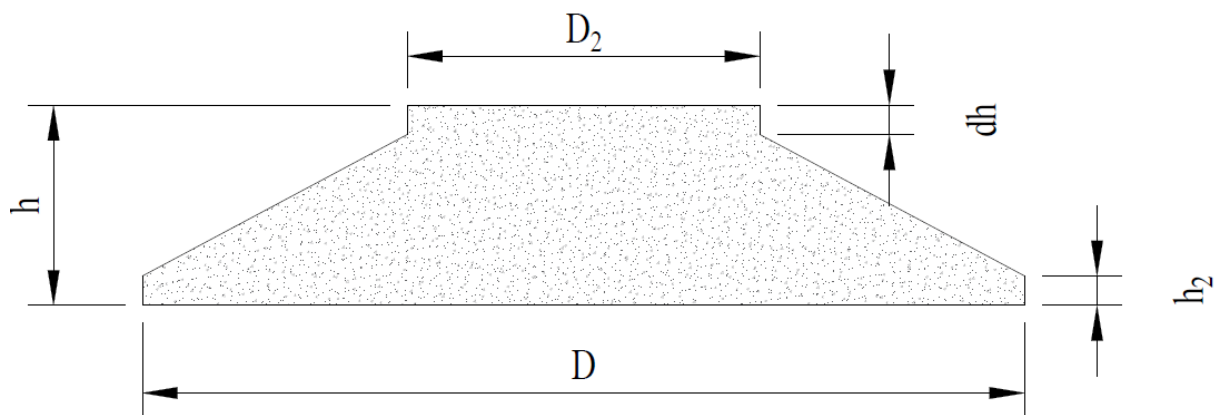


Figure B.1: Generic Foundation Geometry

The effective is calculated based on the guidelines by DNV/Riso (2002). Table ?? shows the results with respect to the definition of parameters shown in Figure B.2.



Table B.2: Effective Area Calculation

Definition	Symbol	Value	Unit
Foundation Radius	R	7.37	m
Simultaneous Horizontal Load	Fres	784	kN
Simultaneous Vertical Load	Fz	5130	KN
Design Overturning Moment	Md	93765	kNm
Design Vertical Load	Vd	17127	kN
eccentricity	e	5.475	m
Effective Foundation Area	A <sub>eff</sub>	25.680	m <sup>2</sup>
ellipse width	b <sub>e</sub>	3.793	m
ellipse length	l <sub>e</sub>	9.871	m
Effective Foundation length	l <sub>eff</sub>	8.175	m
Effective Foundation width	b <sub>eff</sub>	3.141	m
Type of Rapture		Rapture 2	

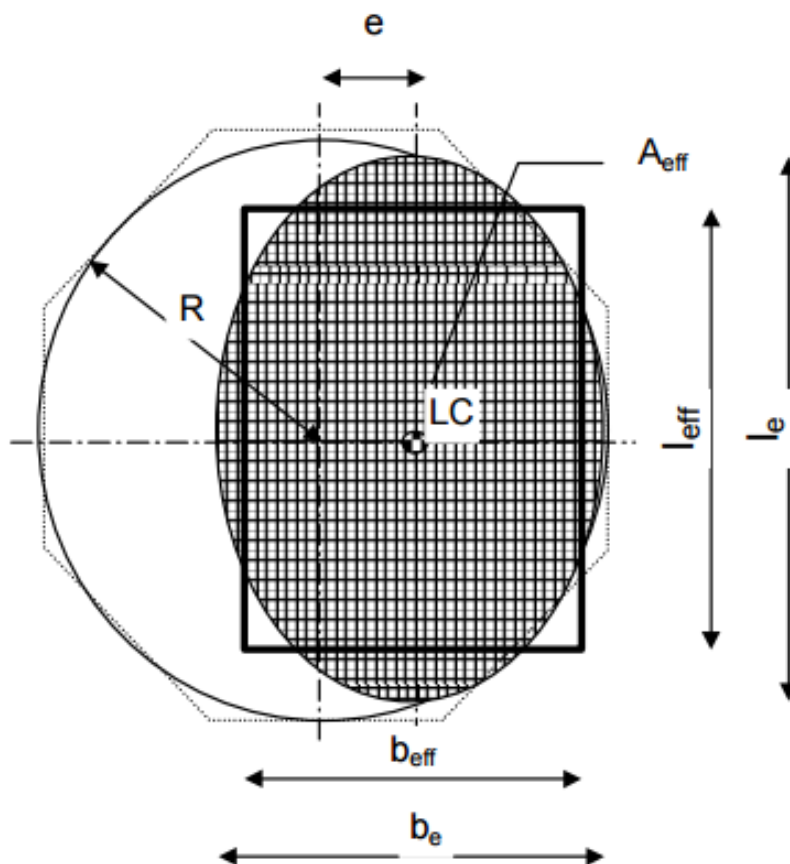


Figure B.2: Effective Area

The design load from the loading document and the equivalent vertical load from the foundation and backfill material used as the total vertical load for the bearing capacity calculations loaded on the effective area calculated. The results are shown in Table B.3 and the factor of safety is calculated.

Table B.3: Bearing Capacity Calculation

Loading			
Turbine+Tower Vertical Load	DL	17127	kN
Horizontal load	H	784	
Foundation Density	$\gamma_{\text{foundation}}$	24	kN/m <sup>3</sup>
Foundation Weight	$G_c$	7308	kN
Back Fill Weight	$G_s$	4689	kN
Overburden Pressure	$q_0$	65	kPa
Gross Bearing Pressure	$q$	667	kPa
Nett Bearing Pressure	$q_{\text{nett}}$	602	kPa
Horizontal Loading (Direction 1)			
Inclination	$\alpha_1$	2.62	degrees
Eccentricity	$e_1$	0.00	m
Foundation Dimensions			
Breadth	B	3.14	m
Length	L	8.18	m
Depth	Z	3.4	m
Effective Breadth	$B'$	3.14	m
Effective Length	$L'$	8.18	m
Soil Properties			
Bulk Density	$\gamma_{\text{bulk}}$	19.2	kN/m <sup>3</sup>
Saturated Density	$\gamma_{\text{sat}}$	21	kN/m <sup>3</sup>
Unit Weight Water	$\gamma_w$	10	kN/m <sup>3</sup>
Submerged Unit Weight	$\gamma'$	11	kN/m <sup>3</sup>
Friction angle		31.5	degrees
Cohesion intercept	$c'$	12	kPa
Water Table			
Depth of WT		100	m
$q_{o\_bar}$		65.28	kPa
$y\_bar$		13.00	kN/m <sup>3</sup>

Bearing Capacity Factors			
Cohesion	$N_c$	34.04	
Surcharge	$N_q$	21.86	
Self-weight	$N_\gamma$	25.57	
Shape Factors		Rapture 1	Rapture 2
Foundation	$s_c$	1.25	1.25
	$s_q$	1.12	1.12
	$s_\gamma$	1.12	1.12
Founding	$d_c$	1.39	1.00
	$d_q$	1.19	1.00
	$d_\gamma$	1.19	1.00
Load Inclination 1	$i_{c,1}$	0.94	1.00
	$i_{q,1}$	0.94	1.00
	$i_{\gamma,1}$	0.84	1.00
Load Inclination 2	$i_{c,2}$	1.00	1.00
	$i_{q,2}$	1.00	1.00
	$i_{\gamma,2}$	1.00	1.00
Bearing Capacity			
Cohesion	$q_c$	664.67	535
Surcharge	$q_q$	1801.68	0
Self-weight	$q_\gamma$	587.56	1175
Total Bearing Capacity	$q_u$	3053.91	1710
Factor of Safety		<b>4.96</b>	<b>2.73</b>

The equation used for the bearing capacity factors are shown below.

$$q_u = c' \cdot N_c (s_c \cdot d_c \cdot i_c) + \gamma \cdot z \cdot N_q (s_q \cdot d_q \cdot i_q) + 0,5 \cdot \gamma \cdot B \cdot N_\gamma (s_\gamma \cdot d_\gamma \cdot i_\gamma)$$

- bearing capacity factors:

$$N_c = (N_q - 1) \cot \phi'$$

$$N_q = e^{\pi \tan \phi'} \tan^2 \left( 45^\circ + \frac{\phi'}{2} \right)$$

$$N_\gamma = 2(N_q - 1) \tan \phi'$$

- shape of foundation (base area = L' x B')

$$\phi' \leq 10^\circ : s_c = 1 + 0,2(B'/L') \tan^2(45^\circ + \phi'/2), \quad s_q = s_\gamma = 1$$

$$\phi' > 10^\circ : s_c = 1 + 0,2(B'/L') \tan^2(45^\circ + \phi'/2), \quad s_q = s_\gamma = 1 + 0,1(B'/L') \tan^2(45^\circ + \phi'/2)$$

- depth of founding (bottom of foundation at Z below ground surface)

$$\phi' \leq 10^\circ : d_c = 1 + 0,2(Z/B') \tan(45^\circ + \phi'/2), \quad d_q = d_\gamma = 1$$

$$\phi' > 10^\circ : d_c = 1 + 0,2(Z/B') \tan(45^\circ + \phi'/2), \quad d_q = d_\gamma = 1 + 0,1(Z/B') \tan(45^\circ + \phi'/2)$$

- inclination of load (load inclined at  $\alpha$  from the vertical, all angles in radians)

$$i_c = i_q = \left( 1 - \frac{2\alpha}{\pi} \right)^2 \quad \alpha < \phi'$$

$$i_\gamma = \left( 1 - \frac{\alpha}{\phi'} \right)^2$$

- factor of safety

$$FoS = \frac{q_u - q_o}{q - q_o}$$

# Appendix C

## FEM Material Properties

This appendix tabulated the material properties used for the FEM for each analysis.

### C.1 Concrete

Two different material models for concrete were used in the study. The linear elastic concrete material model was used for the static push over analysis without reinforcement, the cyclic load analysis as well as the structural eigen value analysis. The total strain based crack model was used for the reinforced concrete foundation model.

#### C.1.1 Linear Elastic Concrete

Table C.1: Linear Elastic Concrete Model material properties

Description	Value	Unit
Young's Modulus	30.8	GPa
Poisson's Ratio	0.2	
Mass Density	2400	$kg/m^3$

### C.1.2 Total Strain Based Crack Model

Table C.2: Total Strain Based Crack Model material properties

Description	Value	Unit
Young's Modulus	30.8	GPa
Poisson's Ratio	0.2	
Mass Density	2400	$kg/m^3$
Tensile Strength	3.93	MPa
Mode-I tensile fracture energy	30	N/m
Residual tensile strength	0	MPa

## C.2 Soil

The founding material used was soil with the material properties as tabulated in Table C.3. The material properties were used in the models for the push over analysis and the cyclic load analysis. For the structural eigen value analysis, the material properties for the soil are reported in Chapter 6.

Table C.3: Soil Material Properties

Description	Value	Unit
Reference secant stiffness	30	MPa
Unloading-reloading stiffness	150	MPa
Oedometer tangent stiffness	36	MPa
Cohesion	12000	Pa
Friction angle and shear failure	44	deg
Initial friction angle	31.5	deg
Dilatancy angle	12	deg
Failure ration of $q_f/q_a$	0.8	
Exponent m	0.5	
Reference Stress	100000	Pa
Poisson's Ratio	0.2	
K-ration for normally consolidated soil	0.3	
Initial void-ratio	0.5	
Maximum void-ratio	0.89	
Tension cut-off value	0	MPa
Mass Density	1750	$kg/m^3$

### C.3 Soil-Structure Interaction

All analysis used the same SSI material model tabulated in Table C.4 to model the interface between the concrete foundation and the soil.

Table C.4: SSI Material Properties

Description	Value	Unit
Normal stiffness modulus z	9500	GPa
Shear stiffness modulus x	95	MPa
Shear stiffness modulus y	95	MPa
Normal Tensile Stiffness	0	MPa

### C.4 Steel

The tower of the model and the reinforcement steel where developed using the steel material properties shown in Table C.5.

Table C.5: Steel material properties

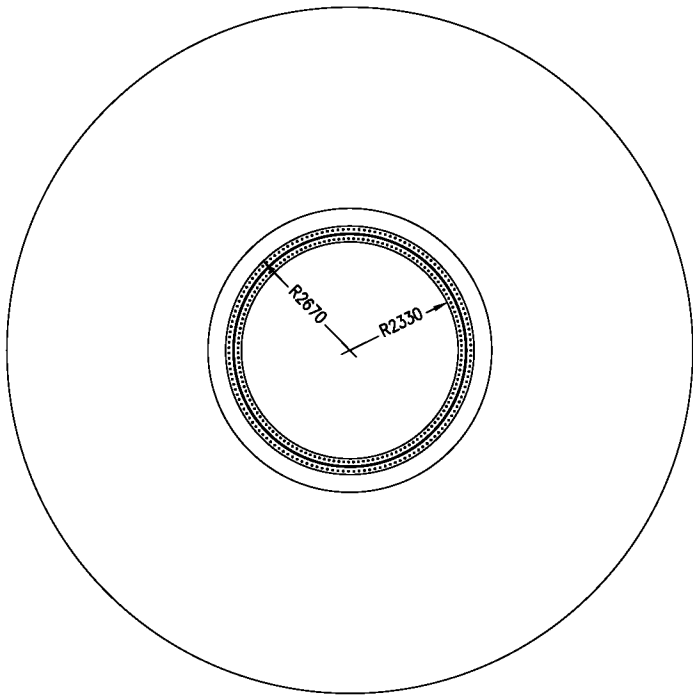
Description	Value	Unit
Young's Modulus	200	GPa
Poisson's Ratio	0.3	
Mass Density	7800	$kg/m^3$

# Appendix D

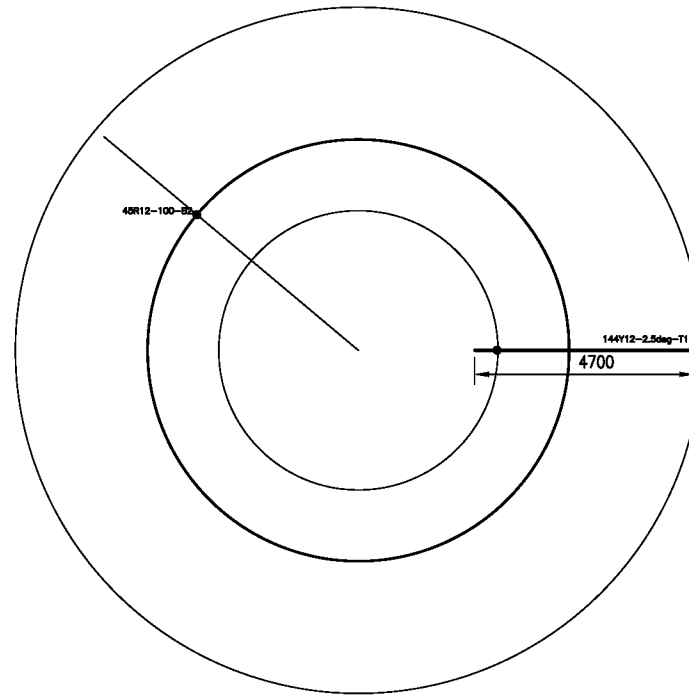
## Foundation Detailed Drawings

The following drawings illustrate the foundation dimension for Model 1 and 2 respectively. The drawings are purely for educational purposes and can not be used for any commercial application without relevant permission from the University of Stellenbosch.

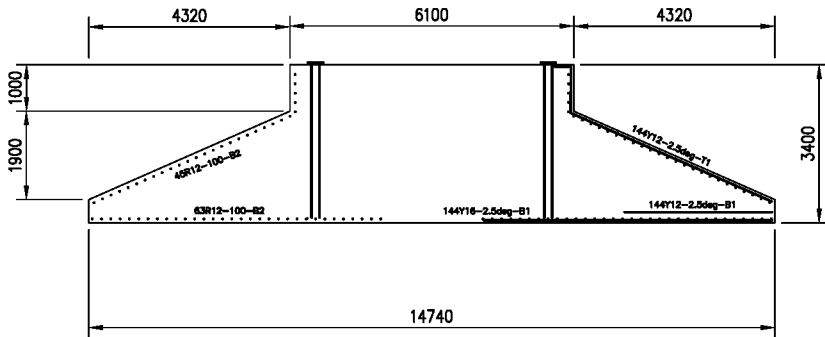




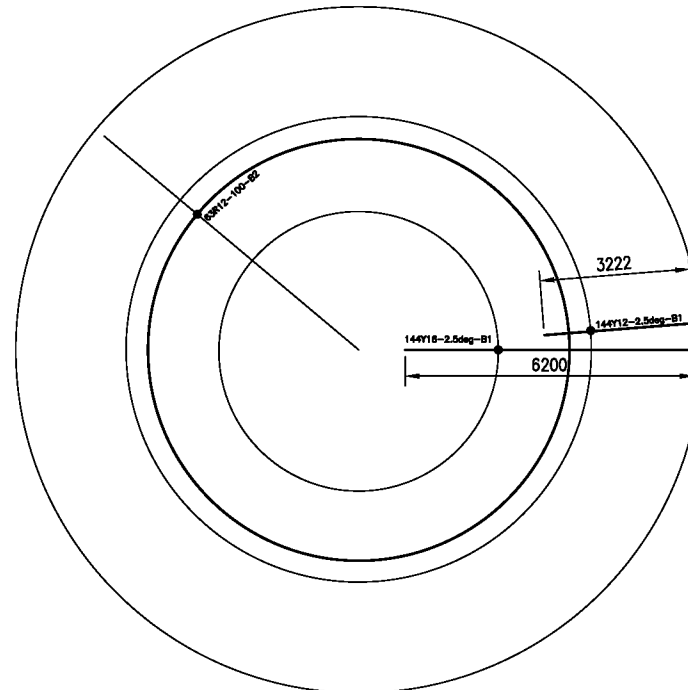
**Plan View**  
1:100



**Top Steel Detail**  
1:100



**Sectional View**  
1:100

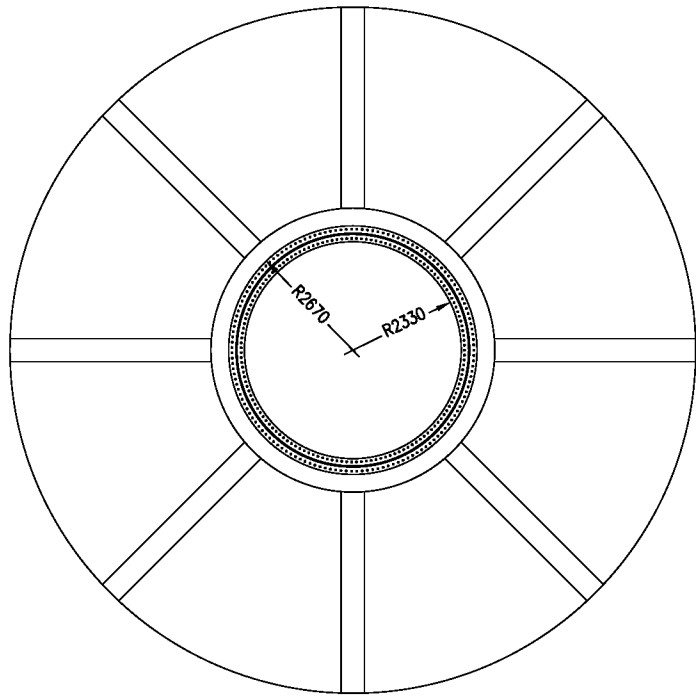


**Bottom Steel Detail**  
1:100

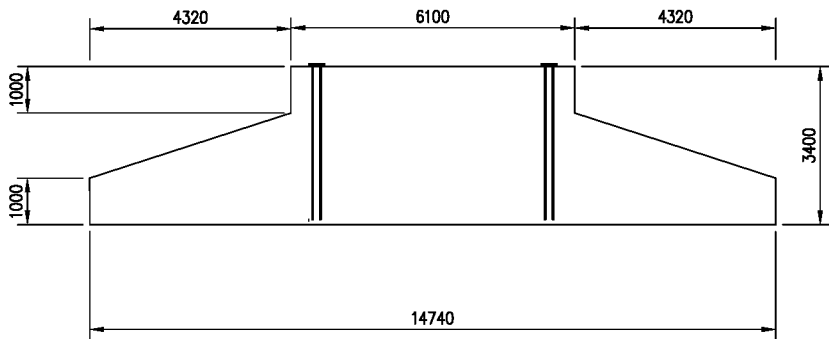
NOTES:  
GENERAL SPECIFICATIONS  
\* 35 MPa Concrete

PROJECT: MEng Thesis Wind Turbine Foundation  
AREA: Stellenbosch University  
TITLE: Model 1 Foundation Design  
Concrete and Steel  
1 OF 1

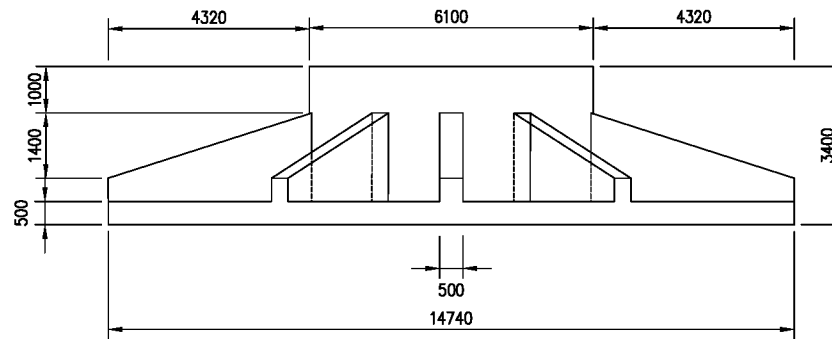
SIZE A3	1234-SP-GA-01	SHT No -	REV C
------------	---------------	-------------	----------



**Plan View**  
1:100



**Sectional View**  
1:100



**Side View**  
1:100

NOTES:  
GENERAL SPECIFICATIONS  
\* 35 MPa Concrete

PROJECT: MEng Thesis Wind Turbine Foundation  
AREA: Stellenbosch University  
TITLE: Model 2 Foundation Design  
Concrete  
1 OF 1

SIZE A3	1234-SP-GA-01	SHT No -	REV C
------------	---------------	-------------	----------

# List of References

- Alexander, M. (2009). *Fulton's concrete technology*. Cement & Concrete Institute.
- ASTM-C-469 (2014). Standard test method for static modulus of elasticity and poisson's ratio of concrete in compression. Tech. Rep., American Society for Testing and Materials (ASTM) International, West Conshohocken, PA, 2014.
- CMW (2015). Windtower foundation opportunities for innovation.
- DIANA (2016). *Diana ( Displacement Analyser) user's Manual and Element Library*. TNO Building and Construction Research, 10th edn.
- DNV/Riso (2002). *Guidelines for Design of Wind Turbine 2nd Edition*.
- Eberhard, A., Kolker, J. and Leigland, J. (2014). South africa's renewable energy ipp procurement program : Success factors and lessons. Tech. Rep., University of Cape Town, World Bank Institute , Private Infrastructure Development Group.
- Eurocode-2 (2004). Design of concrete structures. Tech. Rep., European Committee for Standardization.
- Fitzgerald, B. and Basu, B. (2016). Structural control of wind turbines with soil structure interaction included. *Engineering Structures*.
- GWEC (2015). Global wind energy report.
- Hibbeler, R.C. (2014). *Mechanics of Material*. Pearson.
- Knappett, J.A. and Craig, R.F. (2012). *Craig's Soil Mechanics*. Spon Press.
- Maunu, P. (2006). *Design of Wind Turbine Foundation Slabs*. Master's thesis, Lulea University Of Technology.
- Mawer, B. (2015). *An introduction to Geotechnical Design of South African Wind Turbine Gravity Foundations*. Master's thesis, University of Cape Town.
- Murtagh, P., Basu, B. and Broderick, B. (2005). Response of wind turbines including soil-structure interaction. In: *Proceedings of the Tenth International Conference on Civil, Structural and Environmental Engineering Computing*, 270, pp. 1–17.
- Muzofa, T.D., van Zijl, G.P.A.G. and Day, P.W. (2017). Computational modelling of soil-structure interaction towards reduced concrete foundation volume for tall wind turbine towers. In: *Book of Abstracts for 2017 fib Symposium held in Maastricht, The Netherlands*.
- Nicholson, J.C. (2011). *Design of wind turbine tower and foundation systems*. Master's thesis, University of Iowa.
- Phuly, A. (2010). Fatigue resistant foundation system.

- Prokon (2010). Prokon users guides. Tech. Rep., Prokon Software Consultants (Pty) Ltd.
- Rey, J. and Puertos, Y.C. (2012). ick foundation analysis and design.  
Available at: [http://www.windfarmbop.com/wp-content/uploads/2013/02/iCK\\_Foundation\\_Memory.pdf](http://www.windfarmbop.com/wp-content/uploads/2013/02/iCK_Foundation_Memory.pdf)
- SABS-0100-1 (2000). The structural use of concrete, part 1, design. Tech. Rep., South African Standards.
- SANS-201 (2008). Sieve analysis, fines content and dust content of aggregates. Tech. Rep., SOUTH AFRICAN NATIONAL STANDARD, 1 Dr Lategan Road Groenkloof.
- SANS-3001-AG10 (2012). Civil engineering test methods part ag10: Acv (aggregate crushing value) and 10 aggregates. Tech. Rep., SOUTH AFRICAN NATIONAL STANDARD.
- SANS-5844 (2014). Particle and relative densities of aggregates. Tech. Rep., SOUTH AFRICAN NATIONAL STANDARD, 1 Dr Lategan Road Groenkloof.
- SANS-5862-1 (2006). Concrete tests consistence of freshly mixed concrete slump test. Tech. Rep., SOUTH AFRICAN NATIONAL STANDARD, 1 dr lategan road groenkloof.
- SANS-5863 (2006). Concrete tests - compressive strength of hardened concrete. Tech. Rep., South African National Standards, 1 Dr Lategan Road Groenkloof Private Bag X191 Pretoria 0001.
- SANS-6253 (2006). Concrete tests - tensile splitting strength of concrete. Tech. Rep., South African National Standard, 1 Dr Lategan Road Groenkloof Private Bag X191 Pretoria 0001.
- Selvadurai, A. and Yu, Q. (2005). Mechanics of a discontinuity in a geomaterial. *Science Direct*.
- Svensson, H. (2010). *Design of Wind turbine Foundations*. Master's thesis, Lund University.
- Ti, K.S., Huat, B., Noorzaei, J., Jaafar, M.S. and Sew, G.S. (2009). A review of basic soil constitutive models for geotechnical application. *Electronic Journal for Geotechnical Engineering J*, vol. 14, pp. 1–16.
- van Mier, J.G.M. (1997). *Fracture Processes Of Concrete*. CRC Press.
- Vestas (). Description of standard gravity anchor foundation v80-v90-v100-v112. Restricted Document. Information contained is regarded as proprietary.
- Vestas (2011a). *Foundation Design Guidelines V80-V90-V100-V112*.
- Vestas (2011b). Foundation loads. Tech. Rep., Vestas.
- Way, A. (2014). *A study on the Design and Materials Costs of Tall Wind Turbine Towers in South Africa*. Master's thesis, Stellenbosch University.
- Way, A. and van Zijl, G.P.A.G. (2015). A study on the design and material cost of tall wind turbine towers in south africa. vol. 57, pp. 45–54.